



Forests of the brown macroalgae *Gongolaria abies-marina* (S.G: Gmelin) Kuntze: from phenology to temporal trends in Gran Canaria Island (eastern Atlantic)

Universidad de Las Palmas de Gran Canaria

Programa de Doctorado en Calidad Ambiental y Recursos Naturales

Escuela de doctorado

José Antonio Valdazo Hernández

PhD Tesis

Las Palmas de Gran Canaria

Octubre 2023

D. JESÚS GARCÍA RUBIANO CORDINADOR DEL PROGRAMA DE DOCTORADO EN CALIDAD AMBIENTAL Y RECURSOS NATURALES DE LA UNIVERSIDAD DE LAS PALMAS DE GRAN CANARIA

INFORMA,

De que la Comisión Académica del Programa de Doctorado, en su sesión fecha tomó el acuerdo de dar el consentimiento para su tramitación, a la tesis doctoral titulada *“Forests of brown macroalgae Gongolaria abies-marina (S.G. Gmelin) Kuntze: from phenology to temporal trends in Gran Canaria (eastern Atlantinc)”* presentada por el doctorando D. José Antonio Valdazo Hernández y dirigida por la Dra. María Ascensión Viera Rodríguez y el Dr. Fernando José Tuya Cortés.

Y para que así conste, y a efectos de lo previsto en el Artº 25 del Reglamento de Estudios de Doctorado (BOULPGC 26/01/2023) de la Universidad de Las Palmas de Gran Canaria, firmo la presente en Las Palmas de Gran Canaria, a de de dos mil veinte tres.



**UNIVERSIDAD DE LAS PALMAS DE GRAN CANARIA
ESCUELA DE DOCTORADO**

Programa de doctorado en Calidad Ambiental y Recursos Naturales

Título de la Tesis

FORESTS OF BROWN MACROALGAE *GONGOLARIA ABIES-MARINA* (S.G. GMELIN) KUNTZE: FROM PHENOLOGY TO TEMPORAL TRENDS IN GRAN CANARIA (EASTERN ATLANTIC)

Tesis Doctoral presentada por D. José Antonio Valdazo Hernández

Dirigida por la Dra. D^a María Ascensión Viera Rodríguez

Codirigida por el Dr. D. Fernando José Tuya Cortes

Las Palmas de Gran Canaria, a de octubre de 2023

La Directora,

El Codirector,

El Doctorando,

(firma)

(firma)

(firma)

Index

Agradecimientos	9
CHAPTER 1. General introduction	11
Objectives	16
CHAPTER 2. Massive decline of <i>Gongolaria abies-marina</i> forests in Gran Canaria Island (Canary Islands, eastern Atlantic)	17
Abstract	18
Introduction.....	19
Material and Methods.....	21
Study area.....	21
Mapping historical and current distribution: GIS analysis	22
Comparison of populations: 2008 vs 2016.....	23
Human pressures as drivers of change.....	24
Results	24
Distribution and extent	24
Comparison of populations: 2008 vs 2016.....	27
Human pressures as drivers of regression	29
Discussion.....	30
Supplementary material.....	33
CHAPTER 3. Seasonality in the canopy structure of the endangered brown macroalga <i>Gongolaria abies-marina</i> at Gran Canaria Island (Canary Islands, eastern Atlantic).	40
Abstract	41
Introduction.....	42
Materials and methods	44
Study sites and <i>Gongolaria abies-marina</i> canopy structure	44
Sampling and sorting.....	46
Environmental drivers	47
Statistical analysis.....	47
Results	48
Canopy structure: variation across sites	48
Size structure: evidence of intraspecific relationships	50
Linking environmental variation with canopy structure	51
Annual frond production.....	54
Discussion.....	55
Supplementary material.....	59

CHAPTER 4. Local and global stressors as major drivers of the drastic regression of brown seaweed forests in an oceanic island	69
Abstract	70
Introduction.....	71
Material and Methods.....	73
Target species and historical distribution	73
Small-scale distribution patterns.....	75
Local and global environmental drivers	76
Local geomorphology and wave energy.....	76
Local anthropogenic drivers	76
Climatic drivers.....	77
Effect of predictor variables on <i>Gongolaria abies-marina</i> distribution	77
Survival and growth of early stages.....	78
Temporal changes in frond size	79
Results	80
Historical distribution and drivers of decline	80
Small-scale distribution patterns.....	81
Survival and size of early stages	82
Temporal changes in frond size	83
Discussion.....	84
Supplementary material.....	88
CHAPTER 5. Conclusions	107
RESUMEN EN ESPAÑOL	108
Objetivos	112
Conclusiones	113
FUNDING	115
REFERENCES	116

Agradecimientos

En primer lugar, me gustaría nombrar a mis directores de tesis, Susi Viera y Fernando Tuya, debido a su inestimable ayuda, dedicación, compromiso y aliento. Podría estar toda la vida dándoles las gracias, sin su apoyo esta tesis no se estaría presentado en el tiempo de descuento. En este agradecimiento incluyo también a Ricardo Haroun, porque con él empecé mi andadura en el mundo de la investigación allá por el 2008. Mencionar también a mi tutor de la Tesis, Pedro Sosa, por facilitarme las cosas en todo momento.

También quiero agradecer a todas las personas que me han acompañado del grupo de investigación BIOCON y de la Facultad de Ciencias del Mar por todo su apoyo en las numerosas campañas realizadas y en el trabajo de laboratorio. Un recuerdo especial va para Tony Sánchez, por su genuina manera de ser, sus consejos, enseñanzas de vida y entrega en todo momento. Muchas gracias, Tony, allá donde estés. También me gustaría mencionar a Mascha Stroobant, Francisco Otero, Fernando Espino, Leticia Curbelo, Raúl Triay-Portella, Javier Suárez, que en un momento u otro de esta etapa que llega a su cierre han puesto su granito de arena.

Tampoco quisiera olvidarme de los “compañeros y compañeras” que han coincidido conmigo mientras realizaban sus prácticas y me han ayudado con el arduo trabajo de laboratorio y acompañado en los madrugones para aprovechar las bajamares vivas.

Agradecer también a mis compañeros y compañeras de Elittoral, a los que estuvieron y a los que están, por apoyarme y alentarme en esta etapa. A Oscar Bergasa y Rosana Álvarez por facilitarme las cosas, comprenderme y darme tiempo en el último sprint de esta aventura.

Gracias a todos mis buenos amigos, hermanos de vida, ustedes son parte importante de que esta tesis haya ido tomando forma y esté ahora acabada.

Y como no podía ser de otra manera, el mayor agradecimiento de todos se lo merece mi familia. Gracias a mis padres y hermanos, a mis suegros, a mi amor verdadero y a mi pequeñín. Esto es por y para ustedes. Ellos siempre han estado en los buenos momentos, pero fundamentalmente en los no tan buenos sosteniéndome de manera incondicional. Gracias infinitas por la paciencia que han tenido conmigo, sin ustedes a mi lado, no hubiera sido posible.

CHAPTER 1. General introduction

Marine forests of large brown macroalgae, mostly belonging to the orders Fucales and Laminariales, are unique habitats which support a great variety of organisms in coastal zones worldwide and are comparable to terrestrial forests for the ecosystem services they provide (Steneck et al. 2002). These canopy-forming macroalgae are very important primary producers (Mann 1973) and increase the structural complexity where they live, providing shelter and food for associated species (Schiel and Foster 2006; Cheminée et al. 2013), and increasing biodiversity (Chapman 1995; Steneck et al. 2002; Piazzini et al. 2018). In the past half century, however, threats to canopy-forming brown macroalgae have increased in number and severity, leading to a decline in their abundance in many places of temperate latitudes (Mineur et al. 2015; Krumhansl et al. 2016). The loss of macroalgal forests also implies a damage, or impoverishment, in the provision of ecosystem services (Smale et al. 2019). Thus, the conservation of these habitat-forming species is a crucial goal for ecologists and environmental managers. To achieve this, a better understanding of the structure and dynamics of canopies of algal forests in relation to environmental drivers and intraspecific interactions is crucial (Schiel and Foster, 2006; Bennett & Wernberg, 2014; Smale et al., 2016). Moreover, understanding the causes in declines of macroalgal forests are essential for implementing appropriate conservation and restoration schemes (Coleman and Wernberg 2017).

Subtidal and intertidal algal forests experience large variations in their distribution, abundance, and fitness at a range of spatial and temporal scales (Martínez et al. 2012; Ferreira et al. 2014; Yesson et al. 2015). Their structure and extent are influenced by a variety of environmental variables, including temperature (Tuya et al. 2012), light availability (Creed et al. 1998), nutrients (Piazzini and Ceccherelli 2017) and wave intensity (Engelen et al. 2005). Ecological processes, such as intraspecific and interspecific competition and facilitation, can also affect their structure and functioning (Bennett and Wernberg 2014). Although macroalgae are important habitat-formers in temperate and subtropical rocky ecosystems, there are still few studies on their frond structure, particularly in terms of their temporal dynamics (Åberg 1992; Schiel and Foster, 2006).

Seasonal changes in photoperiod are important in initiating the growth of macroalgae after the winter dormancy period. Likewise, an increase in water temperature is related to the beginning of growth and reproduction (Graiff et al. 2015; de Bettignies et al. 2018). Normally, in temperate seas, there is a mismatch between the period of maximum macroalgal growth and the concentration of nutrients in the water (Ballesteros 1988; Delgado et al. 1994). For example, Laminariales build up reserves of nitrogen (N) which are used to initiate growth in early spring,

when light levels increase (Chapman & Craigie, 1977; Nielsen et al., 2014). Many *Cystoseira* s.l. species can store reserves in their tophules, storage structures situated on the base of the branches (García-Fernández and Bárbara, 2016) although some species such as *Gongolaria abies-marina* lack tophules or alternative structures to store reserves (González and Afonso-Carrillo, 1990). Wave action is one of the primary factors affecting canopy structure and dynamics (Engelen et al. 2005; Kregting et al. 2016), including local adaptation to hydrodynamic forces (de Bettignies et al. 2015).

A combination of natural and anthropogenic stressors often explains the decay of macroalgal forests around the world (Strain et al. 2014; Mineur et al. 2015; Krumhansl et al. 2016). Among these stressors, climate change has become one of the most importance drivers of such global ecological change (Wernberg et al. 2016). Currently, there is evidence that climate change has modified the distribution of species, which has altered the structure and functioning of ecosystems (Pecl et al. 2017). Many species have changed their geographic distribution, colonizing more favourable habitats (Vergés et al. 2014; Bevilacqua et al. 2019; Álvarez-Losada et al. 2020), while becoming extinct in areas previously occupied (Gouvêa et al. 2017; de Bettignies et al. 2018; Gurgel et al. 2020). Extreme events of thermal anomalies, in particular Marine Heat Waves (MHWs), have occurred with increasing intensity, frequency, and duration around the world (Hobday et al. 2016; Oliver et al. 2018; Thorat et al. 2022), which abruptly alter the structure and function of marine ecosystems, including forests of brown macroalgae (Wernberg et al. 2016; Straub et al. 2019; Gupta et al. 2020; Smale 2020; Pesarrodonna et al. 2021). Concurrently, local human disturbances, such as habitat destruction, pollution and eutrophication, act cumulatively and even synergistically, amplifying the effects of climate change on coastal habitats (Gouvêa et al. 2017; Orfanidis et al. 2021). From a conservation point of view, it is critical to ascertain, not only the nature of varying factors involved in declines of macroalgal forests, but also their relative contributions, and how these factors alter processes across levels of organization, from physiological effects to ecological interactions (Côté et al. 2016; Duarte et al. 2018).

The genus *Cystoseira* C. Agardh was described in 1820 and is very diverse; it includes 37 species, and its taxonomy and nomenclature have undergone many changes since then (García-Fernández and Bárbara 2016). The reasons for these changes lie in the fact that variability in this genus occurs not only between species but also between individuals of a single species, even seasonally within the same individual. In recent years, with the aim of completing the knowledge of the genus *Cystoseira*, its taxonomy, origin, and evolution, several studies have been carried out (Draisma et al. 2010; Orellana et al. 2019; Neiva et al 2022). Specifically, Orellana et al. (2019)

studied the diversity and phylogeny of the genus *Cystoseira* in the Mediterranean and the East Atlantic, and because of their studies, made changes in the names of some species, including our study species, *Cystoseira abies-marina* (S.G. Gmelin) C. Agardh, which was renamed *Treptacantha abies-marina* (S.G. Gmelin) Kützing. However, Molinari and Guiry (2020) showed that the genus *Gongolaria* Boehmer had nomenclatural priority over this name, and currently, our study species is called *Gongolaria abies-marina* (S.G. Gmelin) Kuntze.

Brown macroalgae of the genera *Cystoseira* C. Agardh, *Ericaria* Stackhouse and *Gongolaria* Boehmer (Fucales, Phaeophyceae), *Cystoseira* sensu lato (s.l.), are key components of Mediterranean-Atlantic marine forests, essential for biodiversity and ecosystem functioning (Tuya and Haroun 2006), which have suffered severe declines in the last decades (Thibaut et al. 2005; Blanfuné et al. 2016; Valdazo et al. 2017; Bernal-Ibáñez et al. 2021b). Due to their high sensitivity to anthropogenic impacts, several species of *Cystoseira* indicate high quality waters and facilitate the implementation of the EU Water Framework Directive (2000/06/EC) (Ballesteros et al. 2007, Blanfuné et al. 2016b, 2017). All the Mediterranean species of the genus *Cystoseira* s.l., except *C. compressa* (Esper) Gerloff & Nizamuddin, have been protected under the Annex II of the Barcelona Convention (2010). Five species, *Ericaria amentacea* (C. Agardh) Molinari & Guiry, *Ericaria mediterranea* (Sauvageau) Molinari & Guiry, *Ericaria sedoides* Neiva & Serrão, *Gongolaria montagnei* (J. Agardh) Kuntze and *Ericaria zosteroides* C. Agardh) Molinari & Guiry, are protected under the Berne Convention (Annex I, 1979). In addition, all Mediterranean *Cystoseira* species are under surveillance by international organizations, such as IUCN, RAP/ASP and MedPan (Thibaut et al. 2014). All species of *Cystoseira* s.l. are “habitat-forming” and are therefore considered EU habitats of interest (Micheli et al. 2013).

The present study focuses on *Gongolaria abies-marina* (S. G. Gmelin) Kuntze, this species has been considered the most abundant furoid species on rocky shores of the Canary Archipelago (Wildpret et al. 1987, Tuya and Haroun 2006), and its populations typically form extensive stands in both the eulittoral and shallow sublittoral (Fig. 1), mainly on rocky wave-exposed zones (Wildpret et al. 1987, Medina and Haroun 1993).

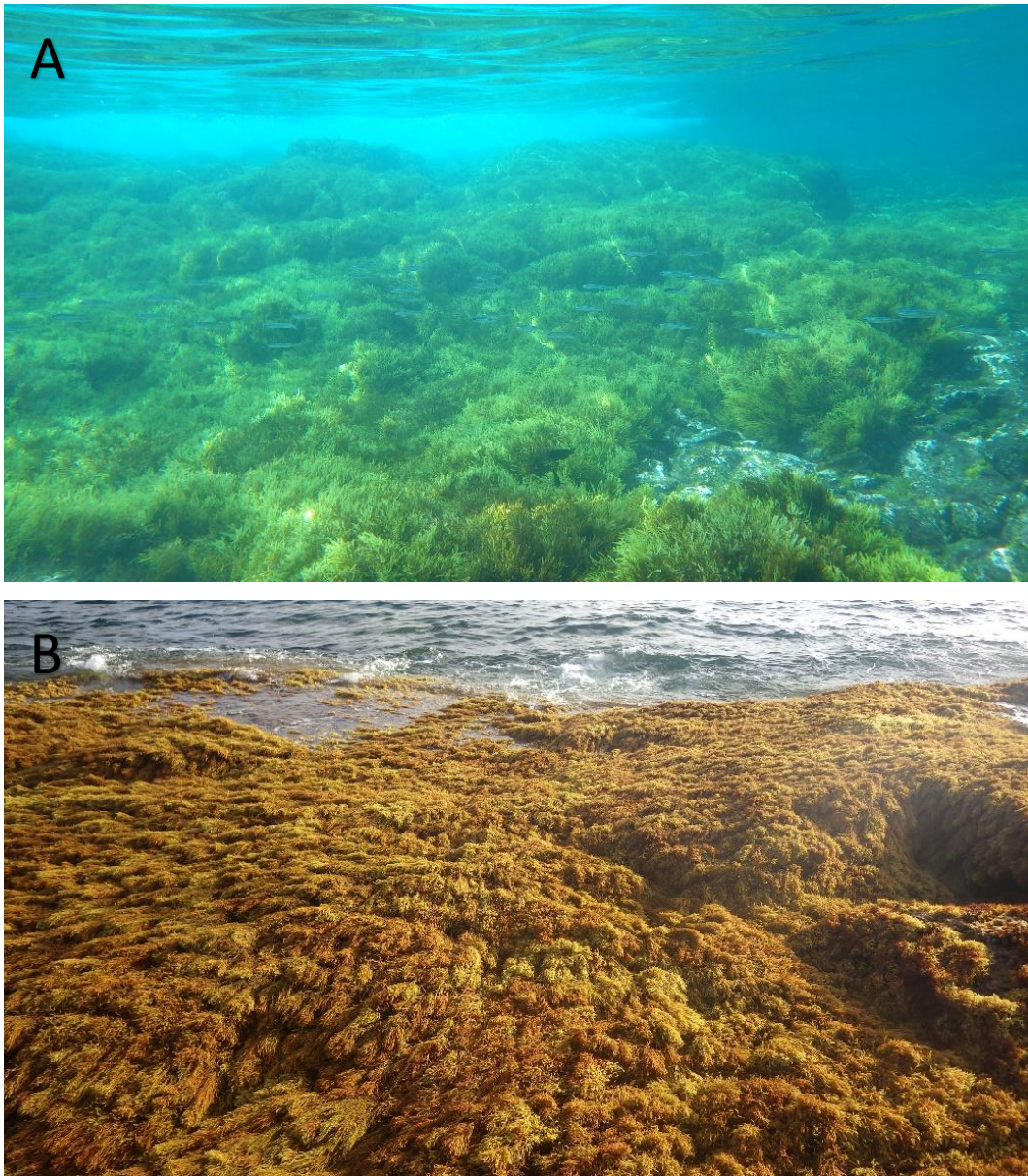


Fig. 1. Stand of *Gongolaria abies-marina* in (A) eulittoral and (B) shallow sublittoral at Salinetas in Gran Canaria Island

G. abies-marina is a caespitose plant with large numbers of erect branches, up to 50 cm long. Similar to other species in the genera *Cystoseira*, this species undergoes an annual thallus loss at the end of summer, when a high proportion of the fronds break down at the base. The holdfasts overwinter and regrow the next year. Therefore, although individuals are perennial, the thalli are annual (Buonomo et al. 2017). However, the plant never goes through a total rest phase: during unfavourable months, branches from different seasons coexist (González-Rodríguez and Afonso-Carrillo 1990). This alga spreads through both vegetative propagation and sexual reproduction (Medina 1997). Similar to other species of the genus, thalli are negatively buoyant, and propagules normally settle at <20-40 cm from the source population (Mangialajo et al. 2012), which gives the species a low-dispersal ability (Bulleri et al. 2002).

G. abies-marina is one of the most productive macroalgae in the Canary Islands (Johnston 1969), and at the end of summer, after the maximum reproductive peak, it is possible to find a large amount of wrack on beaches from nearby forests (Portillo-Hahnefeld 2008). The assemblages of *G. abies-marina* exhibit a complex structure, which allows the presence of many vegetal and animal associate species (Fig. 2)

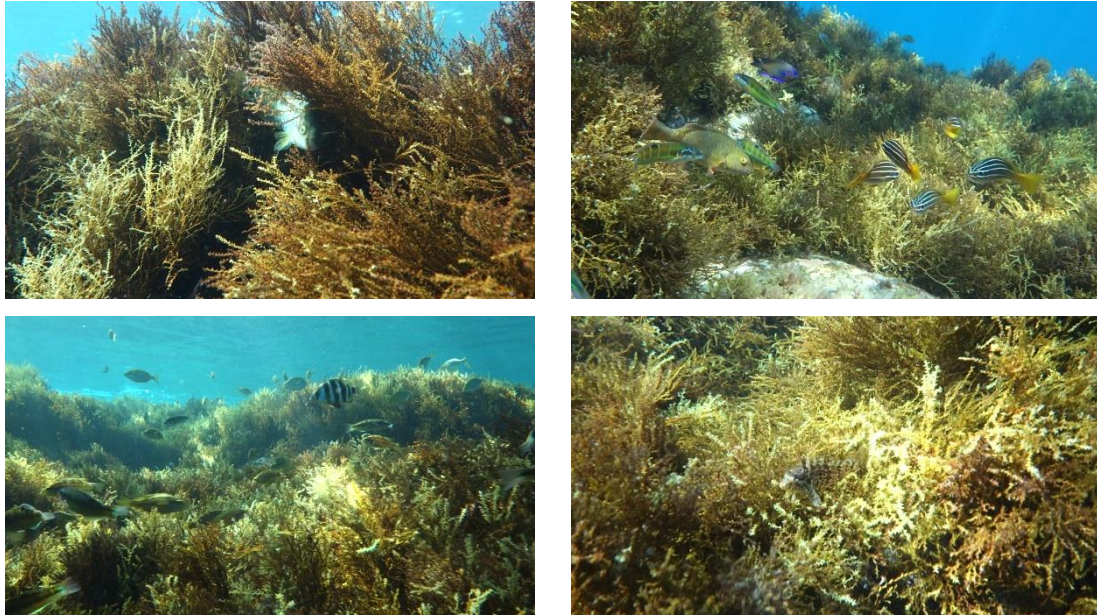


Fig. 2. Biodiversity in a forest of *Gongolaria abies-marina* at Salinetas in Gran Canaria Island.

Across the coasts of the Azores and Webbnesia oceanic archipelagos (eastern Atlantic), a range of local human activities have altered coastal habitats (Tuya et al. 2014; Ferrer-Valero et al. 2017; Bernal-Ibáñez et al. 2021b). At the same time, ocean warming has been attributed to have negative effects on brown seaweeds (Sansón et al. 2013; Geppi and Riera 2022), and the occurrence of MHWs has become more frequent and intense in recent decades (Bernal-Ibáñez et al. 2022). In the NE Atlantic coast, the decline and even disappearance of these species have been reported (Friedlander et al. 2017; Bernal-Ibáñez et al. 2021b; Martín-García et al. 2022), and several processes, such as herbivory by sea-urchins, human development, extreme wave events and MHWs have been pointed in this sense (Bernal-Ibáñez et al. 2021a, b; Martín-García et al. 2022). In the 1990s, regressions of *Gongolaria abies-marina* forests were recorded in the Canary Islands (Medina and Haroun 1994). In the 2000s, Rodríguez et al (2008) recorded great erosion of the populations of *Gongolaria abies-marina* throughout the Canary archipelago. Furthermore, in the 2010s, Martín-García et al (2022) recorded a 90% decline in *G. abies-marina* populations in the western islands (Tenerife, La Gomera, La Palma, and El Hierro). For this reason, this alga is included in the regional catalogue of endangered species (Canary Island Catalogue of

Protected Species; Law 4/2010, 4 June 2010). Recently, the alga was also included in the Spanish national catalogue of endangered species (TEC/596/2019, 8 April 2019).

Objectives

In recent decades, *Gongolaria abies-marina* forests have suffered a significant decline in many coastal areas of the Azores and Webbnesia archipelagos. The existence of historical records of this species in the Canary Islands makes it possible to evaluate temporal changes in its distribution and relate them to time series of local and global anthropogenic variables. In addition, there are few studies on the phenology and canopy structure of this species in the Canary Islands. For these reasons, and taking Gran Canaria Island as the study area, the main objectives of this thesis are:

1. To provide an up-to-date assessment of the current distribution and extent of *Gongolaria abies-marina* and facilitate a comparison with historical data, including populations from certain sites.
2. To link seasonal variation in environmental conditions with the frond structure and reproduction of this canopy-forming macroalga on the island of Gran Canaria through an annual cycle.
3. To evaluate the effects of a variety of environmental and anthropogenic stressors on the temporal distribution of marine forests created by *Gongolaria abies-marina* at an island scale.

CHAPTER 2. Massive decline of *Gongolaria abies-marina* forests in Gran Canaria Island (Canary Islands, eastern Atlantic)

SCIENTIA MARINA 81(4)
December 2017, 499-507, Barcelona (Spain)
ISSN-L: 0214-8358
doi: <http://dx.doi.org/10.3989/scimar.04655.23A>

Massive decline of *Cystoseira abies-marina* forests in Gran Canaria Island (Canary Islands, eastern Atlantic)

José Valdazo, M. Ascensión Viera-Rodríguez, Fernando Espino, Ricardo Haroun,
Fernando Tuya

Abstract

Brown macroalgae within the genus *Cystoseira* s.l. are some of the most relevant “ecosystem-engineers” found throughout the Mediterranean and the adjacent Atlantic coasts. *Cystoseira*-dominated assemblages are sensitive to anthropogenic pressures, and historical declines have been reported from some regions. In particular, *Gongolaria abies-marina*, thriving on shallow rocky shores, is a key species for the ecosystems of the Canary Islands. In this work, we analyse changes in the distribution and extension of *G. abies-marina* in the last decades on the island of Gran Canaria. This alga dominated the shallow rocky shores of the entire island in the 1980s; a continuous belt extended along 120.5 km of the coastline and occupied 928 ha. In the first decade of the 21st century, fragmented populations were found along 52.2 km of the coastline and occupied 12.6 ha. Today, this species is found along 37.8 km of the coastline and occupies only 7.4 ha, mainly as scattered patches. This regression has been drastic around the whole island, even in areas with low anthropogenic pressure; the magnitude of the decline over time and the intensity of local human impacts have not shown a significant correlation. This study highlights a real need to implement conservation and restoration policies for *G. abies-marina* in this region.

Keywords: marine forests; habitat-forming species; human pressures; Fucales; regression; Atlantic Ocean.

Introduction

Coastal ecosystems are suffering severe impacts worldwide due to excessive human pressure. Habitat destruction, pollution, eutrophication, species introduction, overfishing and global warming, which often act synergistically, are affecting species, ecosystems and their ability to provide ecosystem services (Halpern et al. 2008). For example, the Canary Islands are a “hot spot” of marine biodiversity in the North Atlantic (Sansón et al. 2001), which is threatened by human impacts, e.g., pollution, overfishing, occupation of the coast and progressive tropicalization (Riera et al. 2015).

Along rocky shores of temperate and subtropical areas, large canopy-forming brown algae, in particular kelps (Laminariales, Phaeophyceae, Ochrophyta) and fucoids (Fucales, Phaeophyceae, Ochrophyta), are the dominant species in pristine environments (Schiel and Foster 2006). These large perennial macroalgae are considered as “engineering species” (Jones et al. 1994), because their three-dimensional structure dramatically alters the physical, chemical and biological environment. These forests provide shelter, food, habitat and nurseries for a multiplicity of species (Cheminée et al. 2013). The decline of kelps and fucoids is a global phenomenon due, directly, or indirectly, to human mediated activities (Wernberg et al. 2011; Lamela-Silvarrey et al. 2012; Franco et al. 2015). Some species have even been driven to regional and local extinction (Thibaut et al. 2005; Franco et al. 2015; Thibaut et al. 2016a). The loss of these well-structured and diverse ecosystems facilitates the appearance of less complex habitats, such as filamentous algal turfs, ephemeral seaweed assemblages and barren grounds dominated by encrusting algae and sea urchins (Benedetti-Cecchi et al. 2001; Ling et al. 2015).

The genus *Cystoseira* s.l. is distributed in temperate and subtropical coasts around the world, although 80% of the species live in the Mediterranean Sea (Oliveras and Gómez 1989). In the Mediterranean and the adjacent Atlantic Ocean, species of the genus *Cystoseira* are the main group of habitat-forming macroalgae, from the littoral to the lower limit of the euphotic zone (Giaccone et al. 1994; García-Fernández and Bárbara 2016). Losses of *Cystoseira* forests have been reported all around the Mediterranean and attributed to habitat destruction, eutrophication and overgrazing by herbivores (Thibaut et al. 2005; Iveša et al. 2016, Blanfuné et al. 2016a). Due to their high sensitivity to anthropogenic impacts, several species of *Cystoseira* indicate high quality waters and facilitate the implementation of the EU Water Framework Directive (2000/06/EC) (Ballesteros et al. 2007; Blanfuné et al. 2016b, 2017). All the Mediterranean species of the genus *Cystoseira* s.l., except *C. compressa*, have been protected under the Annex II of the Barcelona Convention (2010). Five species, *Ericaria amentacea*, *Ericaria*

mediterranea, *Ericaria sedoides*, *Gongolaria montagnei* and *Ericaria zosteroides*, are protected under the Berne Convention (Annex I, 1979). In addition, all Mediterranean *Cystoseira* species are under surveillance by international organizations, such as IUCN, RAP/ASP and MedPan (Thibaut et al. 2014). All species of *Cystoseira* s.l. are “habitat forming” and are therefore considered EU habitats of interest (Micheli et al. 2013).

The brown alga *Gongolaria abies-marina* (S. G. Gemelin) Kuntze has been considered the most abundant furoid species on rocky shores of the Canarian Archipelago (Wildpret et al. 1987; Tuyá and Haroun 2006), and its populations typically form extensive stands in both the eulittoral and shallow sublittoral, mainly on rocky wave-exposed zones (Wildpret et al. 1987; Medina and Haroun 1993). *G. abies-marina* is a caespitose plant with large numbers of erect branches, up to 50 cm long. Similar to other species in the genera *Cystoseira* s.l., this species undergoes an annual thallus loss at the end of summer, when a high proportion of the fronds break down at the base. The holdfasts overwinter and regrow the next year. Therefore, although individuals are perennial, the thalli are annual (Buonomo et al. 2017). However, the plant never goes through a total rest phase: during unfavourable months, branches from different seasons coexist (González-Rodríguez and Afonso-Carrillo 1990). This alga spreads through both vegetative propagation and sexual reproduction (Medina 1997). Similar to other species of the genus, thalli are negatively buoyant, and propagules normally settle at <20-40 cm from the source population (Mangialajo et al. 2012), which gives the species a low dispersal ability (Bulleri et al. 2002). This is one of the most productive macroalgae in the Canary Islands (Johnston 1969), and at the end of summer, after the maximum reproductive peak, it is possible to find a large amount of wrack on beaches from nearby forests (Portillo-Hahnefeld 2008).

In the last few decades, *Gongolaria abies-marina* forests have declined significantly at certain points of the Canaries (Medina and Haroun 1993, Rodríguez et al. 2008). In order to analyse the long-term patterns in the distribution and extension of *G. abies-marina* along the entire coastal perimeter of the island of Gran Canaria, we collected all available data to reconstruct historical distributions. The aims were: (i) to provide an up-to-date assessment of the current distribution and extent of *C. abies-marina*, (ii) to facilitate a comparison with historical data, including populations from certain sites, and (iii) to evaluate the influence of local anthropogenic pressures, as drivers of regression.

Material and Methods

Study area

The island of Gran Canaria (28°51'N, 15°36'W) is located 200 km off the northwest African coast, in the middle of the Canary Islands (east Atlantic) (Fig. 1). The island has a circular shape of 256 km of coastal perimeter. Abrupt cliffs mostly dominate the north and west sides of the island, with coastal platforms and beaches predominating in the east and south. Although 76.02% of the coastal perimeter is rocky (Ramírez et al. 2008), rocky reefs only account for 17% of the shallow-water bottoms (up to 50 m). Gran Canaria is situated at the centre of a west-east oceanographic gradient along the Canarian archipelago, because of the varying proximity from the upwelling of the African coast (Tuya et al. 2006). The waters are typically oligotrophic, and the surface temperature varies between 18°C in March and 24°C in October.

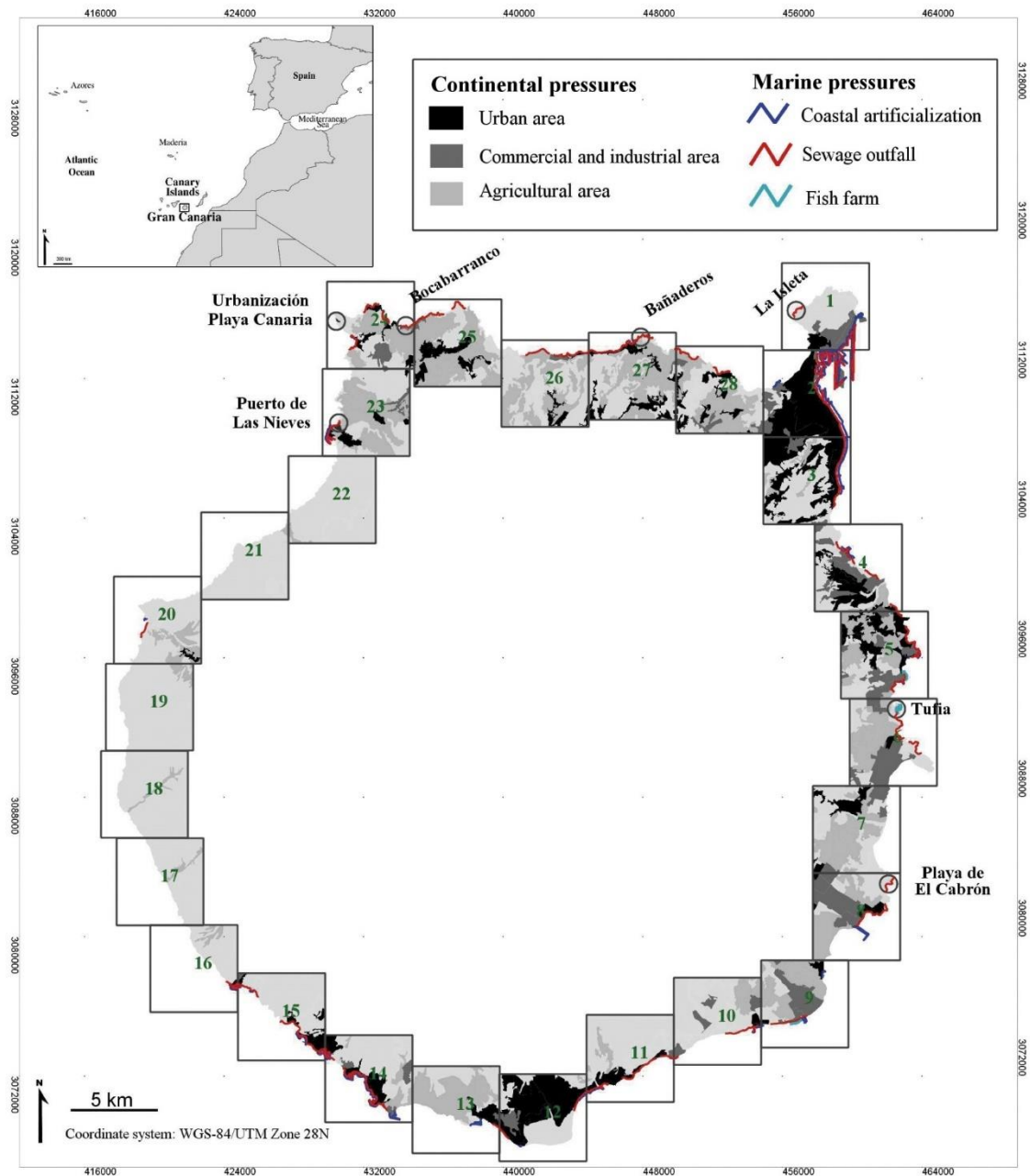


Fig.1. Map of Gran Canaria Island, including the 28 sectors (grids of 5x5 km) encompassing the entire coastal perimeter. The location of the seven analysed populations is also shown, with the circular area (500 m radius) where the HAPI index was calculated.

Mapping historical and current distribution: GIS analysis

Changes in the distribution (km of coastal perimeter) and extent (occupied area in ha) of *Cystoseira abies-marina* over time were analysed with the open-source GIS (gvSIG) and Sextante tools, using a 1:2500 scale and a WGS-84/UTM Zone 28N coordinate system.

Historical records concerning *Gongolaria abies-marina* distribution in the Canary Islands are scarce (Table 1). To reconstruct long-term patterns of change, we used unpublished reports from the late 1980s and 2000s, and oral scientific contributions. However, we did not take into account

herbarium vouchers. The first map dates back to 1985, when Wildpret et al. (1987) defined and mapped 15 types of vegetation between 0 and 10 m depth: 12 correspond to stands of macroalgae, two to seagrass meadows and one to a mixed community of seagrass and algae. Additionally, they mapped three ecosystems devoid of vegetation. We digitalized six of these types of vegetation, in which *G. abies-marina* was the principal floral component (Table S1, Fig. S1A). We used complementary sources to enlarge this map from the 1980s, focusing mainly on the eastern side of the island. Information provided by scientists and technicians, which was contrasted with historical orthophotos (Vuelos históricos: 1989-1991 Costas, Instituto Geográfico Nacional), supplied additional populations to those provided by Wildpret et al. (1987) (Table S1, Fig. S1B).

Table 1. Cartographic sources on the distribution of *Gongolaria abies-marina* in Gran Canaria Island.

1980s	1987	Wildpret et al. (1987)
	1989	Oral scientific communications
2000s	2008	Rodríguez et al. (2008)
2010s	2016	Current study

The first digitalized map of *Gongolaria abies-marina* was undertaken in 2008 by Rodríguez et al. (2008), who mapped the distribution of *G. abies-marina* according to three levels of abundance: as continuous belts, as discontinuous belts, and as isolated individuals (Fig 2B).

Field surveys were carried out between 2015 and 2016, during the maximum development of *Gongolaria abies-marina* (spring to autumn). The entire coast of Gran Canaria was explored on foot or by boat, and the shallow subtidal by snorkelling. Locally, populations were categorized, following Rodríguez et al. (2008), as C1, rare, scattered patches; C2, abundant patches; and C3, continuous belts. All the *G. abies-marina* populations were geo-localized and recorded on A4 format aerial photographs from the IGN (Instituto Geográfico Nacional, 1:2500 scale).

Comparison of populations: 2008 vs 2016

Rodríguez et al. (2008) studied seven populations (Fig. 1), providing the average coverage and belt width of *Gongolaria abies-marina* forests. In 2016, we repeated the study in the same locations, carrying out three transects (ca. 10 m apart), which covered the entire eulittoral and the shallow subtidal. Along each transect, the coverage (n=3) of *G. abies-marina* was obtained with a square (50×50 cm), divided into 25 sub-squares of 10×10 cm; the belt width was measured with a transect. We tested for differences in average coverage and belt width between 2008 and 2016 using a Wilcoxon test (i.e., all populations were pooled).

Human pressures as drivers of change

We assessed the Human Activities and Pressures Index (HAPI) (Blanfuné et al. 2017) on the coast of Gran Canaria. Five water bodies (WD) surround the island, according to the Water Framework Directive (WFD, 2000/60/EC). We divided these WD into 28 coastal sectors (grid cells of 5×5 km, Fig. 1) to identify more precisely the relationship between levels of anthropogenic pressures and the decline of *Gongolaria abies-marina* forests. For this study, we adapted the information available for the method of Blanfuné et al. (2017).

The HAPI index has three metrics to estimate both continental and marine pressures. For continental pressures (urban, industrial, and agricultural areas), the three metrics were expressed as the percentage of land area covered (data from Corine Land Cover 2012, available at centrodedescargas.cnig.es) within each coastal sector. For marine pressures, we estimated (i) the level of artificialization of the coast, expressed as the percentage of the artificialized coastline, (ii) fish farms, expressed as the percentage of rocky coastline potentially impacted (within a 500 m radius), and (iii) sewage outfalls, expressed as the percentage of rocky coastline potentially impacted (within a 500 m radius). This information was provided by the on-line GIS of the Canary Islands Autonomous Government (www.idecanarias.es). For each sector, we calculated the change in the extent of *C. abies-marina* between 1980s (i.e., Wildpret et al. 1987) and 2016 (i.e., this study). We applied a linear regression to test whether varying levels of human pressures explained the magnitude of changes in surface area over time at the island scale. Additionally, the HAPI index was calculated for each of the seven populations under study; we calculated the level of human pressures using a 500 m radius circular buffer from the centre of each population (Fig. 1), following a similar approach to that of Tuya et al. (2014).

Results

Distribution and extent

During the 1980s (Fig. 2A), *Gongolaria abies-marina* dominated the rocky coasts of Gran Canaria, along 120.5 km of coastal perimeter, covering 928 ha. It was abundant on most rocky substrates and the populations were mainly composed of continuous belts (Fig. 2A). Subtidal populations reached up to 9 m depth in many places of the north coast; in the east and southeast coast, stands reached up to 20 m depth in some places. The species was absent from the south and southwestern coast, mainly due to a lack of suitable hard substrates. At the start of the 21st century (Fig. 2B), populations were clearly fragmented, occupying 52.2 km of the coast (19.45% of the coastline) and covering 12.6 ha; this corresponds to a regression of 98.64% in 20 years.

Populations rarely get down into the subtidal, except in a few locations in the north and east, where populations go down to 8-10 m.

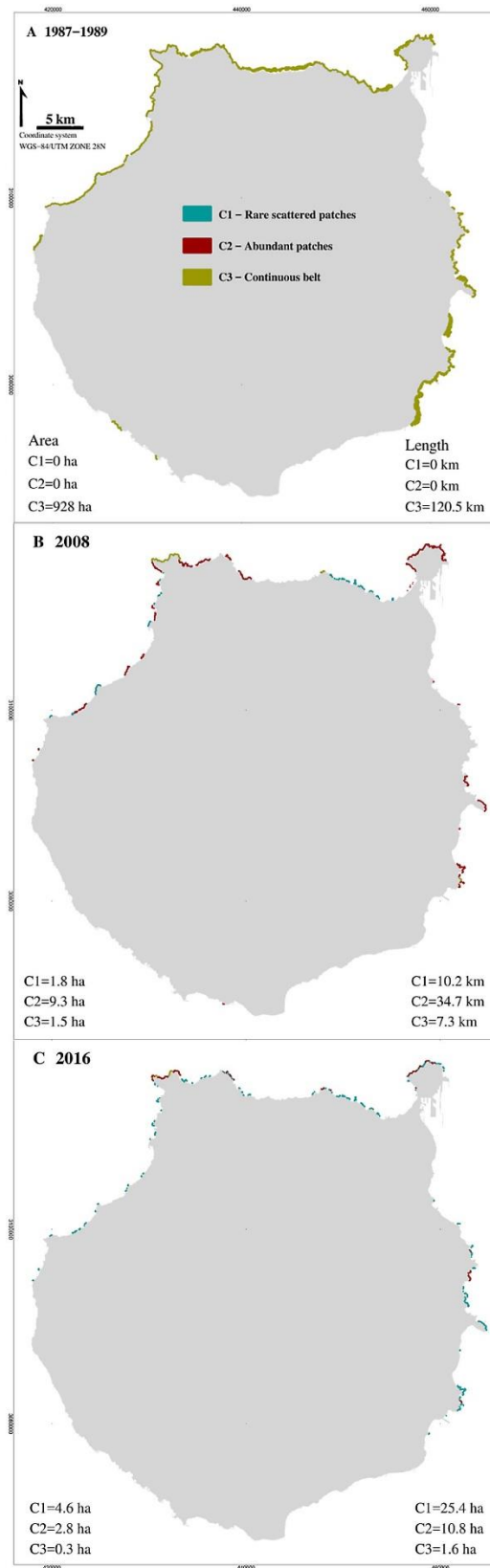


Fig 2. Distribution of *Gongolaria abies-marina* around Gran Canaria Island in the 1980s (A), 2008 (B) and 2016 (C). The area (ha) and length (km) of the three types of stands is included (C1, scattered patches; C2, abundant patches; C3, continuous belt).

Between 2014 and 2016, *G. abies-marina* was present along 37.8 km (14.08% of the coastline) and occupied an area of only 7.4 ha. Populations forming continuous belts have practically disappeared (0.3 ha). Fragmented populations are becoming more prominent and sublittoral populations have totally disappeared. As a result, *ca.* 99% of the area formerly covered by *C. abies-marina* has been lost in a few decades (Fig. 3).

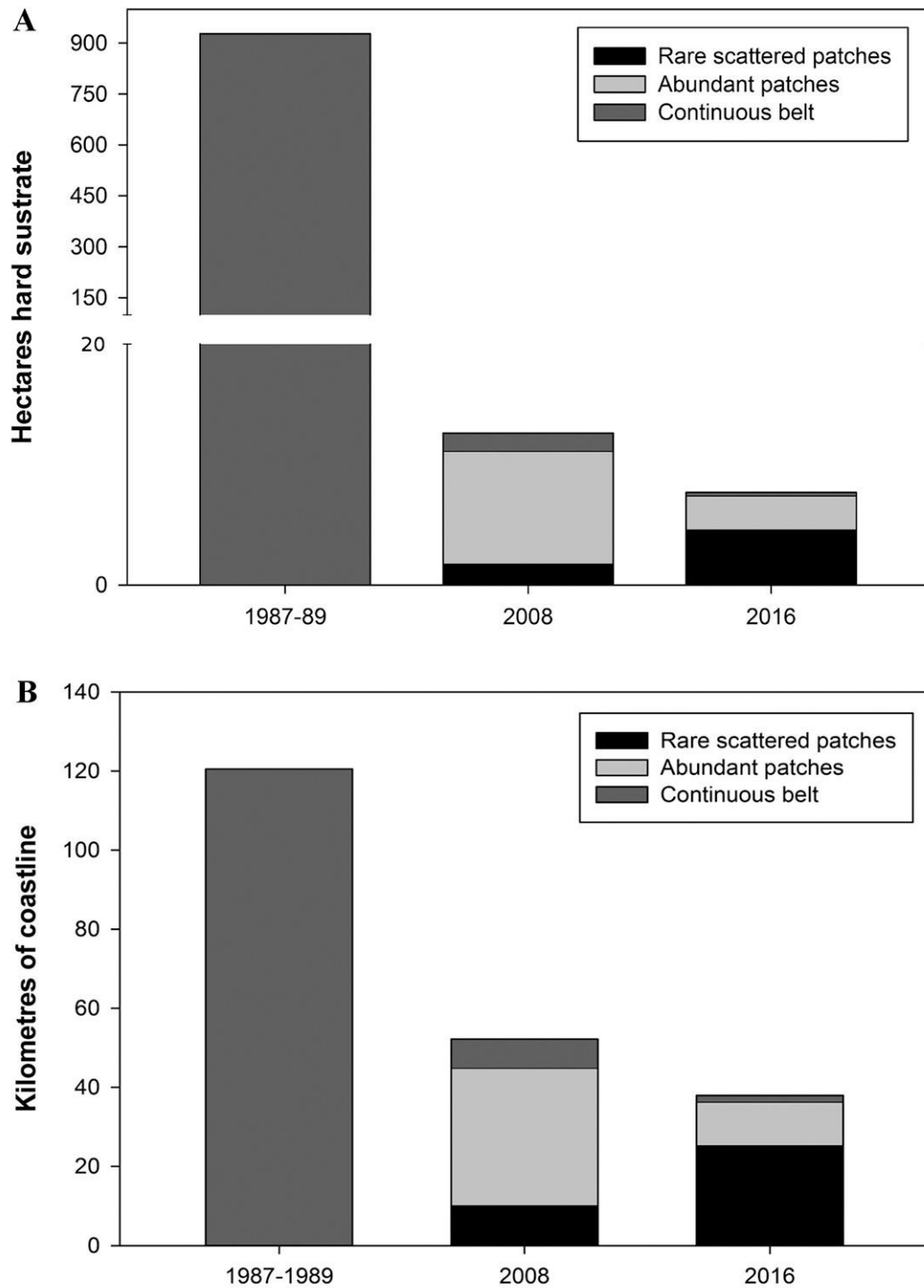


Fig 3. Temporal changes in the extent of *Gongolaria abies-marina*, in terms of the surface in hectares (A) and length in kilometres (B) of the coastline occupied at different times.

Comparison of populations: 2008 vs 2016

Overall, the seven *Gongolaria abies-marina* populations studied in 2016 have suffered a significant decline relative to 2008, in terms of coverage ($V = 231$, $P = 0.00006$, Fig. 4A) and belt width ($V = 231$, $P = 0.0000001$, Fig. 4B). In 2008, all populations had high cover (>50%) and

formed continuous belts; in some localities, belts extended to the subtidal down to 8-10 m depth.

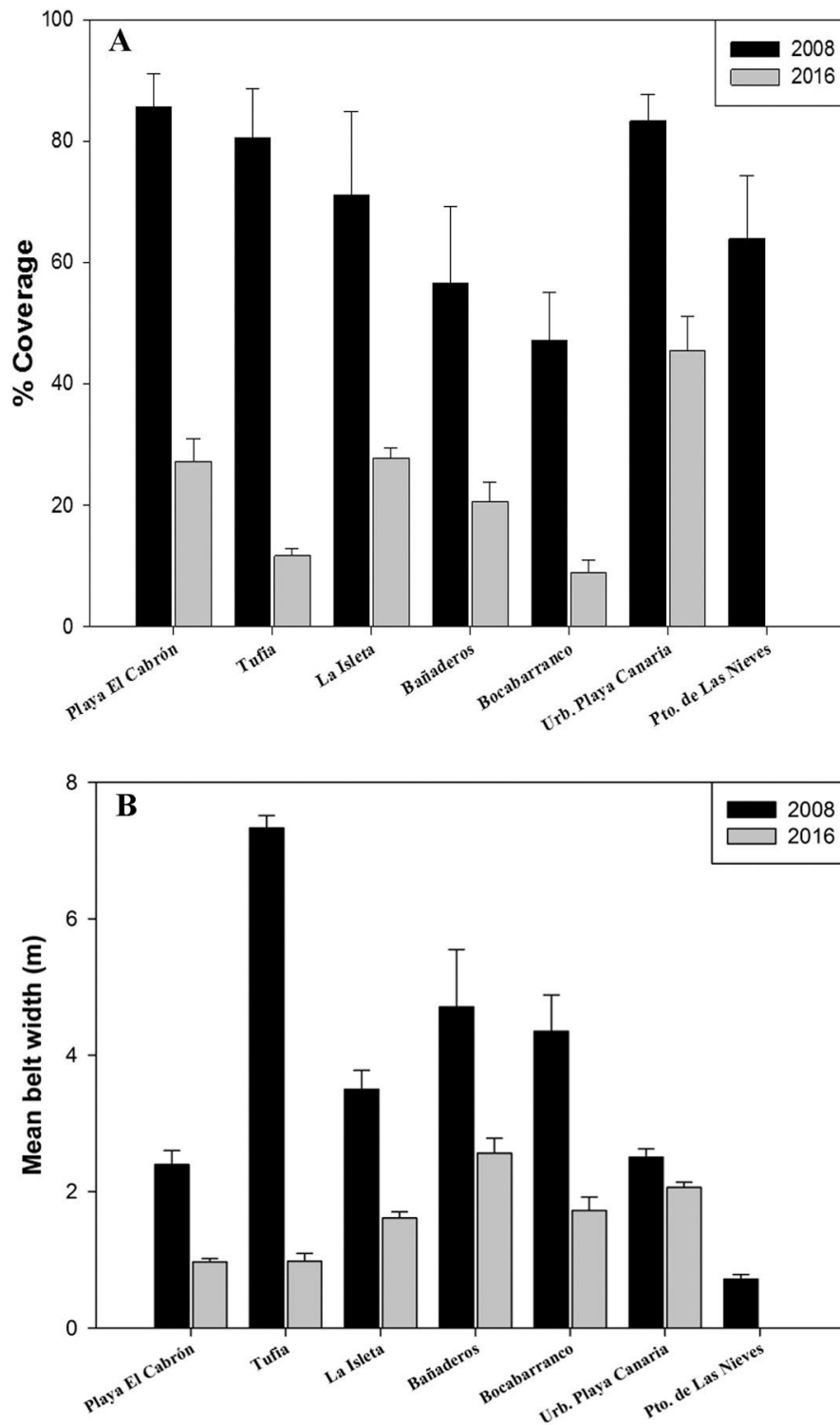


Fig. 4. Average coverage in percentage (A) and belt width in metres (B) of the seven populations of *Cystoseira abies-marina* in 2008 and 2016.

Human pressures as drivers of regression

Values of the HAPI index were calculated for the 28 coastal sectors and 7 populations of Gran Canaria Island (Tables 2 and 3; Table S3). There was no significant effect of varying levels of human pressures on temporal changes for either extent (1980s vs 2016; $R^2 = 0.048$, $F = 0.0423$, $df = 18$, $P = 0.839$) or coverage of *G. abies-marina* (2008 vs 2016; $R^2 = 0.53$, $F = 5.77$, $df = 5$, $P = 0.06$). In general, the magnitude of regression, in terms of both extent and coverage, has been high in all sectors and for all populations, even in areas with low or no human pressure.

Table 1. Values of the HAPI index, area covered and rate of temporal change of *Gongolaria abies-marina* in each of the 28 sectors along the coastal perimeter of Gran Canaria.

Sector	HAPI index	Area (ha)		% Change
		1980s	2016	
1	3.24	83.86	0.81	-99.03
2	5.48	31.72	0	-100
3	4.09	0	0	0
4	3.58	6.73	0.06	-99.11
5	4	30.51	1.75	-94.26
6	2.81	62.65	0.55	-99.12
7	0.83	77.07	0.075	-99.9
8	4.55	131.23	0.46	-99.65
9	4.85	118.9	0	-100
10	3.13	0	0	0
11	4.09	0	0	0
12	4.19	0	0	0
13	3.84	0	0	0
14	4.09	6.6	0	-100
15	4.44	5.66	0	-100
16	4.37	0	0	0
17	0.07	0	0	0
18	0.06	0	0	0
19	0.06	8.61	0.05	-99.42
20	1.8	12.39	0.12	-99.03
21	0.04	29.95	0.09	-99.7
22	0.04	16.53	0.07	-99.58
23	2.44	13.5	0.14	-98.97
24	1.93	42.85	1.5	-96.5
25	1.53	50.64	0.53	-98.96
26	1.42	95.03	0.06	-99.99
27	2.55	58.68	0.47	-99.2
28	1.52	45.04	1.01	-98.99

Table 3. Values of the HAPI index, coverage, and rate of temporal change for each of the seven studied *Gongolaria abies-marina* populations.

	HAPI index	% Coverage		% Change
		2008	2016	
Playa de El Cabrón	1.66	85.56	27.22	-68.19
Tufia	1.88	80.56	11.66	-85.53
La Isleta	1.2	71.11	27.77	-60.95
Bañaderos	2.51	56.67	20.55	-63.74
Bocabarranco	2.19	47.22	8.88	-81.19
Urbanización Playa Canaria	0.11	83.33	45.55	-45.34
Puerto de Las Nieves	2.32	63.89	0	-100.00

Discussion

Changes in the distribution and extent of *Gongolaria abies-marina* on the island of Gran Canaria over the last few decades are evident and dramatic. In the late 1980s, *G. abies-marina* occupied 928 ha (12.84% of the rocky bottoms) and now it only covers 7.4 ha (0.1%). Existing *G. abies-marina* populations have been reduced to narrow belts in the lower eulittoral, i.e., as scattered patches with underdeveloped branches. Our results are in agreement with those found for other *Cystoseira* s.l. species from the Mediterranean Sea (Thibaut et al. 2005, Mangialajo et al. 2008, Sales et al. 2011), for other furoids from the Canary Islands (Rodríguez et al. 2008, Riera et al. 2015) and, in general, for habitat-forming brown algae worldwide (Wahl et al. 2015). Our data show a similar trend to that observed for *Ericaria brachycarpa* (J. Agardh) Molinari & Guiri, a species having the same depth range and ecological function as *G. abies-marina*, including a massive decline from the sublittoral to a narrow fringe immediately below the surface (Thibaut et al. 2015, 2016b).

It is plausible that the area occupied by *Gongolaria abies-marina* in the 1980s is not entirely accurate, because of the lack of technical procedures to accurately trace communities at this time. The map of Wildpret et al. (1987) only reached 10 m depth, so they may even have underestimated the area occupied by *G. abies-marina*. Even assuming these inaccuracies, the regression of *G. abies-marina* is acute, because all sublittoral populations have been lost.

In our study, we found no direct relationship between local levels of anthropogenic pressures and the magnitude of local regression; the decay has been dramatic from almost pristine environments to highly altered coasts. This result contrasts with the disappearance of some *Cystoseira* s.l. species only from highly artificialized areas (harbours, marinas, piers, etc.) and waters severely polluted in the Mediterranean (Thibaut et al. 2014, 2015; Iveša et al. 2016). However, a similar decline has been observed in the pristine environments of the National Park

of Port-Cros in France (Thibaut et al. 2016b). In a similar study, the temporal decay in the vitality of the seagrass *Cymodocea nodosa* (Ucria) Ascherson in Gran Canaria related to an increase in local anthropogenic impacts (Tuya et al. 2014).

The decline of *G. abies-marina* in Gran Canaria has occurred in a period of pronounced urban and tourism development and, therefore, of many local impacts (Tuya et al. 2014; Ferrer-Valero et al. 2017). Today, the population, urbanization and infrastructure are heavily concentrated on the coast of the island, particularly in the northeast, east and south (Fig. 1). Gran Canaria currently has 847830 inhabitants and a very high population density (543 inhabitants km⁻²) (ISTAC 2015); 87% of the population is located along the littoral perimeter, giving a coastal population density of 3142 ind km⁻¹. In addition, about 2 million tourists visit the island every year (e.g., 1805058 tourists in 2015, ISTAC 2015). This has led to the occupation and degradation of most coastal areas (Ferrer-Valero et al. 2017). Importantly, however, populations of *G. abies-marina* in poorly impacted areas have also suffered significant regressions. Hence, it remains elusive to unravel the reasons for the loss of *G. abies-marina*.

The possible causes of the decline may be multiple and cumulative, as happens around the world (Thibaut et al. 2005; Wahl et al. 2015; Franco et al. 2015). Potentially, both local and global stressors are interacting to explain the severe regression of *Gongolaria abies-marina* in Gran Canaria, as is the case with the disappearance of other fucooids from the study region (Riera et al. 2015). In the Canary Islands, sea surface temperature has increased about 1°C in recent decades (Lima and Wethey 2012; Riera et al. 2015). Global warming is a key factor in the ongoing decline of fucooids and their displacement to colder waters (Wernberg et al. 2011). There is recent regional evidence of the adverse effect of warming on species of both brown and red macroalgae (Sansón et al. 2013). The decrease in the size of thalli of these seaweeds, and in their reproductive success (Zhang et al. 2009), have also been correlated with the warming of the Canarian waters (Sansón et al. 2013; Riera et al. 2015). Furthermore, *Cystoseira* s.l. are low-dispersal species whose propagules do not have a planktonic stage, and reproductive drifting thalli in floating rafts are the main mechanism of connectivity between populations (Susini et al. 2007). Therefore, if connectivity is limited, the subsequent smaller population gene pools and sizes render populations more vulnerable to threats (Buonomo et al. 2017).

The regime shifts from marine forests to barren grounds devoid of erect macroalgae is generally linked to overexploitation of predatory fishes (Ling et al. 2015; Thibaut et al. 2015, 2016a). In the Canary Islands, the long-spined sea urchin *Diadema africanum* Rodríguez, Hernández, Clemente & Coppard, 2013 controls the transition from rocky bottoms dominated by erect macroalgae to

barren grounds (Tuya et al. 2004; Sangil et al. 2014). This sea urchin may consume thalli of *G. abies-marina* at rates of 1-2 mg of algae per day and individual (Tuya et al. 2001). In addition, it is plausible that the sea urchin *Paracentrotus lividus* (Lamarck, 1816) and herbivorous fishes (*Sparisoma cretense*, *Sarpa salpa* and *Diplodus* spp.) can contribute to the consumption of *G. abies-marina*, as in the Mediterranean for other *Cystoseira* s.l. species (Verges et al. 2009).

This study highlights the urgent need to monitor remaining *Gongolaria abies-marina* populations of the Canary Islands and compare this data with other Macaronesian islands. It is also necessary to promote urgent actions to conserve current populations, including restoration programmes. Currently, *G. abies-marina* is regionally protected within the framework of the Canary Islands Catalogue of Protected Species (Law 4/2010, of 4 June 2010). This highlights the uselessness of legislation if it is not enforced. Furthermore, in the last update of this catalogue, the species lost the category of “vulnerable”: it now belongs to a recently created category called “species of interest for the Canarian ecosystems”, which only protects the species within zones of the Natura 2000 network. Our results clearly do not support this legislative change.

Cystoseira abies-marina has not yet been assessed for the IUCN Red List, i.e., it is “Not Evaluated” (IUCN 2017), nor is species included in the Catalogue of Life (Roskov et al. 2016). We are aware that *G. abies-marina* is undergoing a very important decline throughout the Canaries (Rodríguez et al. 2008) and on Madeira and the Azores (Ballesteros pers. com.), but more data are needed to verify the magnitude of this decline. Nevertheless, with current data and evidence of the regional decline, we propose that *G. abies-marina* should be classified as “Critically Endangered” under the IUCN criteria CR A2ac. There are only very few algal species in the world whose conservation status has been properly assessed (Blanfuné et al. 2016a), due to lack of historical data. Information provided here could be used as a basis for improving the evaluation of the conservation status of *G. abies-marina*, an ecologically important species.

Supplementary material

Fig. S1. *Gongolaria abies-marina* communities in the 1980s, including those from Wildpret et al. (1987) (A) and from oral scientific communications (B).

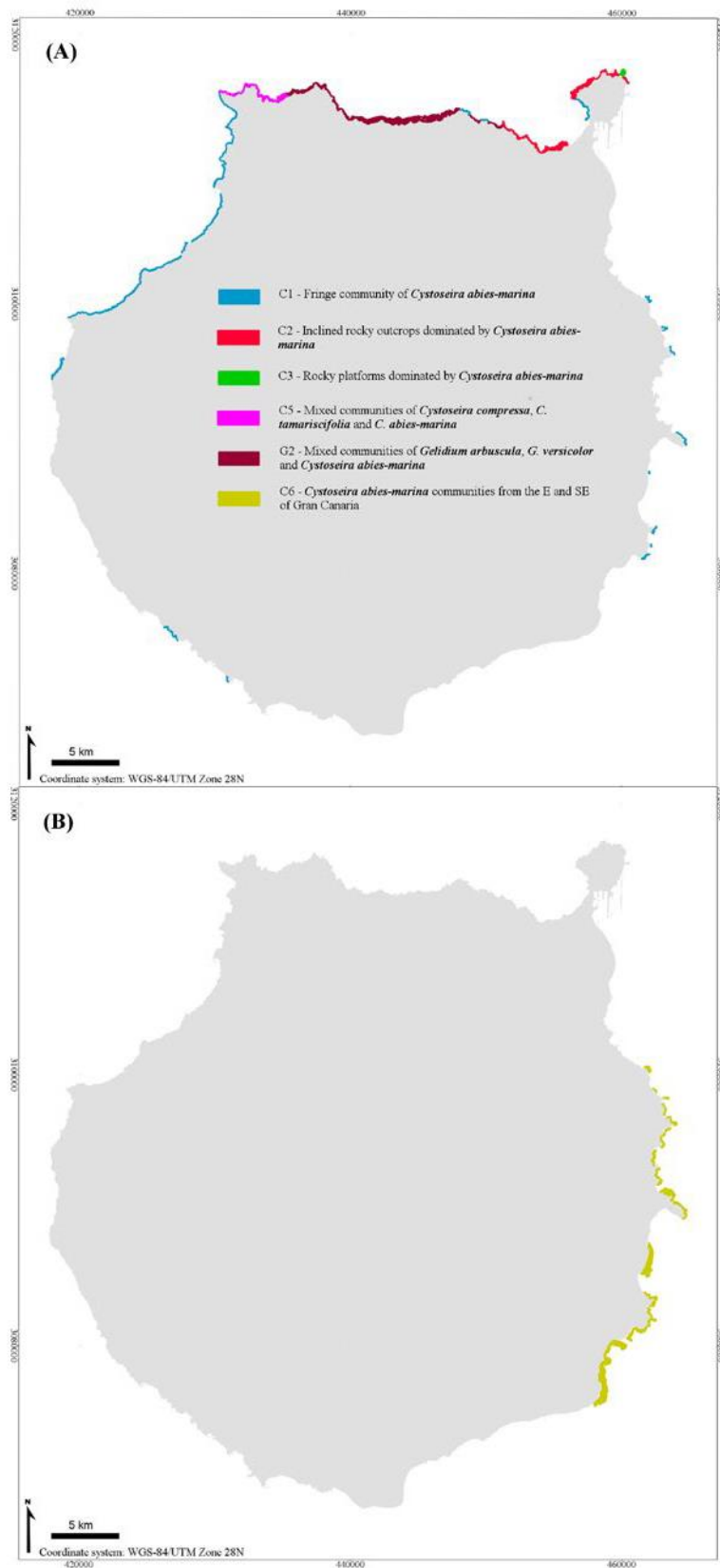


Table S1. Types of human pressures, Corine Land Cover (CLC) codes, area and length percentages, and corresponding scores used in calculations of the HAPI index in coastal sectors and populations of Gran Canaria Island.

Types of pressure	CLC code	Area percentage (%)	Score
Continental pressures			
		0-10	1
Urban area	11, 14	11-35	2
		36-75	3
		>75	4
		0-10	1
Industrial area	12, 13	11-25	2
		26-75	3
		>75	4
		0-5	1
Agricultural area	21-24	6-25	2
		16-30	3
		<30	4
		Marine pressures	
		Length percentage (%)	
Coastal artificialization		0-5	1
		6-25	2
		26-75	3
		>75	4
Sewage outfall		0-5	1
		6-25	2
		26-75	3
		>75	4
Offshore fish farm		0-1	1
		2-15	2
		16-40	3
		>40	4

Table S2. *Cystoseira abies-marina*: historical sources (1980s).

Name	Type	Substrate	Slope (%)	Depth (m)	Cover/Abundant	Source
Fringe community of <i>Cystoseira abies-marina</i>	C1	Rocky	80-100	0-3	Continuous belt	Wildpret et al. 1987
Sloping rocky outcrops dominated by <i>Cystoseira abies-marina</i>	C2	Rocky	50-80	0-9	Continuous belt	Wildpret et al. 1987
Rocky platforms dominated by <i>Cystoseira abies-marina</i>	C3	Rocky	0-50	3-9	Continuous belt	Wildpret et al. 1987
Rocky platform mixed communities	C4	Rocky	0-50	3-9	Continuous belt	Wildpret et al. 1987
Mixed communities of <i>Cystoseira compressa</i> , <i>C. tamariscifolia</i> and <i>C. abies-marina</i>	C5	Rocky	0-100	0-9 3-9	Continuous belt	Wildpret et al. 1987
Mixed communities of <i>Gelidium arbuscula</i> , <i>G. versicolor</i> and <i>Cystoseira abies-marina</i>	G2	Rocky	70-100	0-9 3-9	Continuous belt	Wildpret et al. 1987
<i>Cystoseira abies-marina</i> communities from the E and SE of Gran Canaria	C6	Rocky	0-50	0-20	Continuous belt	Oral scientific communications

Table S3. Percentages of the area and length of each sector according to human pressure. Pressure scores (PS) assigned to each pressure are indicated. Correlation coefficients (R2) between pressures, turnover score (TS) and the HAPI index ($HAPI_j = \sum(P_i \times r_i) / TS_j$) were calculated according to Blanfuné et al. 2017.

Sector	Pressure	% Area	%Length	PS	R ²	TS	HAPI
1	Urban area	9.35		1	0.14	1.33	3.24
	Industrial area	27.91		3	0.31		
	Agricultural area	0		0	0.06		
	Coastal artificialization		44.74	3	0.68		
	Sewage outfall		43.46	3	0.4		
	Fish farm		0	0	0.15		
2	Urban area	72.15		3	0.14	1	5.48
	Industrial area	21.01		2	0.31		
	Agricultural area	0.04		2	0.06		
	Coastal artificialization			4	0.68		
	Sewage outfall			4	0.4		
	Fish farm			0	0.15		
3	Urban area	28.02		3	0.14	1	4.09
	Industrial area	24.93		1	0.31		
	Agricultural area	6.77		2	0.06		
	Coastal artificialization		19.07	3	0.69		
	Sewage outfall		49.29	3	0.4		
	Fish farm		0	0	0.15		
4	Urban area	25.03		2	0.14	1	3.58
	Industrial area	18.75		2	0.31		
	Agricultural area	34.54		2	0.06		
	Coastal artificialization		21.46	2	0.68		
	Sewage outfall		67.63	3	0.4		
	Fish farm		6.77	0	0.15		
5	Urban area	25.03		2	0.14	1	4
	Industrial area	18.75		2	0.31		
	Agricultural area	34.54		4	0.06		
	Coastal artificialization		21.46	2	0.68		
	Sewage outfall		67.63	2	0.4		
	Fish farm		6.77	2	0.15		
6	Urban area	2.1		1	0.14	1	2.81
	Industrial area	28.07		3	0.31		
	Agricultural area	41.16		4	0.06		
	Coastal artificialization		0	0	0.68		
	Sewage outfall		34.56	3	0.4		
	Fish farm		7.09	2	0.15		
7	Urban area	10.31		2	0.14	1	0.83
	Industrial area	7.59		1	0.31		
	Agricultural area	40.97		4	0.06		
	Coastal artificialization		0	0	0.68		
	Sewage outfall		0	0	0.4		
	Fish farm		0	0	0.15		
8	Urban area	6.71		1	0.14	1	4.55
	Industrial area	32.66		3	0.31		
	Agricultural area	31.55		4	0.06		
	Coastal artificialization		36.18	3	0.68		
	Sewage outfall		47.43	3	0.4		
	Fish farm		0	0	0.15		
9	Urban area	4.4		1	0.14	1	4.85
	Industrial area	28.19		3	0.31		
	Agricultural area	50.86		4	0.06		

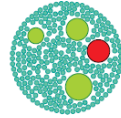
Sector	Pressure	% Area	%Length	PS	R ²	TS	HAPI
	Coastal artificialization		34.83	3	0.68		
	Sewage outfall		32.88	3	0.4		
	Fish farm		13.57	2	0.15		
10	Urban area	2.02		1	0.14	1	3.13
	Industrial area	9.11		1	0.31		
	Agricultural area	12.61		2	0.06		
	Coastal artificialization		20.79	2	0.068		
	Sewage outfall		48.75	3	0.4		
	Fish farm		0	0	0.15		
11	Urban area	11.13		2	0.14	0.8	4.09
	Industrial area	0.84		1	0.31		
	Agricultural area	6.78		2	0.06		
	Coastal artificialization		20.17	2	0.68		
	Sewage outfall		68.83	3	0.4		
	Fish farm		0	0	0.15		
12	Urban area	59.95		3	0.14	0.8	4.19
	Industrial area	4.9		1	0.31		
	Agricultural area	0.93		1	0.06		
	Coastal artificialization		12.06	2	0.68		
	Sewage outfall		29.12	3	0.4		
	Fish farm		0	0	0.15		
13	Urban area	8.28		1	0.14	0.8	3.83
	Industrial area	0.75		1	0.31		
	Agricultural area	58.21		3	0.06		
	Coastal artificialization		32.74	3	0.68		
	Sewage outfall		5.87	1	0.4		
	Fish farm		0	0	0.15		
14	Urban area	17.86		2	0.14	0.8	4.09
	Industrial area	7.29		1	0.31		
	Agricultural area	10.72		2	0.06		
	Coastal artificialization		14.05	2	0.68		
	Sewage outfall		71.96	3	0.4		
	Fish farm		0	0	0.15		
15	Urban area	12.97		2	0.14	0.8	4.44
	Industrial area	0.6		1	0.31		
	Agricultural area	0		0	0.06		
	Coastal artificialization		23	2	0.68		
	Sewage outfall		75.59	4	0.4		
	Fish farm		0	0	0.15		
16	Urban area	1.72		1	0.14	0.8	4.37
	Industrial area	0		0	0.31		
	Agricultural area	11.71		2	0.06		
	Coastal artificialization		29.74	3	0.68		
	Sewage outfall		33.16	3	0.4		
	Fish farm		0	0	0.15		
17	Urban area	0		0	0.14	0.8	0.075
	Industrial area	0		0	0.31		
	Agricultural area	5.67		1	0.06		
	Coastal artificialization		0	0	0.68		
	Sewage outfall		0	0	0.4		
	Fish farm		0	0	0.15		
18	Urban area	0		0	0.14	1	0.06
	Industrial area	0		0	0.31		
	Agricultural area	4.3		1	0.06		
	Coastal artificialization		0	0	0.68		

Sector	Pressure	% Area	%Length	PS	R ²	TS	HAPI
	Sewage outfall		0	0	0.4		
	Fish farm		0	0	0.15		
19	Urban area	0		0	0.14	1	0.06
	Industrial area	0		0	0.31		
	Agricultural area	4.37		1	0.06		
	Coastal artificialization		0	0	0.68		
	Sewage outfall		0	0	0.4		
	Fish farm		0	0	0.15		
20	Urban area	2.34		1	0.14	1	1.8
	Industrial area	0		0	0.31		
	Agricultural area	22.39		3	0.06		
	Coastal artificialization		3.56	1	0.68		
	Sewage outfall		11.13	2	0.4		
	Fish farm		0	0	0.15		
21	Urban area	0		0	0.14	1.33	0.045
	Industrial area	0		0	0.31		
	Agricultural area	1.17		1	0.06		
	Coastal artificialization		0	0	0.68		
	Sewage outfall		0	0	0.4		
	Fish farm		0	0	0.15		
22	Urban area	0		0	0.14	1.33	0.044
	Industrial area	0		0	0.31		
	Agricultural area	2.07		1	0.06		
	Coastal artificialization		0	0	0.68		
	Sewage outfall		0	0	0.4		
	Fish farm		0	0	0.15		
23	Urban area	7.1		1	0.14	1.33	2.44
	Industrial area	3.16		1	0.31		
	Agricultural area	47.59		4	0.06		
	Coastal artificialization		0	0	0.68		
	Sewage outfall		0	0	0.4		
	Fish farm		0	0	0.15		
24	Urban area	10.44		1	0.14	1.33	1.93
	Industrial area	10.71		1	0.31		
	Agricultural area	41.45		4	0.06		
	Coastal artificialization		4.15	1	0.68		
	Sewage outfall		41.74	3	0.4		
	Fish farm		0	0	0.15		
25	Urban area	14.98		2	0.14	1.33	1.53
	Industrial area	0.84		1	0.31		
	Agricultural area	59.7		4	0.06		
	Coastal artificialization		0	0	0.68		
	Sewage outfall		45.91	3	0.4		
	Fish farm		0	0	0.15		
26	Urban area	5.33		1	0.14	1.33	1.42
	Industrial area	1.22		1	0.31		
	Agricultural area	39.31		4	0.06		
	Coastal artificialization		0	0	0.68		
	Sewage outfall		62.18	3	0.4		
	Fish farm		0	0	0.15		
27	Urban area	14.55		2	0.14	1.33	2.55
	Industrial area	0.48		1	0.31		
	Agricultural area	45.37		4	0.06		
	Coastal artificialization		9.99	2	0.68		
	Sewage outfall		67.61	3	0.4		

Sector	Pressure	% Area	%Length	PS	R ²	TS	HAPI
	Fish farm		0	0	0.15		
28	Urban area	13.44		2	0.14	1.33	1.52
	Industrial area	5.98		1	0.31		
	Agricultural area	41.59		4	0.06		
	Coastal artificialization		0	0	0.68		
	Sewage outfall		42.19	3	0.4		
	Fish farm		0	0	0.15		

CHAPTER 3. Seasonality in the canopy structure of the endangered brown macroalga *Gongolaria abies-marina* at Gran Canaria Island (Canary Islands, eastern Atlantic).

EUROPEAN JOURNAL OF PHYCOLOGY, 2019
<https://doi.org/10.1080/09670262.2019.1696989>






British
Phycological
Society
Understanding and using algae



Taylor & Francis
Taylor & Francis Group



Seasonality in the canopy structure of the endangered brown macroalga *Cystoseira abies-marina* at Gran Canaria Island (Canary Islands, eastern Atlantic)

José Valdazo ^{a,b}, María Ascensión Viera-Rodríguez ^c and Fernando Tuya ^a

^aGrupo en Biodiversidad y Conservación, IU-ECOQUA, Universidad de Las Palmas de Gran Canaria, Las Palmas de GC, Canary Islands, Spain; ^belitoral, Parque Científico-Tecnológico de Tafira, Universidad de Las Palmas de Gran Canaria, Las Palmas, Canary Island, Spain; ^cGrupo de Ecofisiología de Organismos Marinos, IU-ECOQUA, Universidad de Las Palmas de Gran Canaria, Las Palmas de GC, Canary Islands, Spain

Abstract

Gongolaria abies-marina is a canopy-forming brown seaweed distributed along the western Mediterranean and the adjacent Atlantic coasts, which has suffered massive declines in recent decades, particularly in the Canary Islands. Here, we describe seasonal variation in the canopy structure of this alga, addressing the role of environmental drivers. Four sites around the island of Gran Canaria were investigated monthly during an entire annual cycle. Annually, the non-fertile stage made up the majority of populations, in terms of frond density, while the fertile stage was comparatively sparser. This fertile stage, however, had the largest biomass and reached the longest lengths, showing significant seasonality. Best fitted GAM models included wave action, PAR and seawater temperature, but only accounted for a moderate variation in the seasonal frond structure of this alga. Total frond biomass, mostly fertile fronds, showed a bimodal pattern, with a peak in spring and a less accentuated peak in late summer–early autumn. This pattern was particularly obvious at sites with a wide annual variation in wave action, with lower biomass at times of high wave action. The frond size-structure was dominated, at all sites and times, by small fronds. The high frond density seems to promote intraspecific facilitation throughout the year. These results provide fundamental knowledge to improve the conservation and potential restoration actions for endangered populations of this alga.

Keywords: Canopy-forming seaweed; conservation; environmental drivers; frond structure; intraspecific interactions; production; phenology.

Introduction

Marine forests of large brown macroalgae, mostly belonging to the orders Fucales and Laminariales, are unique habitats which support a great variety of organisms in coastal zones worldwide and are comparable to terrestrial forests for the services they provide (Steneck et al. 2002). These canopy-forming macroalgae are very important primary producers (Mann 1973) and increase the structural complexity where they live, providing shelter and food for associated species (Schiel and Foster 2006; Cheminée et al. 2013), and increasing biodiversity (Chapman 1995; Steneck et al. 2002; Piazzi et al. 2018). Thus, the conservation of these habitat-forming species is a crucial goal for ecologists and environmental managers. To achieve this, a better understanding of the structure and dynamics of canopies of algal forests in relation to environmental drivers and intraspecific interactions is crucial (Schiel and Foster 2006; Bennett and Wernberg 2014; Smale et al. 2016).

Subtidal and intertidal algal forests experience large variations in their distribution, abundance and fitness at a range of spatial and temporal scales (Martínez et al. 2012; Ferreira et al. 2014; Yesson et al. 2015). Their structure and extent are influenced by a variety of environmental variables, including temperature (Tuya et al. 2012), light availability (Creed et al. 1998), nutrients (Piazzi and Ceccherelli, 2017) and wave intensity (Engelen et al. 2005). Ecological processes, such as intraspecific and interspecific competition and facilitation, can also affect their structure and functioning (Bennett and Wernberg, 2014). Although macroalgae are important habitat-formers in temperate and subtropical rocky ecosystems, there are still few studies on their frond structure, particularly in terms of their temporal dynamics (Åberg 1992; Schiel and Foster, 2006).

Seasonal changes in photoperiod are important initiating the growth of macroalgae after the winter dormancy period. Likewise, an increase in water temperature is related to the beginning of growth and reproduction (Graiff et al. 2015; de Bettignies et al. 2018). Normally, in temperate seas, there is a mismatch between the period of maximum macroalgal growth and the concentration of nutrients in the water (Ballesteros 1988; Delgado et al. 1994). For example, Laminariales build up reserves of nitrogen (N) which are used to initiate growth in early spring, when light levels increase (Chapman and Craigie 1977; Nielsen et al. 2014). Many *Cystoseira* s.l. species can store reserves in their tophules, storage structures situated on the base of the branches (García-Fernández and Bárbara, 2016), although some species such as *Gongolaria abies-marina* lack tophules or alternative structures to store reserves (González and Afonso-Carrillo 1990). Wave action is one of the primary factors affecting canopy structure and dynamics

(Engelen et al. 2005; Kregting et al. 2016), including local adaptation to hydrodynamic forces (de Bettignies et al. 2015).

Subtidal and intertidal temperate reefs are characterized by a dense cover of perennial algal canopies (Schiel and Foster 2006), which promote positive interactions through physical stress amelioration (Bennett and Wernberg 2014). However, competition due to resource availability (light, nutrients, etc) can arise when living at high densities (Santelices 2004; Scrosati 2005). Both interactions can modulate frond dynamics, and consequently the size structure may exhibit seasonal variations. The shade effects on small individuals (or fronds) by large individuals, particularly in peak growth season, may limit their success due to low light, resource availability and wave action (Santelices 2004; Rivera and Scrosati 2008). The opposite effect can also occur, i.e., high-density canopies can favour the recruitment and survival of the smallest individuals in harsh environments, by buffering them against high radiation, temperature, desiccation and salinity (Bulleri 2009; Bennett and Wernberg 2014). In the Mediterranean Sea and the adjacent eastern Atlantic, brown algae of the genus *Cystoseira* s.l. are among the more important canopy-forming species (Giaccone et al. 1994; García-Fernández and Bárbara, 2016). *Cystoseira* species occur from the intertidal down to the lower limit of the euphotic zone (García-Fernández and Bárbara 2016). Losses of *Cystoseira* s.l. assemblages have been reported all around the Mediterranean and the Canary Islands, attributed to habitat destruction, eutrophication and overgrazing by herbivores (Thibaut et al. 2005; Blanfuné et al. 2016; Iveša et al. 2016; Valdazo et al. 2017).

Gongolaria abies-marina (S. G. Gmelin) Kuntze is a habitat-forming species, living in shallow waters (0–20m depth), particularly in places with high wave action and solar radiation. This alga is distributed throughout the Macaronesian region and reports from Morocco and Senegal require confirmation. In the Mediterranean Sea *G. abies-marina* is restricted to the western zone, where populations are reduced (González and Afonso-Carrillo 1990; Ribera et al. 1992). In the Canary Archipelago, it used to be the most abundant and productive furoid species (Johnston 1969), typically forming extensive stands in the lower intertidal to shallow subtidal zone of moderately exposed and exposed rocky reefs (Wildpret et al. 1987; Medina 1997). Morphologically, *G. abies-marina* is an atypical member of the genus (Gil-Rodríguez 1978). With no conspicuous holdfast and no stipe, *G. abies-marina* is a caespitose macroalgae, attached to the substratum by small discoid haptera. The base is sympodial, formed by a creeping axis from which multiple primary axes grow, often at points opposing the attachment structures. Branches can reach 50 cm in length and are replaced annually, while the creeping axis is perennial (Gil-Rodríguez 1978; González and Afonso-Carrillo 1990). During the reproductive season,

receptacles (reproductive structures) develop from secondary and tertiary thorny branches, which can reach 10 cm in length, sprouting from the apical part of branches (González and Afonso-Carrillo 1990). In previous studies, populations of *G. abies-marina* have shown seasonal patterns of growth and reproduction, with peaks of biomass in spring and summer and a period of dormancy in autumn and winter (González and Afonso-Carrillo 1990; Medina 1997). Although many fronds are lost after the reproductive peak, the thalli never go through a total rest phase, because branches from different seasons coexist (González and Afonso-Carrillo, 1990). This alga spreads through both vegetative (clonal) propagation and sexual reproduction (Medina 1997). Similar to other species of the genus, thalli are negatively buoyant, and zygotes are heavy and tend to sink close to the parents (Guern 1962), which gives the species/genus a low dispersal ability (< 20 cm; Mangialajo et al. 2012).

In the 1990s, regressions of *G. abies-marina* forests were recorded in the Canary Islands (Medina and Haroun 1994). Recent mapping of the distribution of *G. abies-marina* populations from Gran Canaria has shown a huge regression, despite a lack of consensus on the reason for such declines (Valdazo et al. 2017). For this reason, this alga is included in the regional catalogue of endangered species (Canary Island Catalogue of Protected Species; Law 4/2010, 4 June 2010). Recently, the alga was also included in the Spanish national catalogue of endangered species (TEC/596/2019, 8 April 2019).

Identifying relevant environmental drivers affecting the structure of canopies of *G. abies-marina* is, therefore, of interest to quantify the ecosystem functions and services they provide (e.g., primary production and nurseries). In this study, we explicitly linked seasonal variation in environmental conditions with the frond structure and reproduction of this canopy-forming macroalga on the island of Gran Canaria through an annual cycle. We predicted that canopy descriptors (density, biomass, length, and frond production) would vary seasonally, associated with environmental conditions, in particular sea surface temperature, light, nutrients, and wave energy. Finally, we analysed variations in the frond size-structure of this alga to assess the prevalence of positive and/or negative frond interactions.

Materials and methods

Study sites and *Gongolaria abies-marina* canopy structure

Our study was performed at four sites on the island of Gran Canaria (Canary Islands, eastern Atlantic, Spain; Fig. 1): two in the north, Playa Canaria (PLC) and El Confital (CON); and two in the east, Clavellinas (CLA) and Salinetas (SAL). These sites cover a large part of *G. abies-marina* distribution on the island, incorporating different types of environmental conditions, mainly in

terms of wave action. The main environmental and anthropogenic characteristics for each site are summarized in Table S1.

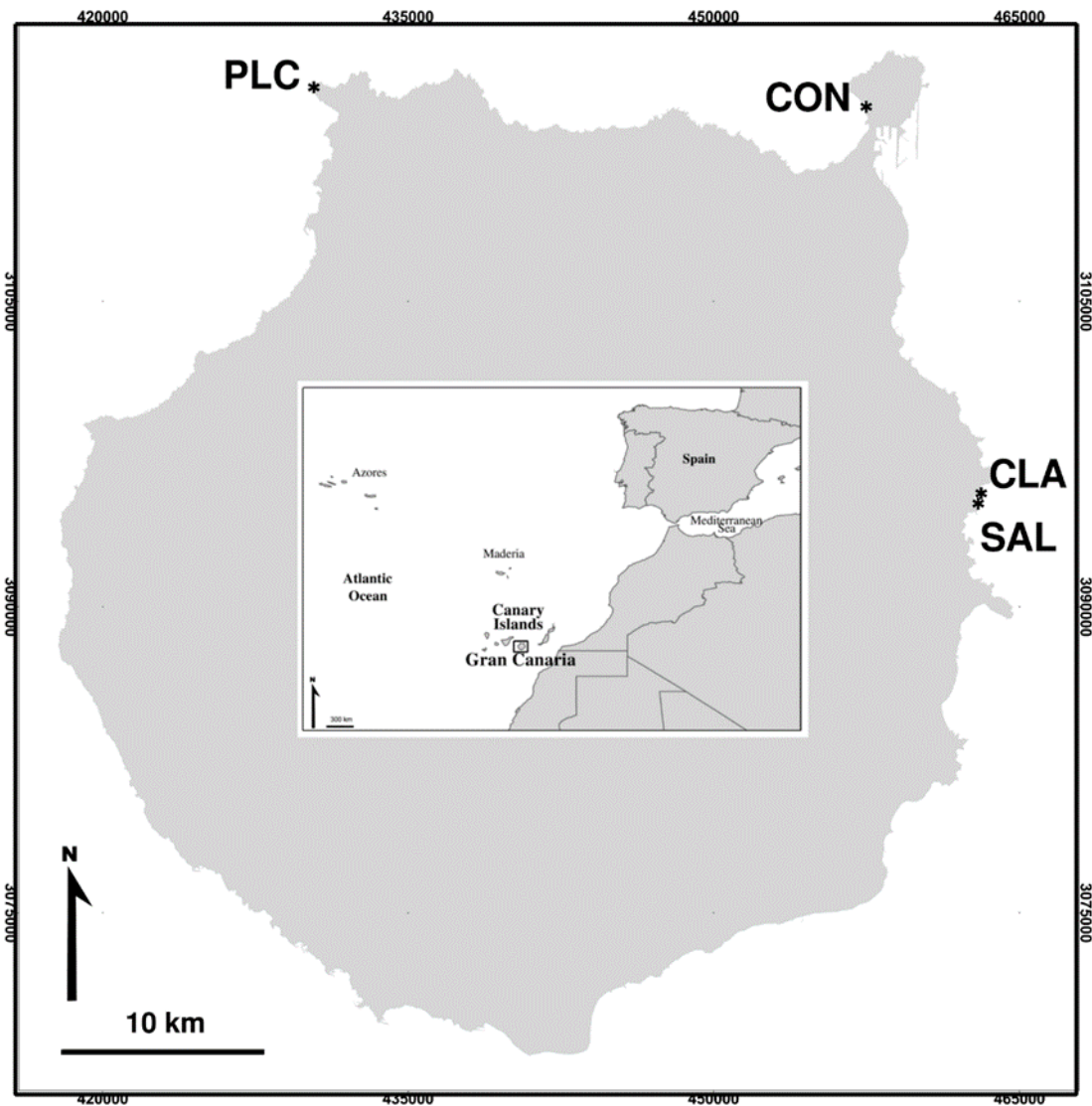
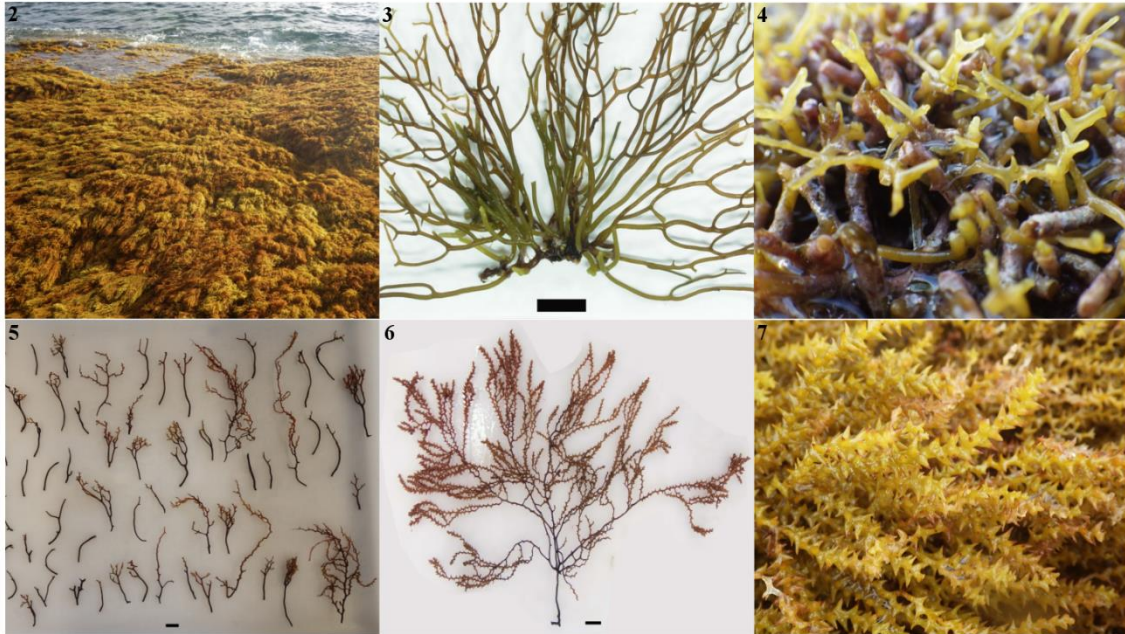


Fig. 1. Map of Gran Canaria Island, showing study sites Playa Canaria (PLC), El Confital (CON), Salinetas (SAL) and Clavellinas (CLA).

Gongolaria abies-marina is a clonal seaweed with modular construction (Santelices 2004) that forms monospecific stands (Fig. 2), made up of ramets or fronds arising from creeping axes, which are attached to the substratum by small haptera (Fig. 3). The entwinement of axes and branching of plants makes ramets difficult to distinguish from genets (Fig. 4). Moreover, it is difficult to accurately age individuals and ramets; in the absence of growth rings, no ageing method is currently available (Blanfuné et al. 2016). For these reasons, we considered 'fronds' as the sample unit. We distinguished two stages in the macroscopic life history of *G. abies-marina*: non-fertile fronds (NF) (Fig. 5), and fertile fronds (F) (Fig. 6). We defined non-fertile fronds as any primary axis without receptacles (reproductive structures). Fertile fronds, which are usually

much branched, carry the receptacles in the distal part of branches (Fig. 7). In this study, we used the length of the primary axis of fronds, despite their deciduous character, to describe algal dynamics.



Figs 2–7. *Gongolaria abies-marina*, showing Fig. 2. monospecific stand; Fig. 3. fronds arising from creeping axes; Fig. 4. entwined creeping axes; Figs 5, 6. non-fertile fronds; Fig. 7. fertile fronds. Scale bars correspond to 1 cm.

Sampling and sorting

At each site, sampling was carried out at the lower limit of the intertidal zone, where *G. abies-marina* forms dense monospecific stands. Subtidal populations have disappeared in Gran Canaria (Valdazo et al. 2017). We decided to use a small sampling unit (25 cm²), because this alga is under protection by national and regional laws. Every month, from May 2014 to April 2015 (except January and March 2015, due to bad weather), at low tide, six samples were haphazardly collected by scraping the substrate to ensure that the creeping and erect fronds were collected complete and intact. Algal samples were placed in sealed bags and carried to the laboratory, where they were immediately frozen.

Once defrosted, algal samples were rinsed, and all epiphytes and sandy and rocky debris eliminated. We first measured the length of the primary axis with a ruler. For each sample, fronds were classified into seven size classes: 0–3, 3.1–6, 6.1–9, 9.1–12, 12.1–15, 15.1–18, and >18 cm to describe their population size structure. The seven classes were established to describe population frond size-structure (Åberg 1992), including non-fertile and fertile fronds. The number of non-fertile/fertile and the total number of fronds were subsequently determined for

each sample. We obtained the mean length of non-fertile (>3cm) and fertile fronds by measuring at least 50% of fronds of each stage. The dry weight (dwt) of each stage was obtained after drying fronds for two days at 80°C. As a result, the stand density (fronds m⁻²) and the stand biomass (g dwt m⁻²) were estimated for each stage over time for each site. Lastly, we calculated the annual mean, including frond densities and biomasses across all sites.

Biomass production (P) was calculated, for each site, between each of two consecutive sampling times by considering all the stages. Fronds are not perennial, and so production of *G. abies-marina* was calculated using its annual biomass cycle. Then, we calculated the daily turnover ratio (r) of fronds, using the formula (Sales and Ballesteros 2012):

$$r = \left(\frac{P}{B_1} + 1 \right) / \Delta t$$

P is the production attained during a given time interval (g dwt), B1 is the initial biomass (g dwt), and Δt is the time length of the interval (days). We calculated the average annual production of the four sites. Finally, we converted the biomass (g dwt) to carbon tissue content according to previous research on a range of *Cystoseira* s.l. species, which indicated that carbon content is ~34% of dwt (Ballesteros 1990a; Delgado et al. 1994).

Environmental drivers

Wave exposure, sea surface temperature, light availability and nutrient concentrations (chlorophyll a, used as a proxy) were obtained, on a monthly basis, for each site (Fig. S1). Data on wave energy were obtained from the Enola project (www.enola.ihcantabria.com). We used averaged monthly power (Kw m⁻¹) as a proxy for wave energy. Monthly sea surface temperature (SST, °C), chlorophyll a (Chla, mg m⁻³) and photosynthetically active radiation (PAR, μmol m⁻² d⁻¹) were obtained from the NASA Giovanni Data Portal (<http://giovanni.gsfc.nasa.gov/giovanni>). Temperature data were monthly means from May 2014 to April 2015, using 9-km² pixel resolution, from the Pathfinder AVHRR satellite. Chla concentration data were monthly means from May 2014 to April 2015, using 4-km² pixel resolution, from the MODIS Aqua satellite. Since there were no PAR data after 2010, we used, as a proxy for light availability through the study period, monthly means from 1997 to 2010, using 9-km² pixel resolution, from the SeaWiFS satellite.

Statistical analysis

Differences in size-frequency distributions between sites and months were tested using the non-parametric Kolmogorov–Smirnov test (Legendre and Legendre 1998). Regression analyses

examined the relationship between densities, biomasses, and length of each of the two stages and environmental predictors. We initially used the 'chart.Correlation' function in the 'PerformanceAnalytics' R package (Peterson and Carl 2014) to explore collinearity in predictor variables, the relationship between response variables and environmental drivers, and relationships between response variables. We identified a strong negative correlation between Chla and SST ($R^2 = -0.77$), so Chla was removed. Data exploration revealed that relationships between predictor and response variables were non-linear and, therefore, a Generalized Additive Model (GAM) strategy was adopted (Zuur et al. 2009). All models were fitted using the R 'mgcv' package (Wood 2006, 2008), which uses the default method of a 'thin-plate regression spline' for smoothing and automatic selection of smoothing parameters by cross-validation. We fitted the models with a gamma error distribution for the non-fertile stage and a Gaussian error distribution for the fertile stage. The GAM models were conceptualized as:

$$Y \sim Pw + s(PAR) + s(SST)$$

Y is the density, biomass and length of each stage (response variables); s is the non-parametric smoothed functions of photosynthetically active radiation (PAR) and sea surface temperature (SST) and Pw is the parametric coefficient of wave energy. We built models with all possible combinations of explanatory variables, then we chose the models with the best fit using the AIC (Akaike Information Criterion) as an indicator of the best fitted model (the lower, the better). We assessed models performance using the 'gam. check' function, which produces graphical diagnostics (QQ-plots, residuals histograms, residuals versus fitted values and fitted values versus observed values). For the models of the fertile stage (biomass, density and length), the plots of residuals against linear predictors for the GAM model displayed some normality problems and, therefore, the dependent variables were square root transformed. We used partial residual plots of the models to contrast the relative influence of each predictor.

Results

Canopy structure: variation across sites

During the study, at all four sites, *G. abies-marina* populations were dominated by non-fertile fronds ($85,911.8 \pm 34,783.3$ fronds m^{-2} ; annual mean \pm SE, Fig. 8). Fertile fronds had a comparatively lower mean annual density ($9,984.4 \pm 433.8$ fronds m^{-2} , Fig. 8). Fertile fronds, however, carried the largest annual biomasses ($2,924.1 \pm 175.4$ gr dwt m^{-2} , Fig. 9). In terms of mean frond length, fertile fronds were longer (14.7 ± 0.1 cm) than non-fertile fronds (6.9 ± 0.04 cm) (Fig. S2).

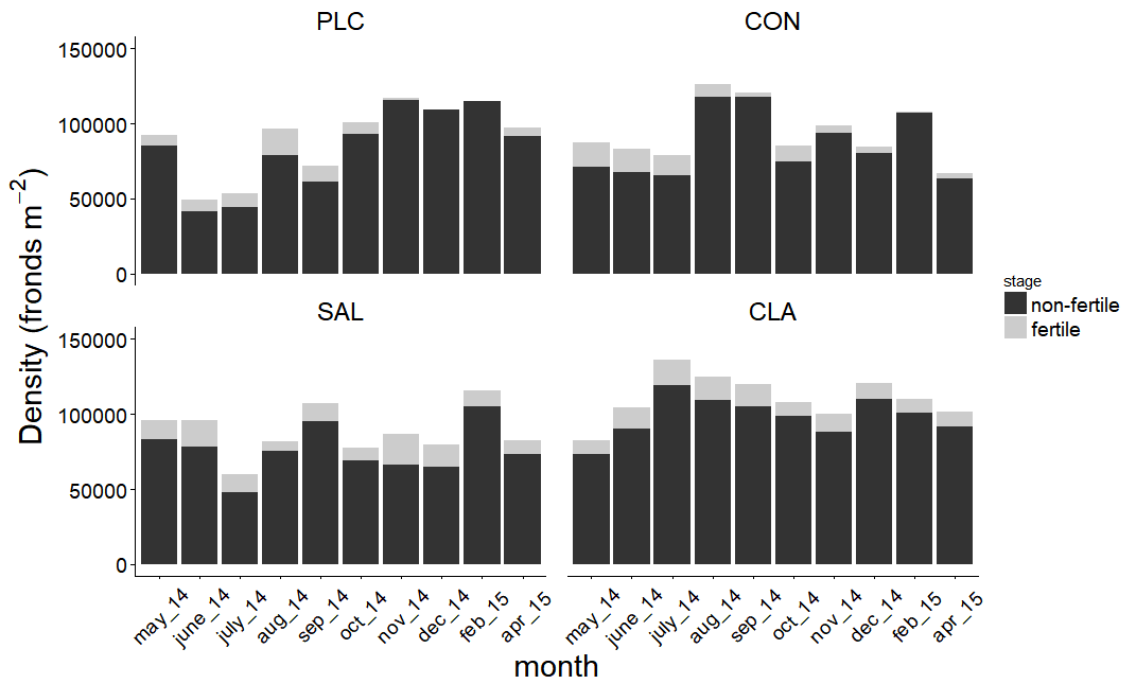


Fig. 8. Temporal variation in *Gongolaria abies-marina* frond densities for Playa Canaria (PLC), El Confital (CON), Salinetas (SAL) and Clavellinas (CLA).

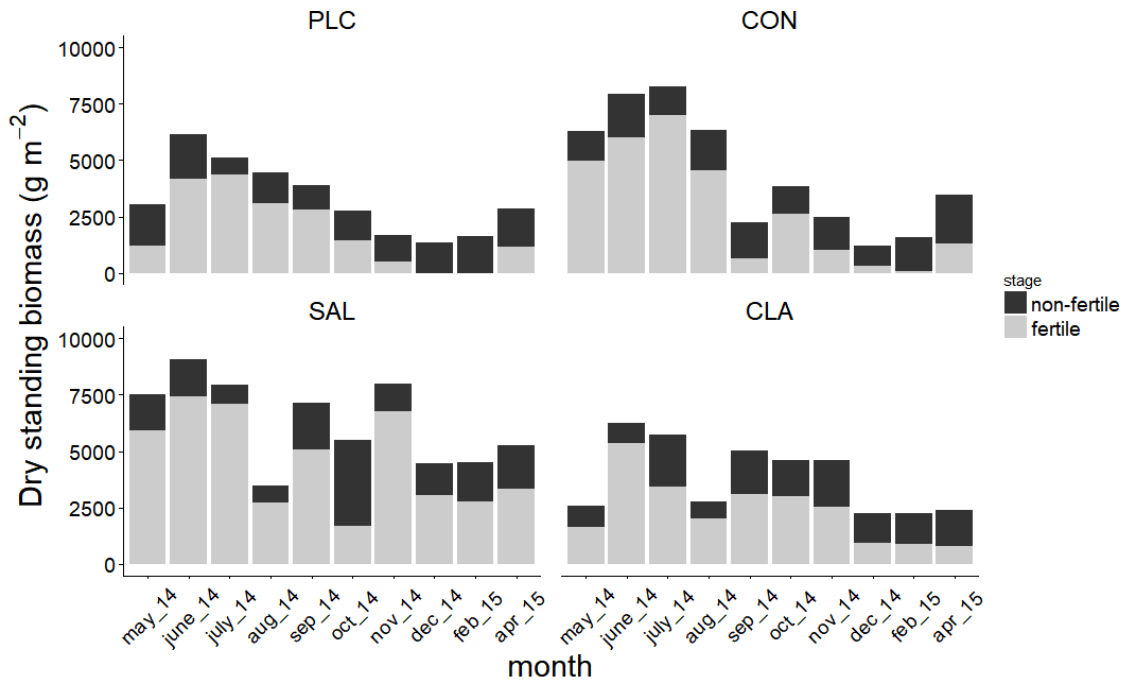


Fig. 9. Temporal variation in *Gongolaria abies-marina* frond biomass for Playa Canaria (PLC), El Confital (CON), Salinetas (SAL) and Clavellinas (CLA).

Size structure: evidence of intraspecific relationships

Within sites, no significant changes in size-frequency distributions were observed through time (Fig. 10; Table S2). Across sites, and throughout the year, *G. abies-marina* stands were mostly dominated by small-sized fronds (classes 1 and 2), so there was no direct indication of negative interaction, even in the season when large-sized fronds increased (May to October, Fig. 10). Large fronds (classes 6 and 7), which were mostly fertile, were always sparse and disappeared during winter from most sites (PLC, CON and CLA) (Fig. 10).

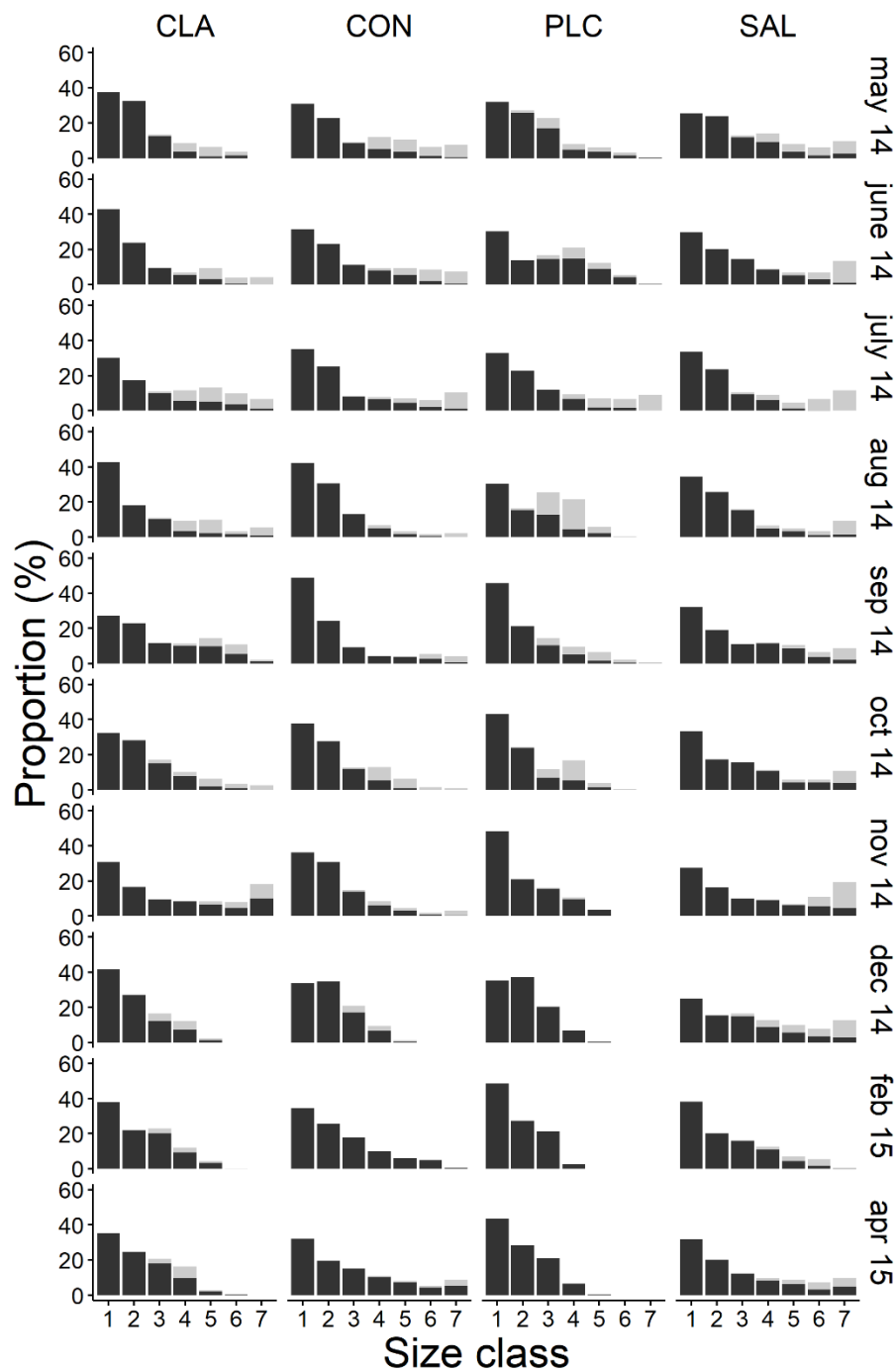


Fig. 10. Temporal changes in the size-frequency distribution of *Gongolaria abies-marina* fronds for Clavellinas (CLA), El Confital (CON), Playa Canaria (PLC) and Salinetas (SAL). Size classes are: 1 (0–3cm), 2 (3.1–6 cm), 3 (6.1–9 cm), 4 (9.1–12 cm), 5 (12.1–15 cm), 6 (15.1–18 cm), 7 (>18 cm). The fertile stage is denoted in light grey, while the non-fertile stage is in dark grey.

Linking environmental variation with canopy structure

The best model explaining variation in the total density of fronds only included photosynthetically active radiation (PAR); the model only explained 8.33% (adjusted $R^2 = 0.07$) of the variance (Table 1 and Table S3). The models accounting for temporal variation in the density of non-fertile fronds only explained 10.9% (adjusted $R^2 = 0.09$) (Table 1 and Table S3). However, variation in the density of fertile fronds was explained by variation in photosynthetically active radiation (PAR), sea surface temperature (SST) and wave power (Pw) (Table 1 and Table S3). The model explained 55% (adjusted $R^2 = 0.51$) of the variance (Table 1). The residual plot of PAR showed a bimodal pattern (Fig. 11a) with a higher density of fertile fronds at high and low radiation levels, which correspond with spring (April, May, June) and autumn (October and November). SST showed a similar pattern of residuals with a higher density at low (< 18°C) and high (> 22°C) temperatures (Fig. 11b). Wave power was the most important predictor, revealing a general pattern of negative residuals (i.e., low frond density) with increasing wave power (Fig. 11c).

Table 1. GAMs explaining variation in the density and biomass of each stage of *Gongolaria abies-marina* according to sea surface temperature (SST), photosynthetically active radiation (PAR) and wave power (Pw).

Model		D ² (%)	Adj R ²	AIC	GCV
B = Total biomass (Gamma(log))					
B1	~ Pw	24.8%	0.174	-68.81	0.31
B2	~ s(SST)	25.8%	0.241	-62.84	0.32
B3	~ s(PAR)	25.4%	0.219	-55.48	0.33
B4	~ s(PAR) + s(SST)	40.5%	0.326	-99.48	0.28
B5	~ Pw + s(PAR)	42.5%	0.352	-118.77	0.26
B6	~ Pw + s(SST)	40.8%	0.336	-119.3	0.26
B7	~ Pw + s(PAR) + s(SST)	50.6%	0.415	-145.04	0.24
NFB = Non-fertile biomass (Gamma(log))					
NFB1	~ Pw	1.03%	0.004	-553.26	0.33
NFB2	~ s(SST)	1.4x10 ⁻⁵ %	4.3x10 ⁻⁷	-552.64	0.33
NFB3	~ s(PAR)	5.01%	0.006	-550.5	0.33
NFB4	~ s(PAR) + s(SST)	14.6%	0.052	-562.39	0.32
NFB5	~ Pw + s(PAR)	6%	0.017	-551.95	0.33
NFB6	~ Pw + s(SST)	1.03%	0.004	-553.26	0.33
NFB7	~ Pw + s(PAR) + s(SST)	14.5%	0.053	-562.1	0.32
FB = Fertile biomass (Gaussian)					
FB1	~ Pw	29.2%	0.29	-19.7	0.05

FB2 ~	s(SST)	32.9%	0.31	-19.7	0.05
FB3 ~	s(PAR)	30.6%	0.28	-9.14	0.06
FB4 ~	s(PAR) + s(SST)	44.1%	0.406	-49.94	0.05
FB5 ~	Pw + s(PAR)	47.3%	0.45	-73.01	0.043
FB6 ~	Pw + s(SST)	46.8%	0.454	-77.55	0.04
FB7 ~	Pw + s(PAR) + s(SST)	55.3%	0.52	-99.33	0.038
<hr/>					
D = Total density (Gamma (log))					
D1 ~	Pw	0.008	-0.004	1258.4	0.133
D2 ~	s(SST)	6.24%	0.058	1245.2	0.127
D3 ~	s(PAR)	8.33%	0.07	1243.8	0.126
D4 ~	s(PAR) + s(SST)	8.48%	0.068	1245.1	0.127
D5 ~	Pw + s(PAR)	8.49%	0.067	1245.4	0.127
D6 ~	Pw + s(SST)	6.26%	0.054	1247.1	0.128
D7 ~	Pw + s(PAR) + s(SST)	7.27%	0.061	1245.7	0.127
<hr/>					
NFD = Non-Fertile density (Gamma (log))					
NFD1 ~	Pw	1.02%	0.007	1256.4	0.17
NFD2 ~	s(SST)	7.9%	0.076	1241.5	0.16
NFD3 ~	s(PAR)	10.9%	0.095	1238.4	0.158
NFD4 ~	s(PAR) + s(SST)	10.9%	0.092	1239.4	0.16
NFD5 ~	Pw + s(PAR)	11%	0.094	1239.9	0.16
NFD6 ~	Pw + s(SST)	8.34%	0.077	1242.3	0.16
NFD7 ~	Pw + s(PAR) + s(SST)	9.43%	0.085	1240.6	0.16
<hr/>					
FD = Fertile density (Gaussian)					
FD1 ~	Pw	35.4%	0.351	174.45	0.120
FD2 ~	s(SST)	18.7%	0.165	240.10	0.158
FD3 ~	s(PAR)	19%	0.162	242.85	0.160
FD4 ~	s(PAR) + s(SST)	31.2%	0.269	215.20	0.143
FD5 ~	Pw + s(PAR)	43.8%	0.416	157.13	0.112
FD6 ~	Pw + s(SST)	45.1%	0.428	152.63	0.110
FD7 ~	Pw + s(PAR) + s(SST)	55%	0.514	120.83	0.097
<hr/>					
NFL = Non-fertile length (Gamma)					
NFL1 ~	Pw	14.8%	0.129	966.51	0.074
NFL2 ~	s(SST)	10.6%	0.066	993.29	0.082
NFL3 ~	s(PAR)	13%	0.097	985.80	0.080
NFL4 ~	s(PAR) + s(SST)	23.9%	0.179	969.68	0.075
NFL5 ~	Pw + s(PAR)	26.7%	0.229	945.70	0.068
NFL6 ~	Pw + s(SST)	26.5%	0.235	943.63	0.067
NFL7 ~	Pw + s(PAR) + s(SST)	32%	0.265	937.52	0.066
<hr/>					
FL = Fertile Length (Gaussian)					
FL1 ~	Pw	32.1%	0.318	726.86	1.2
FL2 ~	s(SST)	16.8%	0.156	780.33	1.5
FL3 ~	s(PAR)	20%	0.171	780.8	0.17
FL4 ~	s(SST) + s(PAR)	30.4%	0.257	760.74	1.39
FL5 ~	Pw + s(PAR)	41.9%	0.396	705.86	1.11
FL6 ~	Pw + s(SST)	43.3%	0.411	700.02	1.08
FL7 ~	Pw + s(PAR) + s(SST)	49%	0.453	688.93	1.03

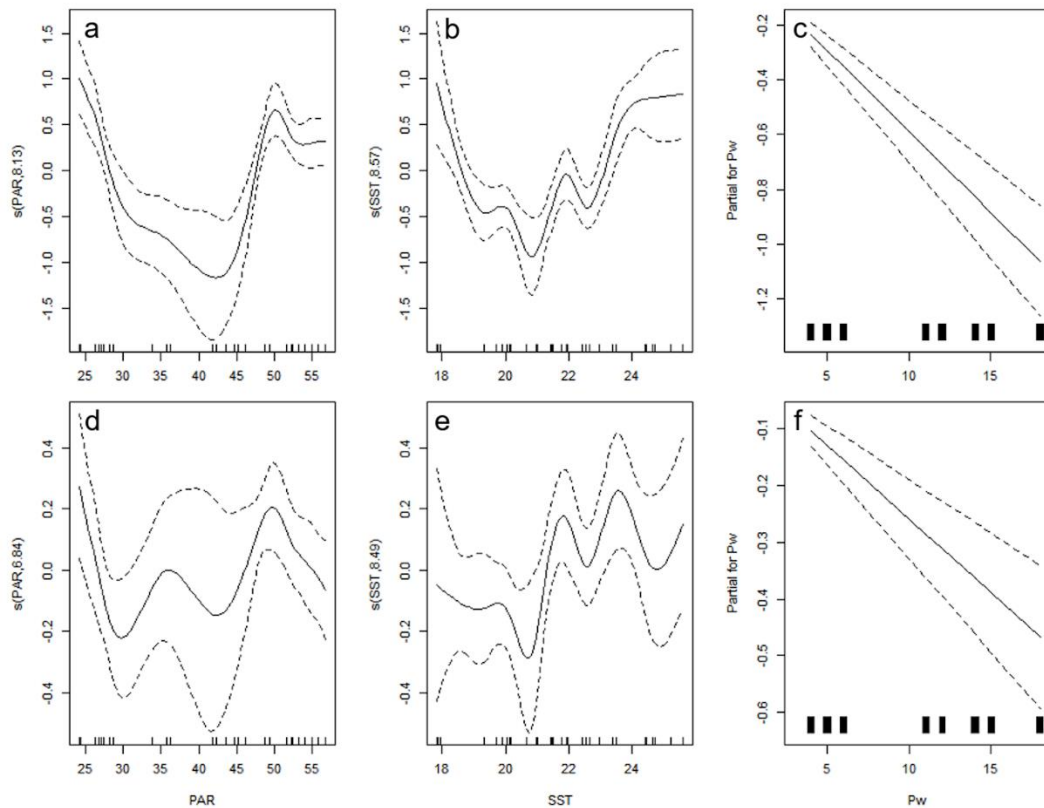


Fig. 11. Partial residual plots for the GAMs terms explaining variation in the density and biomass of fertile *Gongolaria abies-marina*. For fertile frond density: (a) photosynthetically active radiation (PAR), (b) sea surface temperature (SST), (c) wave power (Pw). For fertile frond biomass: (d) photosynthetically active radiation (PAR), (e) sea surface temperature (SST), (f) wave power (Pw). Each panel plots the values for a predictor variable (x-axis) against the partial residuals (y-axis), after removing the effects of the other predictors. The dashed lines show the estimated 95% confidence limits. The y-axis label indicates the estimated degrees of freedom for the smoothed spline term.

As for the density and biomass of fertile fronds, the models that best explained variation in the length of the non-fertile and fertile stages included photosynthetically active radiation (PAR), sea surface temperature (SST) and wave power (Pw) (Table 1 and Table S5). For the length of non-fertile fronds, the model explained 32% of the variance (adjusted $R^2 = 0.27$) (Table 1). The residual plot of PAR showed a bimodal pattern with the higher length at low ($25\text{--}27 \mu\text{mol m}^{-2} \text{d}^{-1}$) and high ($> 45 \mu\text{mol m}^{-2} \text{d}^{-1}$) levels of radiation (Fig. 12a). Similarly, a bimodal pattern was observed for SST, including positive residuals at low (SST values $< 18^\circ\text{C}$) and high temperatures ($> 23^\circ\text{C}$) (Fig. 12b). A weak pattern of positive residuals (i.e., higher length) was observed under increased wave power (Fig. 12c). In terms of the length of fertile fronds, the model explained 49% of the variance (adjusted $R^2 = 0.45$) (Table 1). The residual plot of PAR showed a bimodal pattern with

the higher length at low ($< 25\text{--}27 \mu\text{mol m}^{-2} \text{d}^{-1}$) and high ($35\text{--}50 \mu\text{mol m}^{-2} \text{d}^{-1}$) levels of radiation (Fig. 12d). For SST, we observed a bimodal pattern, with positive residuals between $21\text{--}24^\circ\text{C}$ (Fig. 12e). A clear pattern of negative residuals (i.e., low length) was observed under increased wave power (Fig. 12f).

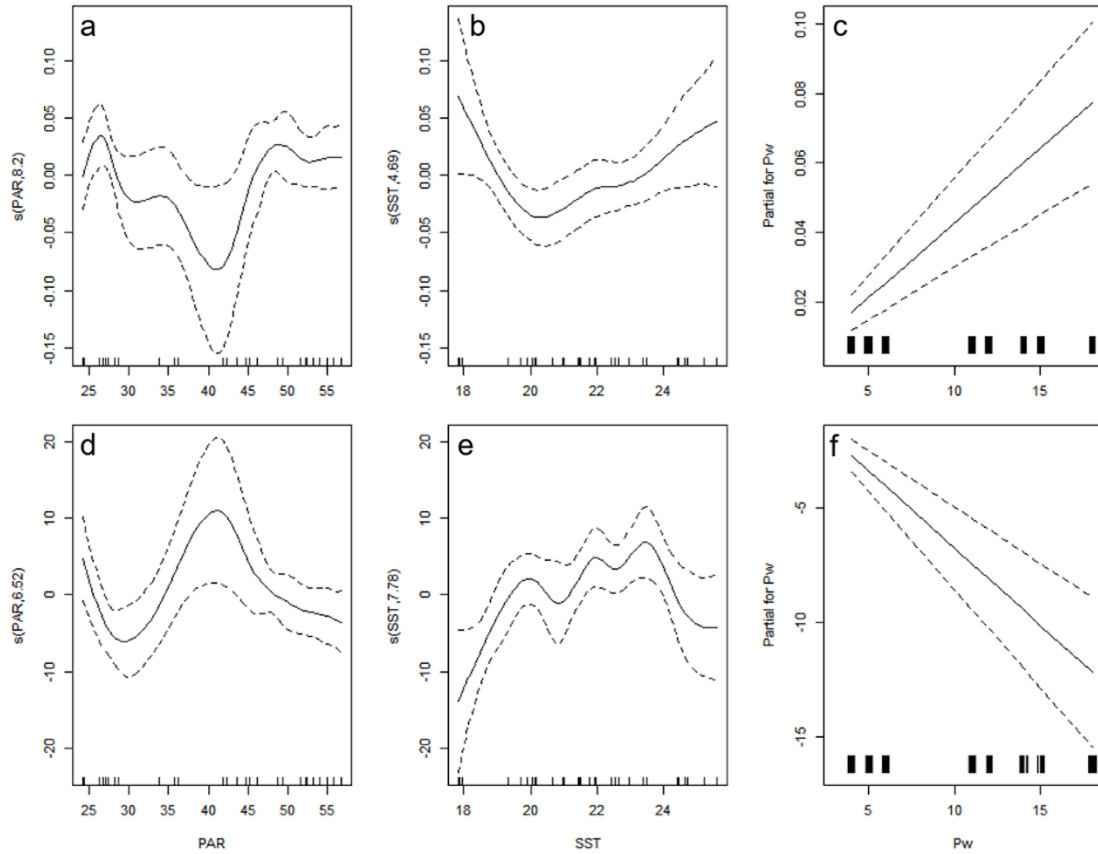


Fig. 12. Partial residual plots for the GAMs terms explaining variation in the length of non-fertile and fertile *Gongolaria abies-marina*. For non-fertile frond length: (a) photosynthetically active radiation (PAR), (b) sea surface temperature (SST), (c) wave power (Pw). For fertile frond length: (d) photosynthetically active radiation (PAR), (e) sea surface temperature (SST), (f) wave power (Pw). Each panel plots the values for a predictor variable (x-axis) against the partial residuals (y-axis), after removing the effects of the other predictors. The dashed lines show the estimated 95% confidence limits. The y-axis label indicates the estimated degrees of freedom for the smoothed spline term.

Annual frond production

The mean annual frond production of *G. abies-marina* in Gran Canaria was $5,380 \text{ g dwt m}^{-2}$ ($1,829.52 \text{ g C m}^{-2}$) (Table S6). Frond production showed two peaks, in spring and autumn, and null values in summer and late autumn–early winter (Fig. 13). The daily turnover ratio was highest in spring for all sites, although CON and SAL also showed high rates in autumn (Table S6).

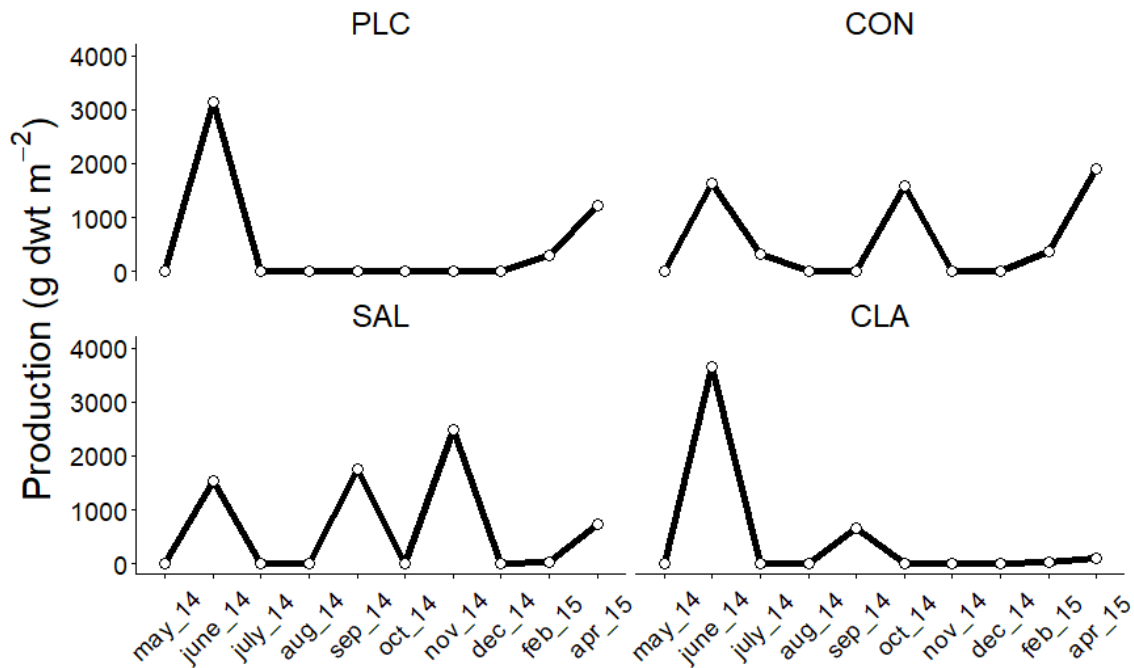


Fig. 13. Annual *Gongolaria abies-marina* frond production for each site on Gran Canaria Island: Playa Canaria (PLC), El Confital (CON), Salinetas (SAL) and Clavellinas (CLA).

Discussion

Despite the important role that the genus *Cystoseira* s.l. plays as a habitat-former on Atlantic coasts, we have a limited knowledge of the population dynamics of most species; this is especially true for less conspicuous species such as *G. abies-marina*. To our knowledge, ours is the first study to address the seasonal dynamics of macroscopic fronds of this species, providing insight into the frond size-structure and possible intraspecific relationships of *G. abies-marina*. We provide a more precise phenology than the descriptive studies carried out previously (González and Afonso-Carrillo 1990; Medina 1997). In particular, we linked quantitative data on canopy structure with seasonality of environmental drivers. However, results should be interpreted with caution, as our study is limited to four sites on one island for one year.

We found a temporal shift in the frond size structure of *G. abies-marina* on the island of Gran Canaria, mainly related to the prevalence of the fertile stage, which showed the largest variability in relation to environmental predictors. The models that best fit included three environmental factors (Pw, PAR and SST) and explained a moderate variation in the seasonality of the fertile stage. Two predictors (PAR and SST) did not differ much between sites, but wave power showed considerable spatial and temporal variation. In general, the density, biomass and length of the fertile stage decreased with increased wave power. The lower, seasonally constant,

wave power observed at the eastern sites (SAL and CLA) seems to be connected with the highest temporal consistency of their canopy descriptors. At these sites, in particular, we found fertile fronds throughout the entire year. In winter, under decreased SST and PAR, the density and biomass of fertile fronds also decreased. At PLC and CON, sites located on the more exposed northern coast, canopy descriptors followed a more seasonal pattern, with the highest density and biomass of fertile fronds in the months of lower wave energy, and minimum density and biomass in the winter months, when the wave energy, mostly induced by NW swells, is maximum, while SST and PAR are low.

Previous work on *G. abies-marina* from the Canarian Archipelago (González and Afonso-Carrillo, 1990; Medina 1997) and some *Cystoseira* s.l. species from the Mediterranean (Ballesteros 1988, 1990a, 1990b; Delgado et al. 1994; Sales and Ballesteros 2012) showed a simple seasonal pattern, with maximum biomass in late spring and early summer, and minimum in autumn and winter. However, in our study, at CON, SAL and CLA, the algal biomass cycle showed a rather bimodal pattern, with production peaking in spring and a less accentuated peak in late summer–early autumn. This pattern is similar to that found for *Gongolaria nodicaulis* (*Withering*) *Molinari & Guiry* on the north coast of Spain (Arenas et al., 1995) and *Ericaria brachycarpa* on the north-western coast of France (Hoffmann et al., 1992). The contrasting seasonality, relative to Mediterranean and northern Atlantic species of *Cystoseira* s.l., may result from the narrower annual environmental variation around the Canarian Archipelago, in comparison with Mediterranean and Atlantic shores (Arenas et al. 1995; Tuya et al. 2006). For example, the seagrass *Cymodocea nodosa*, in the Canary Islands, shows a smoothed seasonal production pattern compared with the Mediterranean (Tuya et al. 2006). There may be other mechanisms which help to explain the second period of production, particularly that the modular construction of *G. abies-marina* allows the plant to regrow following losses suffered in its senescent phase, and the highly efficient nutrient uptake mechanisms (Delgado et al. 1994; Rico and Fernández 1997).

As previously indicated, the population structure of *G. abies-marina* was spatially and temporally variable, associated with wave power, demonstrating the importance of exposure to waves in determining algal canopy density, biomass and morphology (Hurd 2000; Engelen et al. 2005). For many macroalgae, specimens subjected to heavy waves are typically smaller, thicker and have stronger holdfasts than those growing in calmer waters (Hurd 2000; Thomsen and Wernberg 2005). This morphological plasticity modulated by wave energy also reduces hydrodynamic drag forces to minimize dislodgement (de Bettignies et al. 2015). Previous, spatially non-replicated, work on *G. abies-marina* (Medina 1997) showed that canopies from an

exposed location were larger, more branched and had greater biomass than canopies from a less exposed location. Our results were not congruent with Medina (1997), since we found a clear decrease in all canopy descriptors under increased wave exposure scenarios, both spatially (i.e., inter-site differences) and temporally (i.e., in winter for each site).

In this study, we have reported a temporally stable situation in terms of frond size-structure; small fronds (0–6 cm, class 1 and 2) predominate throughout the entire year. This finding suggests the prevalence of positive interactions in the closed canopies of *G. abies-marina*. High-density canopies favour high humidity at low tide, maintaining a low temperature and reducing the water velocity, decreasing the amount of drag experienced by small fronds; this is in accordance with other clonal seaweeds (Collado-Vides 2002; Scrosati 2005; Rivera and Scrosati, 2008). In *G. abies-marina* stands, algal biomass is concentrated in the largest fronds, which are highly branched, so they can induce shading and/or whiplash on the understory of smaller fronds below. However, this effect does not seem to affect their success. In turn, strategies to adapt to the stressful conditions of the low intertidal and upper subtidal, where crowded conditions seem to drive facilitative relationships, may improve population persistence, as demonstrated for other canopy-forming algal populations (Santelices 2004; Bennett and Wernberg 2014). In any case, experimental work, at local scales, would be necessary to unravel the direction of interactions between small and large-sized fronds.

The annual production of *G. abies-marina* in Gran Canaria (5,380.9 g dwt m⁻² year⁻¹) was higher than that previously estimated in the Canary Islands (1,293.2 g dwt m⁻² year⁻¹; Medina 1997) and other Mediterranean *Cystoseira*-dominated assemblages (Ballesteros 1988, 1990a, 1990b; Sales and Ballesteros 2012a). The primary annual production of *G. abies-marina* was as large as that observed for kelps and other fucoids around the world (Chung et al. 2011; Krumhansl and Scheibling 2012). The dramatic decline of *G. abies-marina* forests in recent decades, ~9.2 km² in Gran Canaria (Valdazo et al. 2017), means the loss of high primary production (16,831.6 Mg C year⁻¹). Although more research is key to understanding the carbon flows from macroalgal forests, a considerable proportion of the carbon provided by *G. abies-marina* forests could end up sequestered by means of detrital export into the deep sea, or adjacent marine sediments (Krause-Jensen and Duarte 2016).

Currently, *G. abies-marina* is nationally and regionally protected within the framework of the Spanish and Canarian Catalogues of Protected Species, as over the last few decades, there has been a massive decline across the entire Canarian archipelago (Medina and Haroun 1994; Valdazo et al. 2017). Population dynamics are poorly understood for most of the *Cystoseira* s.l.

species from Macaronesia, so better knowledge of *G. abies-marina* makes an important contribution. More efforts are necessary to better understand key ecological processes shaping these dynamics. For conservation and restoration purposes, it is necessary to know if there are demographic constraints (e.g., Allee effects), whereby population persistence displays positive density-dependence (Berec et al. 2007). In addition, *G. abies-marina* should be considered within blue carbon conservation and restoration strategies to mitigate climate change in response to carbon neutral strategies. These future studies will improve conservation actions for this habitat-forming organism.

Supplementary material

Table S1. Environmental and anthropogenic characteristics of the study sites. PAR = average annual value of photosynthetic active radiation; SST = average annual value of sea surface temperature; Chl a = average annual value of Chlorophyll a concentration; Pw = average annual wave power; HAPI = Human Activities and Pressures Index, according to Valdazo *et al.* (2017)*. Geomorphological variables according to Ballesteros *et al.* (2007).

Site	PAR (E cm ⁻² s ⁻¹)	SST (°C)	Chl a (mg m ⁻³)	Pw (Kw m ⁻¹)	Coastline morphology	Substrate constitution	Coastline slope	Coastline orientation	HAPI
PLC	42.27	21.21	0.19	10.5	Low coast	Basalt	Horizontal	Northwest	1.93
CON	40.56	21.36	0.18	12.75	Low coast	Basalt	Sub-vertical	Northwest	3.24
SAL	41.75	21.09	0.21	4.5	Low coast	Basalt	Horizontal	East	4
CLA	41.74	21.09	0.21	4.5	Low coast	Basalt	Sub-vertical	East	4

*higher values mean more pressures.

Table S2. Results of the two-sample Kolmogorov-Smirnov test (D) checking for differences in size-structure between sites and months.

Population 1		Population 2		D	P-value
Month		Month			
May Playa Canaria	June Playa Canaria	June Playa Canaria	June Playa Canaria	0.286	0.963
May Playa Canaria	July Playa Canaria	July Playa Canaria	July Playa Canaria	0.286	0.963
May Playa Canaria	August Playa Canaria	August Playa Canaria	August Playa Canaria	0.286	0.963
May Playa Canaria	September Playa Canaria	September Playa Canaria	September Playa Canaria	0.143	1
May Playa Canaria	October Playa Canaria	October Playa Canaria	October Playa Canaria	0.286	0.963
May Playa Canaria	November Playa Canaria	November Playa Canaria	November Playa Canaria	0.286	0.963
May Playa Canaria	December Playa Canaria	December Playa Canaria	December Playa Canaria	0.428	0.541
May Playa Canaria	February Playa Canaria	February Playa Canaria	February Playa Canaria	0.428	0.541
May Playa Canaria	April Playa Canaria	April Playa Canaria	April Playa Canaria	0.286	0.963
June Playa Canaria	July Playa Canaria	July Playa Canaria	July Playa Canaria	0.286	0.963
June Playa Canaria	August Playa Canaria	August Playa Canaria	August Playa Canaria	0.286	0.963
June Playa Canaria	September Playa Canaria	September Playa Canaria	September Playa Canaria	0.286	0.963
June Playa Canaria	October Playa Canaria	October Playa Canaria	October Playa Canaria	0.428	0.575
June Playa Canaria	November Playa Canaria	November Playa Canaria	November Playa Canaria	0.286	0.963
June Playa Canaria	December Playa Canaria	December Playa Canaria	December Playa Canaria	0.286	0.937
June Playa Canaria	February Playa Canaria	February Playa Canaria	February Playa Canaria	0.428	0.541
June Playa Canaria	April Playa Canaria	April Playa Canaria	April Playa Canaria	0.286	0.963
July Playa Canaria	August Playa Canaria	August Playa Canaria	August Playa Canaria	0.286	0.963
July Playa Canaria	September Playa Canaria	September Playa Canaria	September Playa Canaria	0.286	0.963
July Playa Canaria	October Playa Canaria	October Playa Canaria	October Playa Canaria	0.428	0.575
July Playa Canaria	November Playa Canaria	November Playa Canaria	November Playa Canaria	0.428	0.575
July Playa Canaria	December Playa Canaria	December Playa Canaria	December Playa Canaria	0.428	0.541
July Playa Canaria	February Playa Canaria	February Playa Canaria	February Playa Canaria	0.571	0.203
July Playa Canaria	April Playa Canaria	April Playa Canaria	April Playa Canaria	0.286	0.963
August Playa Canaria	September Playa Canaria	September Playa Canaria	September Playa Canaria	0.286	0.963
August Playa Canaria	October Playa Canaria	October Playa Canaria	October Playa Canaria	0.286	0.937
August Playa Canaria	November Playa Canaria	November Playa Canaria	November Playa Canaria	0.143	1
August Playa Canaria	December Playa Canaria	December Playa Canaria	December Playa Canaria	0.286	0.937
August Playa Canaria	February Playa Canaria	February Playa Canaria	February Playa Canaria	0.286	0.937
August Playa Canaria	April Playa Canaria	April Playa Canaria	April Playa Canaria	0.143	1

September Playa Canaria	October Playa Canaria	0.285	0.963
September Playa Canaria	November Playa Canaria	0.285	0.963
September Playa Canaria	December Playa Canaria	0.428	0.541
September Playa Canaria	February Playa Canaria	0.428	0.541
September Playa Canaria	April Playa Canaria	0.285	0.963
October Playa Canaria	November Playa Canaria	0.285	0.963
October Playa Canaria	December Playa Canaria	0.143	1
October Playa Canaria	February Playa Canaria	0.285	0.937
October Playa Canaria	April Playa Canaria	0.286	0.937
November Playa Canaria	December Playa Canaria	0.143	1
November Playa Canaria	February Playa Canaria	0.286	0.937
November Playa Canaria	April Playa Canaria	0.143	1
December Playa Canaria	February Playa Canaria	0.143	1
December Playa Canaria	April Playa Canaria	0.286	0.937
February Playa Canaria	April Playa Canaria	0.286	0.937
May Confital	June Confital	0.428	0.575
May Confital	July Confital	0.286	0.963
May Confital	August Confital	0.428	0.575
May Confital	September Confital	0.571	0.212
May Confital	October Confital	0.286	0.963
May Confital	November Confital	0.286	0.963
May Confital	December Confital	0.428	0.541
May Confital	February Confital	0.286	0.963
May Confital	April Confital	0.286	0.963
June Confital	July Confital	0.286	0.963
June Confital	August Confital	0.571	0.212
June Confital	September Confital	0.571	0.212
June Confital	October Confital	0.428	0.575
June Confital	November Confital	0.571	0.212
June Confital	December Confital	0.428	0.541
June Confital	February Confital	0.428	0.575
June Confital	April Confital	0.285	0.962
July Confital	August Confital	0.428	0.575
July Confital	September Confital	0.571	0.212
July Confital	October Confital	0.428	0.575
July Confital	November Confital	0.428	0.575
July Confital	December Confital	0.428	0.575
July Confital	February Confital	0.428	0.575
July Confital	April Confital	0.286	0.963
August Confital	September Confital	0.286	0.963
August Confital	October Confital	0.286	0.963
August Confital	November Confital	0.143	1
August Confital	December Confital	0.428	0.541
August Confital	February Confital	0.143	1
August Confital	April Confital	0.428	0.575
September Confital	October Confital	0.286	0.963
September Confital	November Confital	0.286	0.963
September Confital	December Confital	0.428	0.541
September Confital	February Confital	0.286	0.963
September Confital	April Confital	0.571	0.212
October Confital	November Confital	0.286	0.963
October Confital	December Confital	0.286	0.937

October Confital	February Confital	0.143	1
October Confital	April Confital	0.428	0.575
November Confital	December Confital	0.428	0.541
November Confital	February Confital	0.143	1
November Confital	April Confital	0.428	0.575
December Confital	February Confital	0.285	0.937
December Confital	April Confital	0.428	0.541
February Confital	April Confital	0.428	0.575
May Salinetas	June Salinetas	0.143	1
May Salinetas	July Salinetas	0.286	0.963
May Salinetas	August Salinetas	0.286	0.937
May Salinetas	September Salinetas	0.286	0.937
May Salinetas	October Salinetas	0.143	1
May Salinetas	November Salinetas	0.428	0.575
May Salinetas	December Salinetas	0.428	0.575
May Salinetas	February Salinetas	0.143	1
May Salinetas	April Salinetas	0.286	0.963
June Salinetas	July Salinetas	0.286	0.963
June Salinetas	August Salinetas	0.428	0.575
June Salinetas	September Salinetas	0.286	0.937
June Salinetas	October Salinetas	0.286	0.963
June Salinetas	November Salinetas	0.286	0.937
June Salinetas	December Salinetas	0.286	0.963
June Salinetas	February Salinetas	0.286	0.963
June Salinetas	April Salinetas	0.285	0.963
July Salinetas	August Salinetas	0.143	1
July Salinetas	September Salinetas	0.286	0.937
July Salinetas	October Salinetas	0.286	0.963
July Salinetas	November Salinetas	0.286	0.963
July Salinetas	December Salinetas	0.428	0.575
July Salinetas	February Salinetas	0.143	1
July Salinetas	April Salinetas	0.286	0.963
August Salinetas	September Salinetas	0.428	0.541
August Salinetas	October Salinetas	0.143	1
August Salinetas	November Salinetas	0.428	0.575
August Salinetas	December Salinetas	0.428	0.575
August Salinetas	February Salinetas	0.143	1
August Salinetas	April Salinetas	0.286	0.963
September Salinetas	October Salinetas	0.286	0.937
September Salinetas	November Salinetas	0.286	0.937
September Salinetas	December Salinetas	0.286	0.937
September Salinetas	February Salinetas	0.286	0.937
September Salinetas	April Salinetas	0.286	0.937
October Salinetas	November Salinetas	0.286	0.963
October Salinetas	December Salinetas	0.428	0.575
October Salinetas	February Salinetas	0.143	1
October Salinetas	April Salinetas	0.286	0.963
November Salinetas	December Salinetas	0.286	0.963
November Salinetas	February Salinetas	0.286	0.963
November Salinetas	April Salinetas	0.286	0.963
December Salinetas	February Salinetas	0.428	0.575
December Salinetas	April Salinetas	0.428	0.575

February Salinetas	April Salinetas	0.286	0.963
May Salinetas	June Salinetas	0.286	0.963
May Salinetas	July Salinetas	0.286	0.963
May Salinetas	August Salinetas	0.286	0.963
May Salinetas	September Salinetas	0.428	0.575
May Salinetas	October Salinetas	0.286	0.963
May Salinetas	November Salinetas	0.571	0.212
May Salinetas	December Salinetas	0.143	1
May Salinetas	February Salinetas	0.143	1
May Salinetas	April Salinetas	0.286	0.937
June Salinetas	July Salinetas	0.1423	1
June Salinetas	August Salinetas	0.143	1
June Salinetas	September Salinetas	0.428	0.575
June Salinetas	October Salinetas	0.286	0.963
June Salinetas	November Salinetas	0.428	0.575
June Salinetas	December Salinetas	0.428	0.541
June Salinetas	February Salinetas	0.286	0.963
June Salinetas	April Salinetas	0.428	0.575
July Salinetas	August Salinetas	0.286	0.963
July Salinetas	September Salinetas	0.428	0.575
July Salinetas	October Salinetas	0.286	0.963
July Salinetas	November Salinetas	0.428	0.575
July Salinetas	December Salinetas	0.428	0.541
July Salinetas	February Salinetas	0.286	0.963
July Salinetas	April Salinetas	0.428	0.575
August Salinetas	September Salinetas	0.428	0.575
August Salinetas	October Salinetas	0.286	0.963
August Salinetas	November Salinetas	0.571	0.212
August Salinetas	December Salinetas	0.428	0.541
August Salinetas	February Salinetas	0.286	0.963
August Salinetas	April Salinetas	0.286	0.963
September Salinetas	October Salinetas	0.286	0.963
September Salinetas	November Salinetas	0.286	0.963
September Salinetas	December Salinetas	0.286	0.937
September Salinetas	February Salinetas	0.286	0.963
September Salinetas	April Salinetas	0.286	0.963
October Salinetas	November Salinetas	0.428	0.575
October Salinetas	December Salinetas	0.286	0.937
October Salinetas	February Salinetas	0.286	0.963
October Salinetas	April Salinetas	0.286	0.963
November Salinetas	December Salinetas	0.428	0.541
November Salinetas	February Salinetas	0.428	0.575
November Salinetas	April Salinetas	0.428	0.575
December Salinetas	February Salinetas	0.143	1
December Salinetas	April Salinetas	0.143	1
February Salinetas	April Salinetas	0.143	1

Sites

May Playa Canaria	May Confital	0.286	0.963
May Playa Canaria	May Salinetas	0.428	0.575
May Playa Canaria	May Clavellinas	0.143	1
May Confital	May Salinetas	0.286	0.963

May Confital	May Clavellinas	0.286	0.963
May Salinetas	May Clavellinas	0.286	0.963
June Playa Canaria	June Confital	0.428	0.575
June Playa Canaria	June Salinetas	0.286	0.963
June Playa Canaria	June Clavellinas	0.428	0.575
June Confital	June Salinetas	0.285	0.963
June Confital	June Clavellinas	0.428	0.575
June Salinetas	June Clavellinas	0.428	0.575
July Playa Canaria	July Confital	0.428	0.575
July Playa Canaria	July Salinetas	0.143	1
July Playa Canaria	July Clavellinas	0.286	0.963
July Confital	July Salinetas	0.286	0.963
July Confital	July Clavellinas	0.143	1
July Salinetas	July Clavellinas	0.286	0.963
August Playa Canaria	August Confital	0.286	0.963
August Playa Canaria	August Salinetas	0.286	0.963
August Playa Canaria	August Clavellinas	0.286	0.963
August Confital	August Salinetas	0.428	0.575
August Confital	August Clavellinas	0.286	0.963
August Salinetas	August Clavellinas	0.143	1
September Playa Canaria	September Confital	0.286	0.963
September Playa Canaria	September Salinetas	0.428	0.541
September Playa Canaria	September Clavellinas	0.428	0.575
September Confital	September Salinetas	0.571	0.203
September Confital	September Clavellinas	0.428	0.575
September Salinetas	September Clavellinas	0.286	0.937
October Playa Canaria	October Confital	0.286	0.963
October Playa Canaria	October Salinetas	0.428	0.575
October Playa Canaria	October Clavellinas	0.286	0.963
October Confital	October Salinetas	0.428	0.575
October Confital	October Clavellinas	0.143	1
October Salinetas	October Clavellinas	0.428	0.575
November Playa Canaria	November Confital	0.286	0.963
November Playa Canaria	November Salinetas	0.428	0.575
November Playa Canaria	November Clavellinas	0.428	0.575
November Confital	November Salinetas	0.428	0.575
November Confital	November Clavellinas	0.571	0.212
November Salinetas	November Clavellinas	0.143	1
December Playa Canaria	December Confital	0.143	1
December Playa Canaria	December Salinetas	0.571	0.203
December Playa Canaria	December Clavellinas	0.143	1
December Confital	December Salinetas	0.428	0.541
December Confital	December Clavellinas	0.143	1
December Salinetas	December Clavellinas	0.428	0.541
February Playa Canaria	February Confital	0.428	0.541
February Playa Canaria	February Salinetas	0.428	0.541
February Playa Canaria	February Clavellinas	0.286	0.937
February Confital	February Salinetas	0.286	0.963
February Confital	February Clavellinas	0.286	0.963
February Salinetas	February Clavellinas	0.286	0.963
April Playa Canaria	April Confital	0.286	0.963
April Playa Canaria	April Salinetas	0.428	0.575

April Playa Canaria	April Clavellinas	0.143	1
April Confital	April Salinetas	0.286	0.963
April Confital	April Clavellinas	0.428	0.575
April Salinetas	April Clavellinas	0.428	0.575

Table S3. Optimal GAM models explaining annual variation in the frond density of *G. abies-marina*.

Models and terms	Estimate	df	t value	F value	P
Total density (D3)					
Intercept	2.254		99.69		<2x10 ⁻¹⁶ ***
Pw	-		-	-	-
s(PAR)	4.345			2.083	0.0007 ***
s(SST)	-			-	-
Non-fertile density (NFD5)					
Intercept	2.14		84.72		<2x10 ⁻¹⁶ ***
Pw	-		-	-	-
s(PAR)	4.953			2.87	5.5x10 ⁻⁵ ***
s(SST)	-			-	-
Fertile density (FD7)					
Intercept	1.36		28.18		<2x10 ⁻¹⁶ ***
Pw	-0.059		-10.45		<2x10 ⁻¹⁶ ***
s(PAR)	8.125			4.893	7.10x10 ⁻⁷ ***
s(SST)	8.571			5.567	7.78x10 ⁻⁸ ***

*P<0.05; **P < 0.01; ***P < 0.001

Table S4. Optimal GAM models explaining annual variation in the frond biomass of *G. abies-marina*.

Model term	Estimate	df	t value	F value	P
Total biomass (B7)					
Intercept	-0.429		-5.899		1.3x10 ⁻⁷ ***
Pw	-0.062		-7.305		4.8x10 ⁻¹² ***
s(PAR)	6.126			4.213	4x10 ⁻⁷ ***
s(SST)	8.302		-	5.316	2.7x10 ⁻⁸ ***
Non-fertile biomass (NFB4)					
Intercept	-1.90		-51.81		<2x10 ⁻¹⁶ ***
Pw	-		-	-	-
s(PAR)	7.427			2.741	0.0004 ***
s(SST)	7.568			2.144	0.004 **
Fertile biomass (FB7)					
Intercept	0.669		22.164		<2x10 ⁻¹⁶ ***
Pw	-0.026		-7.341		3.9x10 ⁻¹² ***
s(PAR)	6.891			3.811	6.9x10 ⁻⁶ ***
s(SST)	8.509			5.027	1.8x10 ⁻⁷ ***

*P<0.05; **P < 0.01; ***P < 0.001

Table S5. Optimal GAM models explaining annual variation in the length of *G. abies-marina*.

Models and terms	Estimate df	T value	F value	P
Adult length (LA11)				
Intercept	0.115	22.56		<2x10 ⁻¹⁶ ***
Pw	0.004	6.691		1.7x10 ⁻¹⁰ ***
s(PAR)	8.195		2.050	0.0065 **
s(SST)	4.687		1.382	0.0103 *
Fertile length (LF10)				
Intercept	17.87	22.844		<2x10 ⁻¹⁶ ***
Pw	-0.675	-7.446		2.1x10 ⁻¹² ***
s(PAR)	6.523		2.634	0.0003 ***
s(SST)	7.784		2.979	0.00015 ***

*P<0.05; **P < 0.01; ***P < 0.001

Table S6. Annual production of *G. abies-marina* fronds. t: time (days), B₁ and B₂ are the biomasses (g dwt m⁻²) at the start and the end of each period, P: production (g dwt m⁻²), r (daily biomass turnover ratio).

Site	Period	t	B ₂	B ₁	P	r
PLC	May 14 – Jun 14	30	6185	3033.3	.	0.024
	Jun 14 - Jul 14	30	5111.7	6185.0	-	
	Jul14 - Aug 14	30	4460	5111.67	-	
	Aug14 –Sep 14	30	3908.3	4460.0	-	
	Sep 14 - Oct 14	30	2811.6	3908.33	-	
	Oct 14 – Nov 14	30	1680.0	2811.67	-	
	Nov 14 – Dec 14	30	1350.0	1680.0	-	
	Dec 14 – Feb 15	60	1653.3	1350.0	303.3	0.003
	Feb 15 – Apr 15	60	2880.0	1653.3	1226.6	0.009
Annual production					4681.7	
CON	May 14 – Jun 14	30	7936.7	6295.0	1641.7	0.008
	Jun 14 - Jul 14	30	8265.0	7936.7	328.3	0.001
	Jul14 - Aug 14	30	6361.6	8265.0	-	
	Aug14 –Sep 14	30	2260.0	6361.6	-	
	Sep 14 - Oct 14	30	3838.3	2260.0	1578.3	0.017
	Oct 14 – Nov 14	30	2471.7	3838.3	-	
	Nov 14 – Dec 14	30	1206.7	2471.7	-	
	Dec 14 – Feb 15	60	1578.8	1206.7	372.1	0.004
	Feb 15 – Apr 15	60	3485.0	1578.8	1906.3	0.013
Annual production					5823.7	
SAL	May 14 – Jun 14	30	9063.33	7536.67	1526.66	0.006
	Jun 14 - Jul 14	30	7926.67	9063.33	-	
	Jul14 - Aug 14	30	5398.33	7926.67	-	
	Aug14 –Sep 14	30	7156.67	5398.33	1758.34	0.009
	Sep 14 - Oct 14	30	5483.33	7156.67	-	
	Oct 14 – Nov 14	30	7968.33	5483.33	2485.00	0.012
	Nov 14 – Dec 14	30	4475.00	7968.33	-	
	Dec 14 – Feb 15	60	4515	4475.00	40	0.0001
	Feb 15 – Apr 15	60	5248.33	4515.00	733.33	0.002
Annual production					6543.33	
CLA	May 14 – Jun 14	30	6228.33	2565.00	3663.33	0.029
	Jun 14 - Jul 14	30	5713.33	6288.33	-	
	Jul14 - Aug 14	30	4348.33	5713.33	-	
	Aug14 –Sep 14	30	5010.00	4348.33	661.67	0.005
	Sep 14 - Oct 14	30	4620.00	5010.00	-	

Oct 14 – Nov 14	30	4610.00	4620.00	-	
Nov 14 – Dec 14	30	2236.67	4610.00	-	
Dec 14 – Feb 15	60	2275.00	2236.67	38.4	0.0003
Feb 15 – Apr 15	60	2386.67	2275.00	111.67	0.0008
Annual production (g dwt m⁻²)				4475.07	
Mean annual frond production (g dwt m⁻²)				5380.95	

Figure S1. Temporal changes in environmental predictors. **(A)** photosynthetically active radiation (PAR, Einstein $s^{-1} cm^{-2}$); **(B)** sea surface temperature (SST, $^{\circ}C$); **(C)** wave power (Pw, $Kw m^{-1}$); **(D)** Chlorophyll a (Chl a, $mg m^{-3}$).

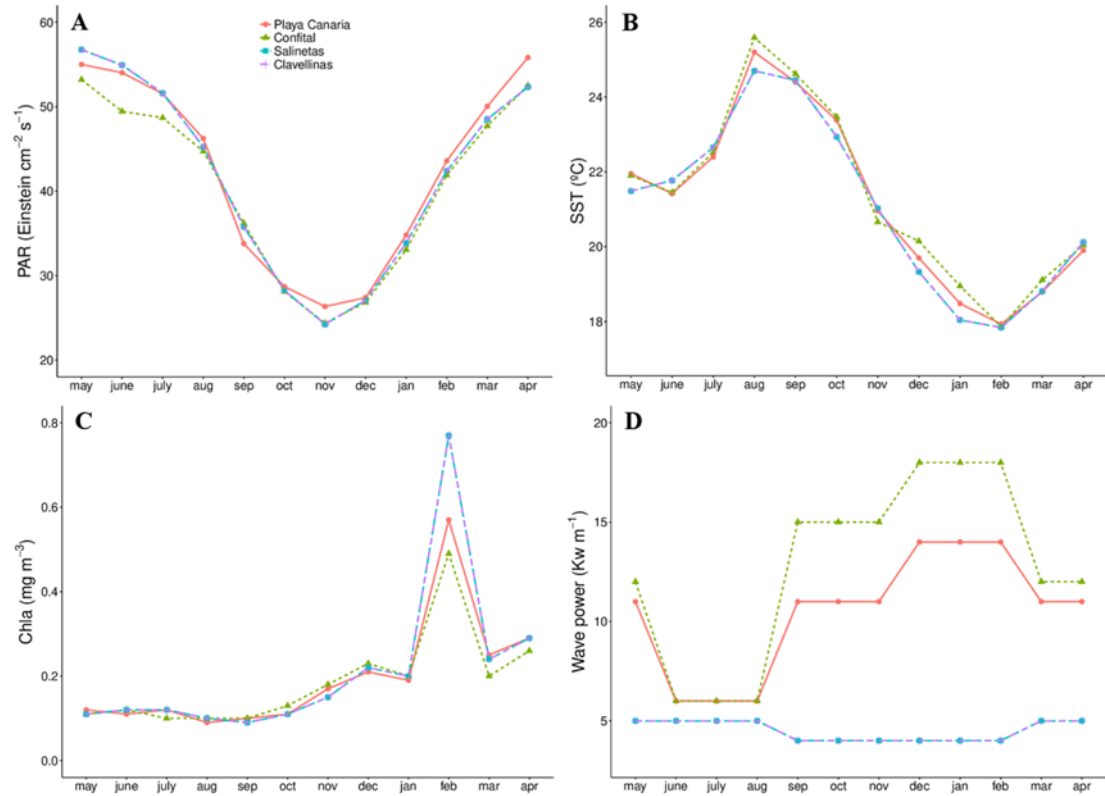
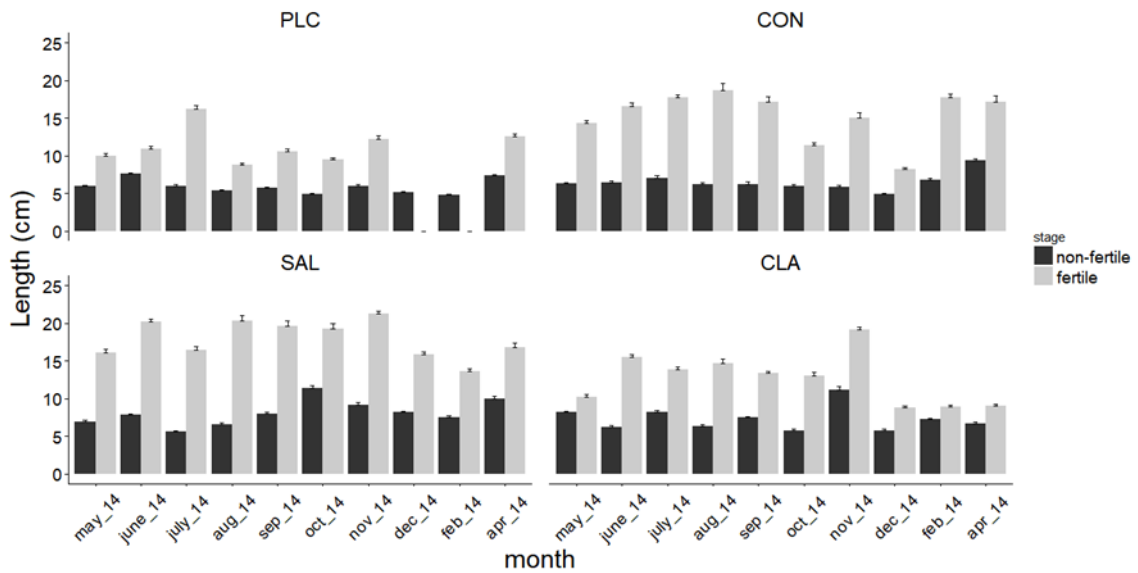


Figure S2. Temporal variations in the frond length of *Gongolaria abies-marina* for each site.



CHAPTER 4. Local and global stressors as major drivers of the drastic regression of brown seaweed forests in an oceanic island

Regional Environmental Change

Local and global stressors as major drivers of the drastic regression of brown seaweed forest in an oceanic island --Manuscript Draft--

Manuscript Number:	REEC-D-23-00746
Full Title:	Local and global stressors as major drivers of the drastic regression of brown seaweed forest in an oceanic island
Article Type:	Original Article
Keywords:	Global change, Conservation, Atlantic, Seaweed, habitat forming, marine heatwaves
Corresponding Author:	Jose Antonio Valdazo, MSc Universidad de las Palmas de Gran Canaria Facultad de Ciencias del Mar Las Palmas de Gran Canaria, Las Palmas SPAIN
Corresponding Author Secondary Information:	
Corresponding Author's Institution:	Universidad de las Palmas de Gran Canaria Facultad de Ciencias del Mar
Corresponding Author's Secondary Institution:	
First Author:	Jose Antonio Valdazo, MSc
First Author Secondary Information:	
Order of Authors:	Jose Antonio Valdazo, MSc Josep Coca, PhD Ricardo Haroun, PhD Oscar Bergasa, MSc María Ascensión Viera-Rodríguez, PhD Fernando Tuya, PhD

Abstract

Similar to other coastal regions worldwide, forests created by brown macroalgae have severely declined in recent decades across the Macaronesian oceanic archipelagos (northeastern Atlantic), eroding the provision of ecosystem services. However, the putative effects of natural and anthropogenic stressors (both local and global) on such declines across spatial and temporal scales remain unresolved. Using data collected from the oceanic island of Gran Canaria (Canary Islands) over the last four decades, we initially investigated the relationship between time series of global (ocean warming, marine heat waves, and solar radiation) and local anthropogenic stressors (levels of local human activity) with changes in the distribution and extent of the canopy-forming brown macroalgae *Gongolaria abies-marina* on the rocky intertidal and adjacent shallow subtidal zones. We also quantified the presence of populations at small scales in two types of microhabitats (“open rock” versus “refugia”). Through herbarium records, we additionally analysed the historical variation in the thallus size of the species. Finally, we experimentally assessed the thermotolerance of embryonic stages to warming. The main environmental drivers explaining the regression of *G. abies-marina* were the increasing number of marine heatwaves, while the number of local human impacts (quantified through the HAPI index) also accounted for further regression in the extent of marine forests. Warming experimentally reduced the survival and size of macroalgal embryos. A progressive miniaturisation of the species, currently restricted to micro-habitat refuges as a survival strategy, seems likely to be the final stage in the progressive disappearance of this macroalgae from the island rocky shores.

Keyword: global change; conservation; Atlantic, seaweed; habitat-forming; marine heatwaves

Introduction

Marine forests created by canopy-forming brown macroalgae (Laminariales, Tilopteriales, and Fucales) globally form highly productive ecosystems on rocky coastlines, increasing structural complexity and providing habitats for associated species (Wernberg and Filbee-Dexter 2019). Macroalgal forests, because of their high primary productivity rates, are important contributors to the benthic carbon cycle of rocky coasts (Krause-Jensen and Duarte 2016), aside from other relevant ecosystem services provided, such as nutrient cycling, food production, nursery habitat and control of water quality (De La Fuente et al. 2019; Eger et al. 2023). In the past half century, however, threats to canopy-forming brown macroalgae have increased in number and severity, leading to a decline in their abundance in many places of temperate latitudes (Mineur et al. 2015; Krumhansl et al. 2016). The loss of macroalgal forests also implies a damage, or impoverishment, in the provision of ecosystem services (Smale et al. 2019). Understanding the causes in declines of macroalgal forests are essential for implementing appropriate conservation and restoration schemes (Coleman and Wernberg 2017).

A combination of natural and anthropogenic stressors often explains the decay of macroalgal forests around the world (Strain et al. 2014; Mineur et al. 2015; Krumhansl et al. 2016). Among these stressors, climate change has become one of the most importance drivers of such global ecological change (Wernberg et al. 2016). Currently, there is evidence that climate change has modified the distribution of species, which has altered the structure and functioning of ecosystems (Pecl et al. 2017). Many species have changed their geographic distribution, colonizing more favourable habitats Vergés et al. 2014; Bevilacqua et al. 2019; Álvarez-Losada et al. 2020), while becoming extinct in areas previously occupied (Gouvêa et al. 2017; de Bettignies et al. 2018; Gurgel et al. 2020). Extreme events of thermal anomalies, in particular Marine Heat Waves (MHWs), have occurred with increasing intensity, frequency, and duration around the world (Hobday et al. 2016; Oliver et al. 2018; Thorat et al. 2022), which abruptly alter the structure and function of marine ecosystems, including forests of brown macroalgae (Wernberg et al. 2016; Straub et al. 2019; Gupta et al. 2020; Smale 2020; Pesarrodonna et al. 2021). Concurrently, local human disturbances, such as habitat destruction, pollution and eutrophication, act cumulatively and even synergistically, amplifying the effects of climate change on coastal habitats (Gouvêa et al. 2017; Orfanidis et al. 2021). From a conservation point of view, it is critical to ascertain, not only the nature of varying factors involved in declines of macroalgal forests, but also their relative contributions, and how these factors alter processes across levels of organization, from physiological effects to ecological interactions (Côté et al. 2016; Duarte et al. 2018).

Chronic warming and MHWs affect the phenology and physiology of macroalgal species creating marine forests, harming their performance, growth, and size (Doney et al. 2012; Smith et al. 2023), increasing their vulnerability to other stressors, and eventually leading to population decline and local extinction (Wernberg et al. 2010, 2016). A large body of literature has evaluated thermal stress on the physiology and biology of brown algae, both for early and adult stages (Andrews et al. 2014; Capdevila et al. 2019; Falace et al. 2021; Verdura et al. 2021). Overall, the pattern that has emerged is a high sensitivity for the early life stages, and a relative ability of adults to survive over broader temperature ranges, physiologically compensating thermal stress (Falace et al. 2021; Verdura et al. 2021). The speed, extent and magnitude of species' range shifts following MHWs, as well as their capacity to recover, are highly variable and may be dependent on species' traits and local and regional processes (Sunday et al. 2015; Smale et al. 2019; Smith et al. 2023). For example, corals, seaweeds, and seagrasses are more sensitive to MHWs than mobile species (Garrabou et al. 2009; Stipcich et al. 2022; Smith et al. 2023), often exhibiting sharp declines after exposure to anomalously high temperatures (Garrabou et al. 2009; Wernberg et al. 2016). Often, due to warming and/or extreme events, species find refuge in cryptic habitats, as a survival strategy, allowing their persistence and recovery, or ultimately as a final stage before its disappearance (Franco et al. 2015; Shay et al. 2021; Verdura et al. 2021; Zarco-Perello et al. 2021; Grimaldi et al. 2023).

Brown macroalgae of the genera *Cystoseira*, *Ericaria* and *Gongolaria* (Fucales, Phaeophyceae), *Cystoseira* sensu lato (s.l), are key components of Mediterranean-Atlantic marine forests, essential for biodiversity and ecosystem functioning (Tuya and Haroun 2006), which have suffered severe declines in the last decades (Thibaut et al. 2005; Blanfuné et al. 2016; Valdazo et al. 2017; Bernal-Ibáñez et al. 2021b). Populations of these species are particularly vulnerable to anthropogenic impacts and, therefore, are indicators of good environmental status (Blanfuné et al. 2017). Across the coasts of the Macaronesian oceanic archipelagos (eastern Atlantic), a range of local human activities have altered coastal habitats (Tuya et al. 2014; Ferrer-Valero et al. 2017; Bernal-Ibáñez et al. 2021b). At the same time, ocean warming has been attributed to have negative effects on brown seaweeds (Sansón et al. 2013; Geppi and Riera 2022), and the occurrence of MHWs has become more frequent and intense in recent decades (Bernal-Ibáñez et al. 2022). In the NE Atlantic coast, the decline and even disappearance of these species have been reported (Friedlander et al. 2017; Valdazo et al. 2017; Bernal-Ibáñez et al. 2021b; Martín-García et al. 2022), and several processes, such as herbivory by sea-urchins, human development, extreme wave events and MHWs have been pointed in this sense (Bernal-Ibáñez et al. 2021a, b; Martín-García et al. 2022).

In this study, we collected data in the oceanic island of Gran Canaria (Canary Islands, eastern Atlantic) through the last four decades, as a regional case-study, to initially link time series of local (levels of local human activity) and global anthropogenic stressors (ocean warming, marine heatwaves and solar radiation) with spatio-temporal decreases in the distribution of the brown macroalgae *Gongolaria abies-marina* on the rocky intertidal and adjacent shallow subtidal. We also compared the presence of *G. abies-marina*, at small-scales, according to local micro-habitat topography (“open rock” versus “refugia”). Through herbarium sheets, we also analysed the historical variation in the thallus size of the species to assess whether miniaturization of the species occurs as a final stage in the regression of the macroalgae. This observational data was then complemented with an experimental assessment of the thermo-tolerance of early stages of this macroalgae to warming. At the end, we aimed to partition the effects of a range of environmental and anthropogenic drivers on the progressive disappearance in marine forests created by *G. abies-marina* at the island scale.

Material and Methods

Target species and historical distribution

Gongolaria abies-marina (S.G. Gmelin) Kuntze is a species of *Cystoseira* s.l. that thrives almost exclusively in the NE Atlantic coasts (Macaronesia and adjacent coasts of north-western Africa) with marginal populations in the western Mediterranean Sea (Ribera et al. 1992). In the Canarian Archipelago, this is a habitat-forming species that created extensive marine forests from the lower intertidal to the shallow subtidal in coasts exposed to high wave action (Tuya and Haroun 2006; Sangil et al. 2011; Martín-García et al. 2022). This is a perennial caespitose macroalgae with no conspicuous holdfast and no stipe, attached to the substratum by small discoid haptera (Gil-Rodríguez et al. 1988; Gomez Garreta et al. 2000). Individuals are monoecious, with male and female gametes housed within the same conceptacle, which are grouped in terminal (apical) receptacles (Gil-Rodríguez et al. 1988). Reproduction is oogamic (large non-motile eggs and biflagellate sperm) and fertilization is external (Guern 1962; Gómez-Garreta et al. 2000). After fertilization, large and free-living zygotes (~70– 100 µm) rapidly sink on the bottom, where they are fixed during the first 12– 24 hr (Verdura et al. 2021). This gives the species a low dispersal ability (< 20 cm; Mangialajo et al. 2012). In the study area, the growth pattern is seasonal (Medina et al. 1997; Valdazo et al. 2021), and reproductive structures are present throughout the entire year, but are more abundant from May to November (Valdazo et al. 2020).

Valdazo et al. (2017) presented the historical distribution of *G. abies-marina* in Gran Canaria (Figs. 1A and 1B) from the 80s to 2016, which included an up-to-date current distribution through

field surveys between 2015 and 2016. Locally, the distribution of populations was categorized as: rare, scattered patches (small patches normally thriving in crevices), abundant patches (large patches forming irregular belts) and continuous belts (wide and continuous belts irrespective of local topography). All *G. abies-marina* populations were geo-localized and recorded on A4 aerial photographs from the IGN (Instituto Geográfico Nacional, 1:2500 scale). Changes in the distribution (Km de coastal perimeter) and extent (occupied area in ha) over time were analysed with the open-source QGIS (<http://www.qgis.org>), using a 1:2500 scale and a WGS-84/UTM Zone 28N coordinate system.

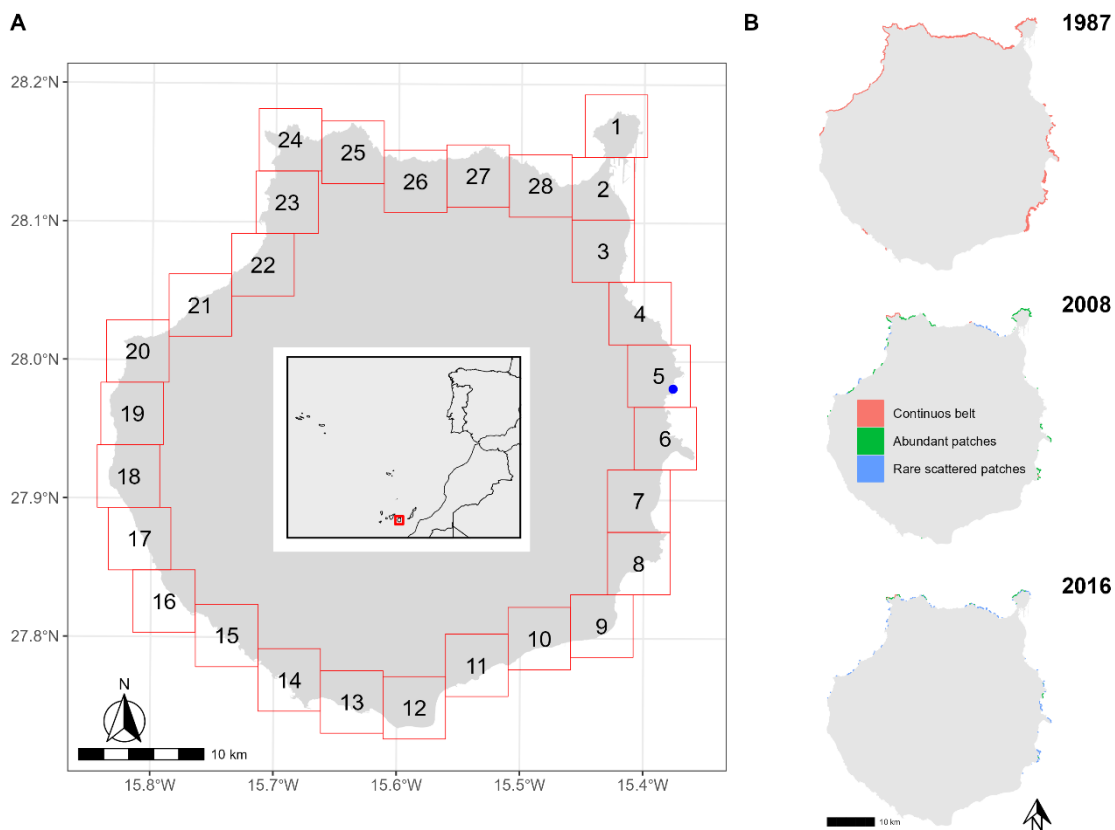


Fig. 1 (A) Location of Gran Canaria Island in the eastern Atlantic and the distribution of the grid used to map the temporal distribution of *G. abies-marina*. The blue dot corresponds to the location of Salinetas, where sample collection of reproductive tissue took place. (B) Historical distribution of *G. abies-marina* around Gran Canaria.

In this study, to relate spatio-temporal changes in the distribution of populations with spatio-temporal changes in local and global stressors, the coast was divided in a grid of (5 x 5 Km) 28 sectors (Fig. 1A), where several environmental drivers were estimated (see below). To operationally link changes in the temporal distribution of *G. abies-marina* with sets of local and global stressors, we finally considered three temporal frames: 1981-1986 (algal distribution data provided by Wildpret et al. 1987; Valdazo et al. 2017), 1987-2007 (Rodríguez et al. 2008), and 2008-2016 (Valdazo et al. 2017).

Small-scale distribution patterns

To describe small-scale patterns in the distribution of *G. abies-marina*, populations were classified into two different micro-habitat types: “open rock” (individuals living in open rocky areas) (Fig. 2A) and “refugia” (individuals living in topographical refuges, e.g., crevices, Fig. 2B), as reported for other brown macroalgae (Franco et al. 2015).

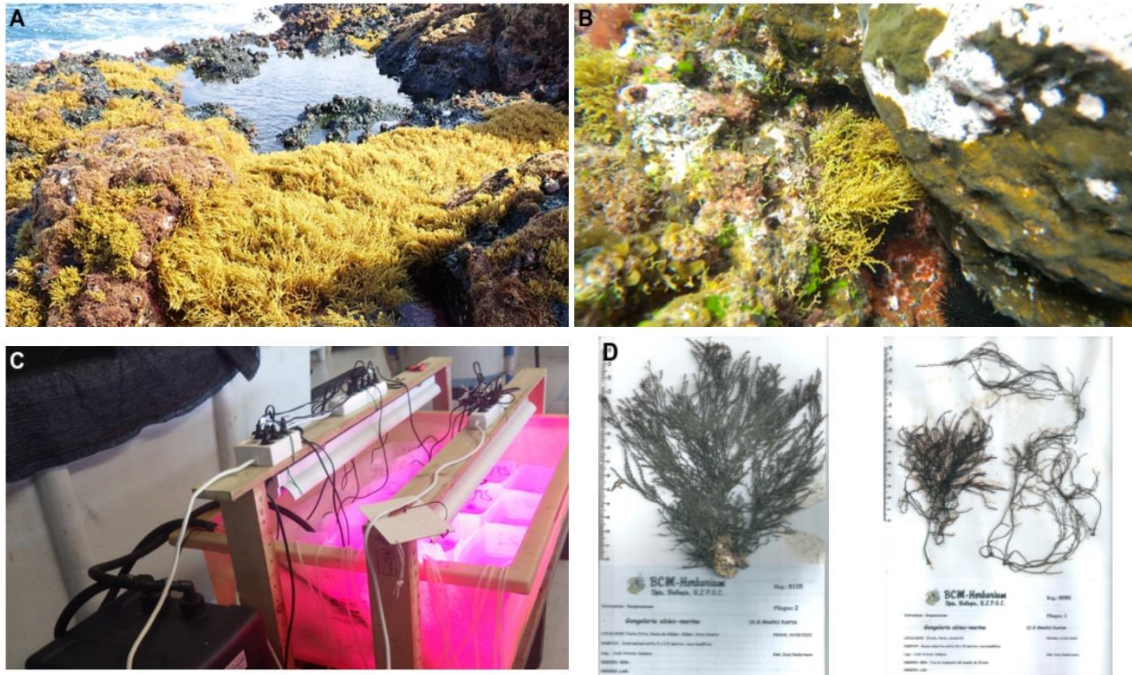


Fig. 2 (A) Large intertidal patch of *G. abies-marina* (“open rock” micro-habitat); (B) presence of *G. abies-marina* in a crevice (“refugia” micro-habitat); (C) Experimental mesocosm where early-stages of the macroalgae were subjected to varying thermal treatments; (D) herbarium sheets of two specimens of the studied macroalgae.

To compare temporal patterns in the local-scale distribution of *G. abies-marina*, we used the proportion occupied in each micro-habitat (“open rock” vs “refugia”) in each sector around the island. A Generalized Mixed-effects Linear Model (GLMM) then tested whether the proportion differed between micro-habitats through times (two-way interaction, ‘time × micro-habitat’). Sector was included as a random effect. The model was implemented in the R ‘glmmTMB’ package (Brooks et al. 2023), as a zero-inflated model with a “beta” error distribution family. Model assumptions were checked through the R ‘performance’ package (Lüdecke et al. 2021). Also, we fitted a linear regression with local distribution data collected in 2016 to test whether the extent (area) occupied by *G. abies-marina* per sector predicted the local proportion of populations in “open rock” and “refugia”.

Local and global environmental drivers

To explain changes in the distribution of *G. abies-marina* over time, we used time series of potential environmental drivers affecting the distribution of the species, according to previous studies on this species (Tuya and Haroun 2006; Sangil et al. 2014; Martín-García et al. 2022) and other brown canopy-forming macroalgae (Álvarez-Losada et al. 2020). Local (small-scale) environmental drivers describe the population-level conditions throughout the study area, such as coastal geomorphology, exposure to waves, and anthropic pressures. Whereas global environmental drivers here refer to climatic conditions that account for global warming, extreme events, and variation solar radiation.

Local geomorphology and wave energy

We used the digital terrain model from the eco-cartographic study of Gran Canaria Island (M.M.A. 2001, 2005), which delimitate the type of coastal substrates between 0 and 50 m depth, to obtain the surface and length of the rocky substrate, for each sector, as well as the slope and orientation (eastness and northness) along the island coastal perimeter. We calculated variables describing the structure of the shallow rocky bottom using QGIS and the R 'sf' (Pebesma 2023) and 'terra' (Hijmans 2023) packages. Data on wave energy were obtained from Losada et al. (2010); we used the average annual wave power (kW m^{-1}), for each of the 28 sectors, by using values at 20 m depth downscaled to a resolution of 0.05° .

Local anthropogenic drivers

Because local human activities may account for declines in the presence of brown macroalgae (Blanfuné et al. 2017; Orfanidis et al. 2021), we used the Human Activities and Pressures Index (HAPI, Blanfuné et al. 2017), previously adapted by Valdazo et al. (2017) to the study area. The index includes three metrics for both terrestrial and marine human-related pressures (see Table S1 for sources and metrics). For terrestrial pressures (presence of urban, industrial and agricultural areas), the three metrics were calculated as the percentage area covered in each 5 x 5 Km sector (data from CORINE Land Cover, available at <https://land.copernicus.eu/pan-european/corine-land-cover>). For marine pressures, we calculated the level (percentage) of shoreline artificialization, and the level of aquaculture facilities and sewage effluents to the sea, both calculated as the percentage of shoreline, by considering a 500 m radio circle around each facility within each 5 x 5 Km sector. This information was obtained from the Spatial Data Infrastructure of the Canary Islands (<https://www.idecanarias.es/>). The HAPI index was calculated over the three time periods (1990, 2006 and 2018; Table S1 and Fig. S1), which approximately correspond to the historical distribution data of *G. abies-marina* here considered.

Climatic drivers

We collected long-term satellite-derived data from Copernicus Marine Environment Monitoring Service (CMEMS, <https://www.copernicus.eu/>) and the European Centre for Medium-Range Weather Forecast (ECMWF, <https://www.ecmwf.int/>) for three climatic variables: Sea Surface Temperature (SST), Surface Solar Radiation Downwards (SSRD) and Ultraviolet Radiation (UV) (see Table S2 for details). SST data were used, not only to describe spatio-temporal patterns in SST (Fig. S2), but to detect monthly SST anomalies and MHWs, which were defined as periods when daily mean temperatures exceeded the 90th percentile (relative to the baseline climatology) for at least five consecutive days (Hobday et al. 2016; Oliver et al. 2018). We calculated four metrics for each climatic driver: the slope, mean, standard deviation and maximum value for each of the three time periods (1981-1986, 1987-2007 and 2008-2016) in each of the 28 sectors (Figs. S3 to S5). In addition, daily SST was used to quantify seven key MHW metrics: (a) the number of events in each period, (b) the duration of the events (number of days), (c) the variability (standard deviation) of the duration (d) the mean intensity (the mean temperature anomaly relative to the climatological, seasonally-varying, mean, in °C), (e) the variability (standard deviation) of the intensity (f) the maximum intensity (the maximum temperature anomaly relative to the climatological, seasonally-varying, mean, in °C) and (g) the cumulative intensity (integrated temperature anomaly over the season/year, in °C x days) (Fig. S6). Metrics of MHWs were calculated using the R 'heatwaveR' package (Schlegel and Smit 2018).

Effect of predictor variables on *Gongolaria abies-marina* distribution

We implemented Generalized Linear Models (GLMs) to explore the relative contribution of predictor environmental drivers on spatio-temporal changes in the area (ha) covered by *G. abies-marina* across the 28 sectors around the island perimeter. To prevent collinearity among predictors, we selected those of a larger biological significance among those that were significantly correlated. A cut-off threshold of 0.7 was used in all cases (Zuur et al. 2009). Firstly, a correlation analysis was carried out between those geomorphological drivers consistent through time (Fig. S7). Northness and eastness were not included in further modelling, as both significantly correlated with wave power and slope. Then, separate correlation analyses were implemented for metrics of each climatic predictor (Figs. S8 to S12) and uncorrelated metrics of climatic predictors (Fig. S13). A final correlation matrix between each pair of predictors including geomorphological and climatic was obtained (Fig. S14). Because mean values of UV and SSRD significantly correlated with wave power, these metrics were not considered in the model selection approach.

A model selection approach was implemented, through the R ‘MuMIn’ package (Barton 2023), by considering those uncorrelated predictors (Table 1). Initially, all possible combinations were included using the “dredge” function (Tables S2 and S3). All models were subsequently ranked according to the Akaike Information Criterion corrected for small sample sizes (AICc), and importance weights (w_i) obtained for each model. Then, we estimated potential collinearity among predictors via Variance Inflation Factors (VIF) using the ‘car’ R package (Fox and Weisberg 2008). Finally, we performed a multimodel averaging to consider model selection uncertainty (Table S4). We also estimated the relative importance of each predictor variable, as the sum of the Akaike weights over all possible models. All models were fitted with a “Gaussian” error distribution family and a “log” link function. Model assumptions were checked via the R ‘performance’ package (Lüdecke et al. 2021) and the Breusch-Pagan heteroscedasticity test.

Table 1. Summary of environmental predictors, obtained for each of the 28 sectors across the island perimeter of Gran Canaria Island, finally implemented in the model selection statistical approach.

Predictors	Type	Variation
Surface of the rocky shore	Geomorphological	Spatial
Length of the rocky shore		
Wave power		
Slope of the rocky shore		
HAPI Index	Local stressors	
Nº of MHWs		Spatio-temporal
SD in the duration of MHWs	Global stressors	
Maximum values of SSRD		

Survival and growth of early stages

In October 2015, during the autumn reproductive peak of *G. abies-marina* (Valdazo et al. 2020), healthy apical fronds, including ca. 3-5 cm length of mature receptacles, were collected from the intertidal at Playa Salinetas, Gran Canaria (27°58'49.5"N, 15°22'34.6"O; Fig. 1). Receptacles were wrapped with seawater-wetted towels and placed in plastic bags without seawater, and rapidly transported to the laboratory under cold and dark conditions. The bags were then stored in the fridge (at 4°C and dark conditions) to promote subsequent gametes liberation (Irving et al. 2009). After 24 h, the same biomass of receptacles (~10 gr FW) was placed in fifteen 5 L aquaria, where ten microscope slides (75 x 26 mm) were set on the bottom, as a substrate for zygote settlement. To examine the effects of temperature on survival and growth of early stages, five temperature treatments were established: 18, 20, 22, 24 and 25°C, with 3 replicated 5 L aquaria for each treatment. Temperatures were chosen to reflect the annual temperature range and MHWs in the study area (Fig. S15). The photoperiod was set to a 12:12 h light: dark cycle. Light was

provided by two 20 W LED light bars (LD1034011, LEDBOX), supplying $125 \mu\text{mol m}^{-2} \text{s}^{-1}$. All aquaria contained filtered seawater, which was renewed every 2 days, and was vigorously aerated using 200 mm air stones. All tanks were immersed in a “cool bath” held at 17-18°C by a TECO TR10 chiller unit. Except for the 18°C treatment, all aquaria kept their temperature stable using 50 W adjustable Jager aquarium heaters, calibrated using multi-parametric sensors. Temperature and salinity were daily monitored.

At the start of the experiment, receptacles were suspended on the surface of each aquarium with a 1 mm plastic mesh for 24 h to induce the release of gametes; after this time, receptacles were discarded to avoid interference with zygote settlement. After 1, 5, 11, 14 and 25 days, 2 randomly selected settlement slides were collected from each aquarium. Survival of germlings was then evaluated, i.e., each embryo was considered either dead or alive, and the size (μm^2) of 10 random germlings from each slide measured (Fig. S16). Germlings that had structurally collapsed, or failed to attach, were considered dead. The size of embryos was assessed via the ‘ImageJ’ software (ImageJ, NIH US Department of Health and Human Services) after taking photographs through a microscope (Leica, DM1000, Berlin, Germany).

To quantify the effect of temperature on survival and growth of germlings, we fitted GLMMs, with a “binomial” family error distribution and a “logit” link function, and a “Gamma” family error distribution and a “log” link function, respectively. We included date as a random factor. Models were fitted through the R ‘glmmTMB’ package (Brooks et al. 2023). We assessed the significance of model terms using Wald chi-squared and F tests (Zuur et al. 2009); model assumptions were checked via the R ‘performance’ package (Lüdecke et al. 2021). For multiple comparisons, we applied the Tukey test using ‘emmeans’ package (Lenth et al. 2023).

Temporal changes in frond size

We compiled a frond size database from herbarium vouchers (Fig. 2D), deposited in the BCM (Depart. of Biology, University of Las Palmas, <http://www.geoportal.ulpgc.es/herbariobcm/>), from 1990 to 2021, which included a total of 145 measured thallus at 10 sites around Gran Canaria Island. Thallus length was measured from the base to the apex (Riera et al. 2015; Geppi and Riera 2022) of entire fronds with the help of the ImageJ software. Temporal changes in frond size were analysed using a General Additive Model (GAM), fitted using “cubic regression” splines through the R ‘mgcv’ package (Wood 2010), which captured strong non-linear temporal patterns. The basis dimensions “k” of the smoothers was limited to five, to avoid overfitting and ensure monotonic relationships. The model was visually inspected for residual patterns.

Results

Historical distribution and drivers of decline

Overall, populations of *G. abies-marina* have progressively disappeared during the last four decades around Gran Canaria Island (Fig. 1B). This alga dominated the intertidal and shallow rocky shores of the entire island in the 1980s, where a continuous belt extended along 120.5 km of the coastline and occupied 928 ha. In the first decade of the 21st century, fragmented populations were found along 52.2 km of the coastline and occupied 12.6 ha. Finally, in 2016, this species was found along 37.8 km of the coastline and occupied only 7.4 ha, mainly as scattered patches.

Results of the model selection (Table S3, $R^2 = 91.4\%$) initially identified that the surface (Estimate = 0.0009, $P = 1e^{-07}$) and length (Estimate = 0.0142, $P = 0.046$) (Table S4, Fig. 3) of the rocky coast positively influenced the area covered by *G. abies-marina*, i.e., the larger the presence of rocky habitat, the larger the area occupied. Wave power positively influenced the area covered by *G. abies-marina* (Estimate = 0.02, $P = 0.079$), while the reverse was observed for the slope of the rocky coast (Estimate = -0.214, $P = 9e^{-05}$) (Table S4, Fig. 3).

The number of MHWs affected negatively the area covered by *G. abies-marina* (Estimate = -0.027, $P = 2e^{-16}$), while the maximum SSRD showed a positive effect on the area (Estimate = 0.000003, $P = 0.0016$) (Table S4, Fig. 3). Both were selected as the most important environmental predictors driving variation in the area of *G. abies-marina* through scales of spatial (i.e., across sectors) and temporal (i.e., time periods) variation. The number of local human impacts (i.e., HAPI index) also significantly contributed to explain the decay in the area covered by the macroalgae across scales of spatial and temporal variation (Estimate = -0.052, $P = 0.002$, Table S4, Fig. 3).

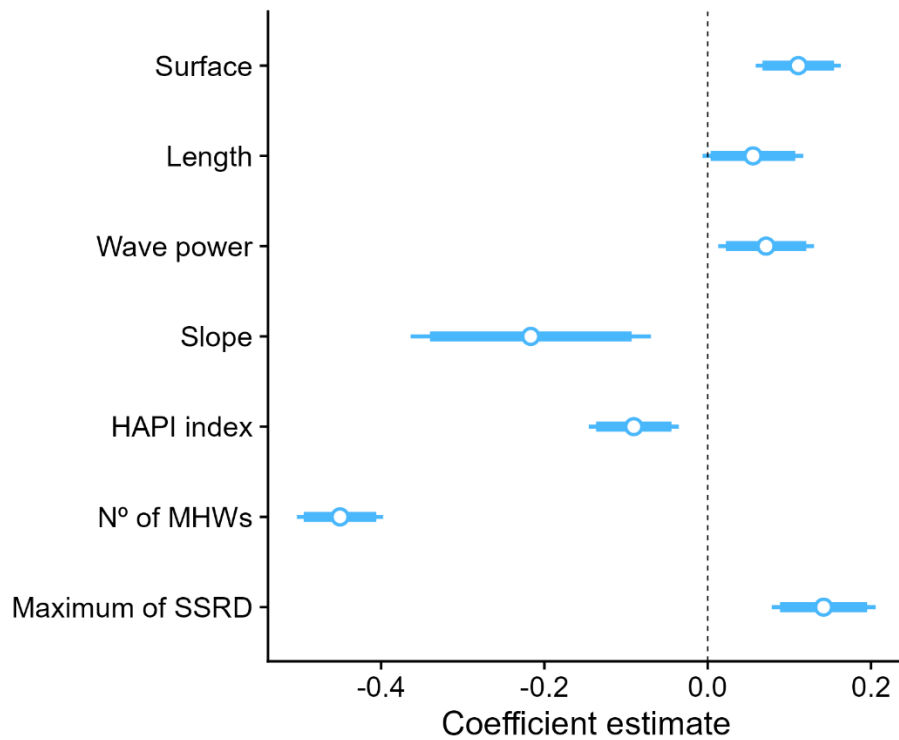


Fig. 3 Estimates for each predictor variable of the more parsimonious model explaining spatio-temporal variation in the area of *G. abies-marina* around Gran Canaria Island. Blue dots are means of coefficients and blue bars are $\pm 95\%$ confidence intervals.

Small-scale distribution patterns

We observed a significant temporal change in the proportion of *G. abies-marina* (Fig. 4A, B) in each micro-habitat ('time period x micro-habitat', $P = 2.2e^{-16}$, Table S5). While in the 1980s and early 2000s, most individuals were locally present in "open rock", individuals in 2016 were majorly in "refugia". In 2016, the local presence of *G. abies-marina* in "open rock" increased with the extent (area) of the macroalgae in each sector (Fig. 4C, $P = 8e^{-4}$, Table S6), while a reversal pattern was observed for the presence of the macroalgae in "refugia" (Fig. 4D, $P = 8e^{-4}$, Table S6).

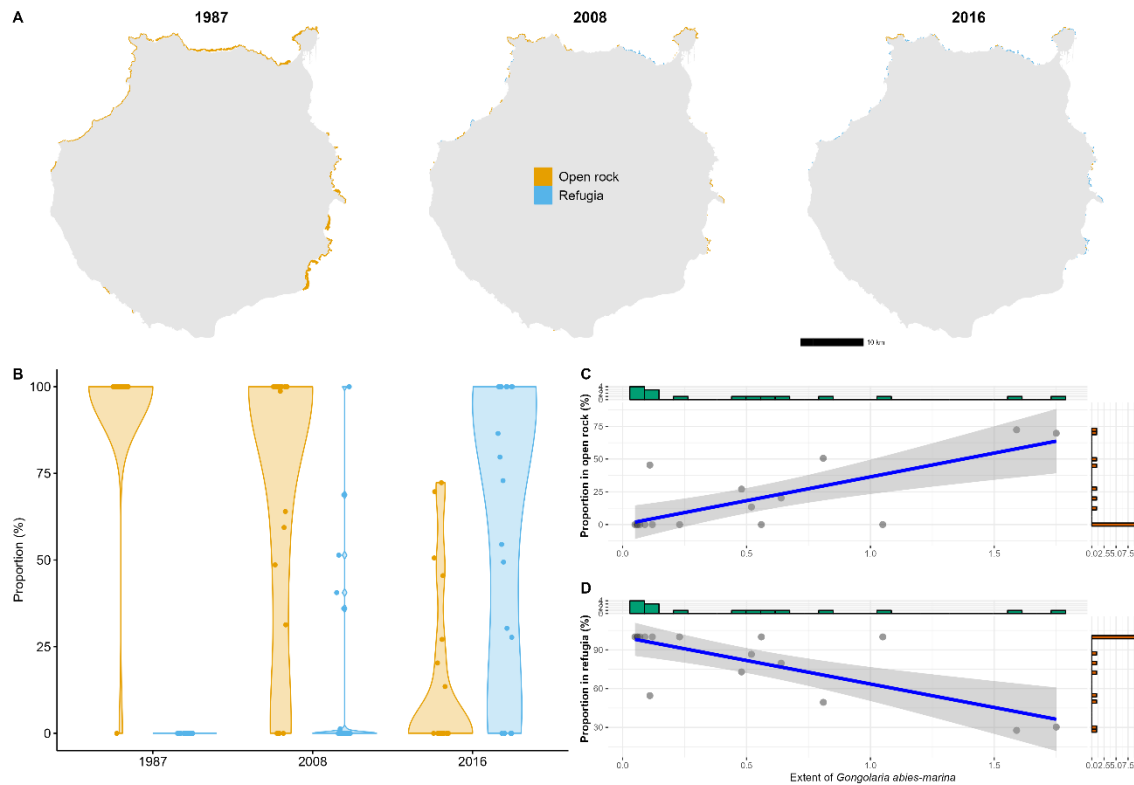


Fig 4 (A) Distribution and (B) proportion of *G. abies-marina* at two local micro-habitat types (“open rock” and “refugia”) through time periods. Linear fit between the proportion of *G. abies-marina* in (C) “open rock” and (D) “refugia” and the area (extent) occupied by the macroalgae in each of the 28 sectors around Gran Canaria in 2016.

Survival and size of early stages

Both survival and size of algal embryos was significantly affected by sea water temperatures ($P = 2.2e^{-16}$, Table S7, Fig. 5A, B). Despite the survival of embryos progressively decreased through the experimental time for all treatments (Fig. 5A), a large reduction in survival ($< 25\%$) was observed for those treatments at 24° and 25°C (Fig. 5A, Table S8). Similarly, embryos at 24°C and 25°C showed smaller sizes relative to 18 , 20 and 22°C (Table S9; Tukey tests, $P = 0.001$ for all pairwise comparisons).

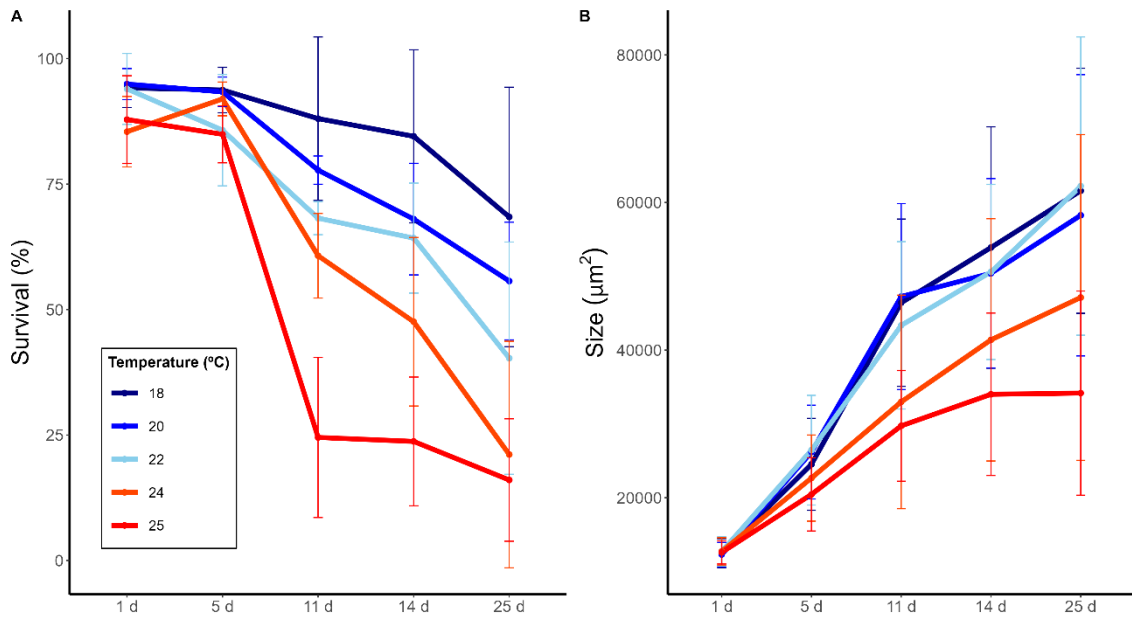


Fig 5 (A) Survival (B) and size of algal embryos according to thermal treatments through the 25 days experiment. The errors bars show confidence intervals (\pm SD) around means.

Temporal changes in frond size

The macroalgal frond size progressively decreased through time, with the fitted GAM depicting a sharp decrease since 2010 onwards (Table S10, Fig. 6; 9.35% of total explained deviance).

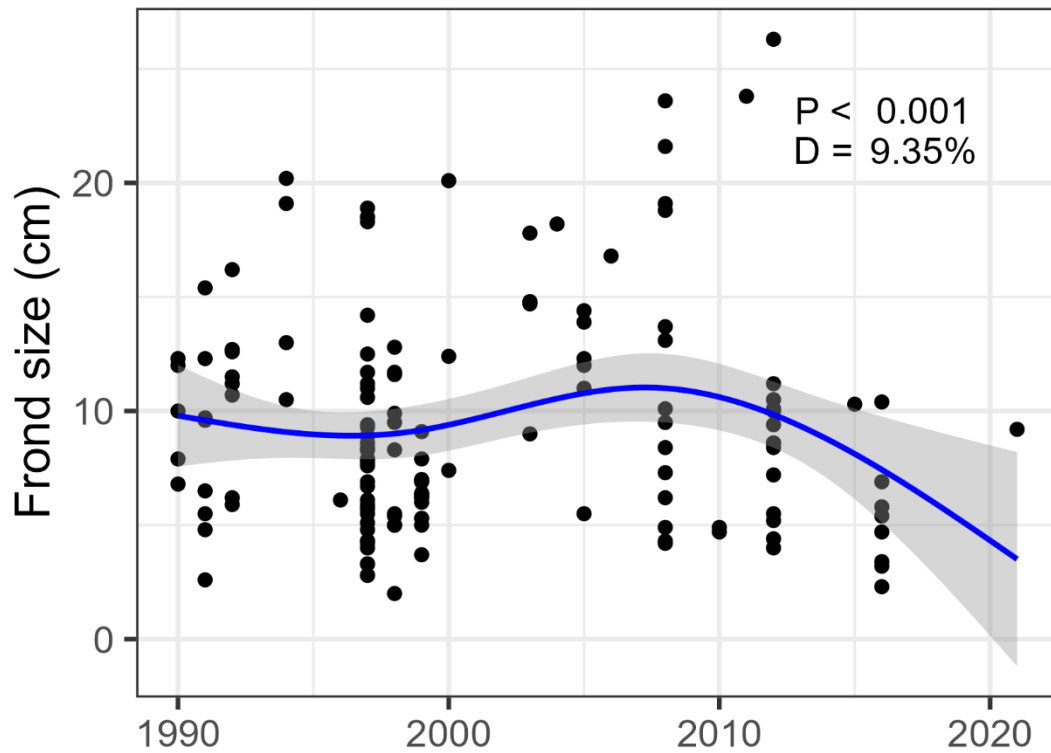


Fig 6. Changes in *G. abies-marina* frond size over the last three decades in Gran Canaria Island. The blue line represents the fitted (smooth) GAM function, and the grey shaded area a 95% confidence interval.

Discussion

Results obtained by this study has improved our knowledge on the causes of marine forests decline in the Northeast Atlantic, where only a few algal species have been adequately evaluated over decades, due to a lack of historical information (Blanfuné et al. 2016; Filbee-Dexter and Wernberg 2018). Our study is relevant because historical data on the distribution and extension of *G. abies-marina*, together with times series of environmental stressors and human pressures, allowed us to elucidate the causes, and their relative weights, on such historical changes. Our study showed that the area covered by *G. abies-marina* around Gran Canaria Island followed a declining trajectory over the last decades (1987-2016), which was mainly related to a combination of human-driven environmental stressors operating at both global and local scales. Results from the early stages thermo-tolerance assay, together with the increased severity in MHWs, provide solid evidence to explain declines of *G. abies-marina*, as reported for sibling species from the Mediterranean (Falace et al. 2021; Verdura et al. 2021). Along most of the rocky coasts of Gran Canaria, there is a considerable probability that *G. abies-marina* is functionally near extinction, in accordance with what has occurred in other islands of the Canary (Martín-García et al. 2022) and Madeira archipelagos (Bernal-Ibáñez et al. 2021b). These fragmented populations, in Gran Canaria Island, mostly persist in topographic micro-habitats, where they find small-scale refugia, as reported for other large brown macroalgae (Franco et al. 2015; Shay et al. 2021; Grimaldi et al. 2023).

According to our modelling, the most extensive forests of *G. abies-marina* developed along the east and southeast of Gran Canaria, where the large surface and length of the rocky coast (i.e., gently slopes) receives considerable solar irradiance (SSRD). However, current populations that persist are found in the north and northwest coast, under high wave energy regimens and low anthropogenic pressures. Our model selection approach showed that the main environmental predictor of temporal changes in the extent of *G. abies-marina* forests was the increase in the number of MHWs. Our best candidate model explained a considerable amount of spatio-temporal variability (91.4%), even without including biotic drivers. However, there is sufficient evidence that increased coastal impacts (habitat destruction, pollution, eutrophication, overfishing, etc.), coupled with ocean warming and MHWs, increase severity of biotic drivers on brown macroalgae, such as grazing by sea-urchins and fishes, and competition from massive turf development (Vergés et al. 2014; Filbee-Dexter and Wernberg 2018; Roma et al. 2021; Mancuso

et al. 2022). It is possible that, in combination with those stressors included in our model selection approach, several biotic stressors not considered here (e.g., overgrazing, increased competition with invasive species and turfs) are concurrently involved with additive or even synergistic effects.

Superimposed to decadal-scale increases in mean coastal temperatures (Espino et al. 2019), MHWs are increasing in frequency, duration, and intensity in Gran Canaria Island, with a sharp increase in the number of events since the late 1980s (Fig. S6). In the first period (1981-1986), the mean number of events per sector was 0.32 (0.05 events per year); in the second period (1987-2007), the mean number of events was 37.11 (1.85 events per year); and in the last period (2008-2016), the average number of events was 26.67 (2.67 events per year). This pattern does not only occur for the number of MHWs, but also for their duration and intensity (Fig. S6), with likely effects on the physiology and phenology of *G. abies-marina*, impairing their performance and increasing their vulnerability to other stressors, as pointed out for similar species (Gouvea et al. 2017; de Bettignes et al. 2018; Bernal-Ibañez et al. 2021b). These trends are consistent with those observed globally (Oliver et al. 2018; Thorat et al. 2021) and in the Macaronesian region (Bernal-Ibañez et al. 2022). In addition, warming also influences the appearance of tropical herbivorous fish (Vergés et al. 2014; Zarco-Perello et al. 2021), invasive species (Mancuso et al. 2022), the expansion of algal species with tropical affinities (Sangil et al. 2012) and the rise of turfs that compete for space with brown macroalgae (Pesarrodona et al. 2021). In the study region, there is a relationship between large abundances of the key herbivorous sea-urchin *Diadema africanum* and overfishing of natural predators (Tuya et al. 2004a), which created large sea-urchin barrens (Tuya et al. 2004b). In recent years, however, this herbivore has suffered massive mortalities (Hernández et al. 2020).

Although the HAPI index did not show significant temporal differences between the three temporal periods, human pressures on the coast were higher in the 2000s and 2010s (Fig. S1). Our model selection approach also included the HAPI index, mostly to explain spatial differences in the presence of *G. abies-marina*. In turn, current remaining populations persist in those sectors of the coast under less local anthropogenic pressures (north and northwest), but also where wave exposure is maximum. The value of the HAPI index in the 1980s was calculated with land use data corresponding to the 1990s and discharge censuses from 2003, so the value of the HAPI index, in this first period, may be overestimated; for this reason, there is no evidence of a temporary change in local anthropic pressures. In any case, as a result of the emergence and rapid rise of the tourist industry, urban expansion in Gran Canaria took place at a fast pace, with a more or less constant rate of construction since the 1960s–1970s (García-Romero et al. 2023).

The first records of the disappearance of *G. abies-marina* subtidal forests begin in the early 1990s (Medina and Haroun 1994); at this time, anthropogenic pressures were already high in the Canary Islands, because of 20-30 years of intense urban development on the coast. The artificialization of the coast, and concurrent increased pollution and eutrophication of nearshore waters, for example due to wastewater discharges during that time, could have affected the resilience of *G. abies-marina* populations. This has been advocated to explain the erosion in the extent of other “foundation” species in the study area, such as the seagrass *Cymodocea nodosa* (Tuya et al. 2014).

We here determined the thermal tolerance thresholds of the early stages of *G. abies-marina*, showing that higher temperatures affected the performance of germlings. In particular, we found a tolerance threshold of 24°C, from which the survival and size of the embryos notably decreased. These results agree with studies in similar shallow-water *Cystoseira* s.l. species from the Mediterranean Sea, such as *Ericaria selaginoides* (Linnaeus) Molinari & Guiry (Campos-Cáliz et al. 2019) and *Ericaria crinita* (Duby) Molinari & Guiry (Verdura et al. 2021). For these species, the tolerance threshold was 28°C; they are species adapted to higher temperatures than those from the NE Atlantic. On the contrary, our results contrast with the thermal optimum of *Ericaria giacconeii* D. Seri & G. Furnari, which requires lower temperatures (12-15°C) than other *Cystoseira* s.l. (Falace et al. 2021).

In general, adults of brown macroalgae are more tolerant to high temperatures than their early-life stages (Román et al. 2020; Verdura et al. 2021; Falace et al. 2021). However, these studies have also pointed to the presence of thermal thresholds for adults. In the case of *Ericaria crinita*, when a threshold of 28°C is surpassed, there is a sharp decline in the reproductive biomass, which seems more sensitive to thermal stress than other parts of the thallus (Verdura et al. 2021). This is particularly relevant for intertidal macroalgae under direct contact with the atmosphere at low tides because they can suffer simultaneous atmospheric and marine heatwaves (Román et al. 2020). Since *G. abies-marina* can thrive in the low intertidal, it is plausible that concurrent atmospheric and marine heatwaves can notoriously erode apical branches with receptacles, in particular if this occurs in the reproductive season, as we here detected for MHWs (Fig. S15). This would lead to massive mortality of zygotes and embryos, thus defeating the reproductive efforts of the species. Furthermore, the negative effects of warming and MHWs on recruitment could be exacerbated by other stressors that have been shown to negatively affect the early developmental stages of *Cystoseira* s.l., such as herbicides, pollutants (de Caralt et al. 2020) and grazing (Monserrat et al. 2023). Successful recruitments of new individuals may be a critical bottleneck for the population persistence of large brown seaweeds

(Schiel and Foster 2006). If the duration and intensity of MHWs exceeds certain thresholds, it can lead to decreased population densities, fragmentation and, ultimately, survival in refugia, as our results seem to indicate. In this sense, the frond size of the species has been decreasing in recent decades. Because the size of the thallus determines the species' reproductive performance, i.e., the amount of biomass allocated to reproductive structures (Valdazo et al. 2020), a progressive decrease in the size (i.e., miniaturization) of *G. abies-marina* puts the viability of the populations at risk, due to a reduction in the reproductive efforts.

In conclusion, our results evidenced that increasing MHWs in a context of global warming, coupled with increasing human activities along the coastal zone, had major impacts on macroalgal forests created by *G. abies-marina*. This information is pertinent to identify appropriate management actions at local scales to halt losses of marine forests. Reducing local stressors, while maintaining favourable environmental conditions, and prioritizing cooler areas of ideal habitat availability (i.e., large rocky areas with gently slopes) for conservation, are useful management approaches. Such actions can, to some extent, reduce the susceptibility of this habitat-forming furoid species and their associated communities to MHWs intensification in upcoming decades.

Supplementary material

Table S1. Sources of information to calculate the HAPI index at different times, e.g., the Corine Land Cover (CLC) (<https://land.copernicus.eu/pan-european/corine-land-cover>). The census of sewage outfalls began in 1998, so there is no data prior to 1990, and data from the 2003 census were used as a proxy for 1987 period. For aquaculture facilities, historical data was extracted from the Strategic Plan for Aquaculture in the Canary Islands (PEACAN, 2014-2020) and IDE Canarias (www.idecanarias.com).

Period	Pressures	Metric	Source
1987	Terrestrial	All	CLC 1990
	Marine	Artificialization	Historical photographs https://idecan2.grafcan.es/ServicioWMS/Fototeca?
		Aquaculture facilities	PEACAN
		Sewage effluents	Effluents survey 2003
2008	Terrestrial	All	CLC 2006
	Marine	Artificialization	Historical photographs https://idecan2.grafcan.es/ServicioWMS/Fototeca?
		Aquaculture facilities	PEACAN
		Sewage effluents	Effluents survey 2008
2016	Terrestrial	All	CLC 2018
	Marine	Artificialization	Current photographs https://idecan1.grafcan.es/ServicioWMS/OrtoExpress?
		Aquaculture facilities	https://idecan2.grafcan.es/ServicioWMS/Acuicultura?
		Sewage effluents	Effluents survey 2021

Figure S1. HAPI index for each of the three time periods.

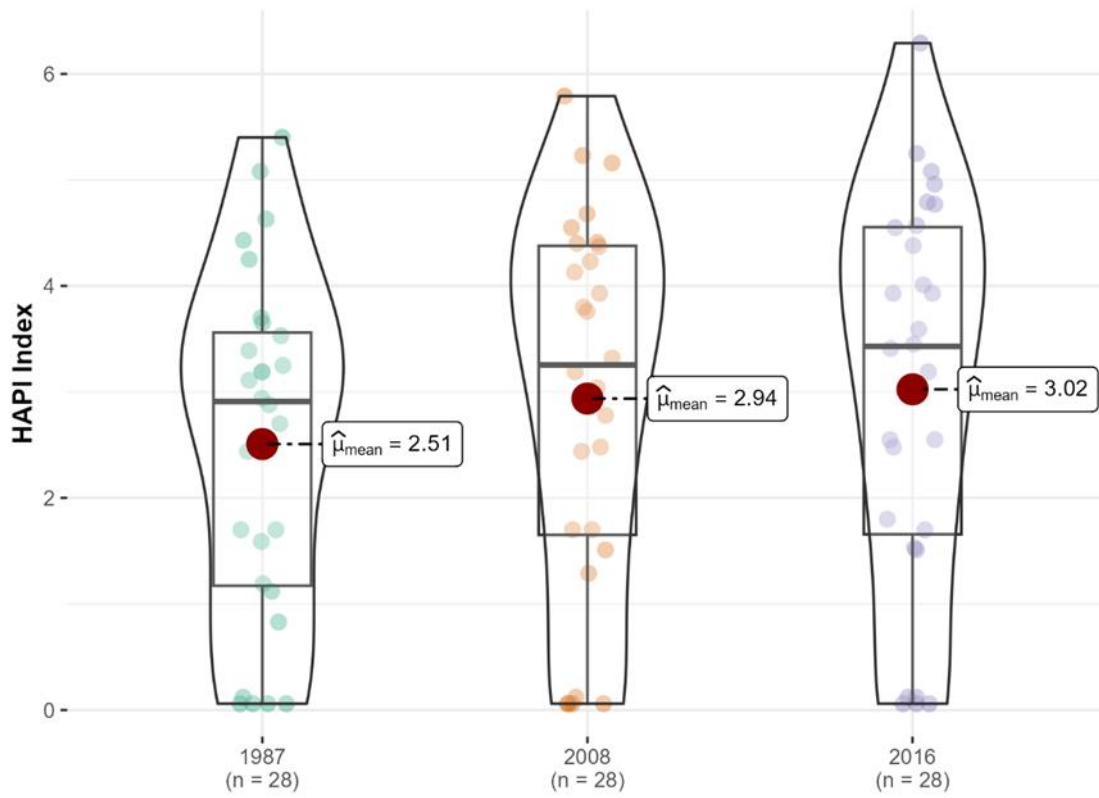


Table S2. Climatic drivers and derived metrics used in the study were provided by the Copernicus Marine Environment Monitoring Service (CMEMS, <https://www.copernicus.eu/en>) and the European Centre for Medium-Range Weather Forecast (ECMWF, (<https://www.ecmwf.int/>)). ERA5 is the 5th generation ECMWF atmospheric reanalysis of the global climate, covering the period from January 1940 to the present. ERA5 is produced by the Copernicus Climate Change Service (C3S) at ECMWF.

Driver	Source	Frequency	Unit	Spatial resolution	Temporal resolution	Metrics
SST	Satellite gap-free CMEMS (010_011 and 010_001 products)	Daily	°C	0.05°	1981/10/01-2022/12/31	Slope, mean, standard deviation, maximum value
SSRD	ECMWF Reanalysis (ERA5)	Daily	J/m ²	0.25°	1981/10/01-2022/10/31	Slope, mean, standard deviation, maximum value
UV	ECMWF Reanalysis (ERA5)	Daily	J/m ²	0.25°	1981/10/01-2022/10/31	Slope, mean, standard deviation, maximum value
Anomalies of SST	Derived from CMEMS daily SST	monthly		0.05°	1981/10/01-2022/12/31	Slope, mean, standard deviation, maximum value
MHWs	Derived from SST	Daily		0.05°	1981/10/01-2022/12/31	N° events, duration, mean intensity, maximum intensity, cumulative intensity

SST: Sea Surface Temperature

SSRD: Surface Solar Radiation Downwards

UV: Ultraviolet Radiation

MHW: Marine Heat Waves

Figure S2. Metrics of patterns in daily SST for each of the three time periods.

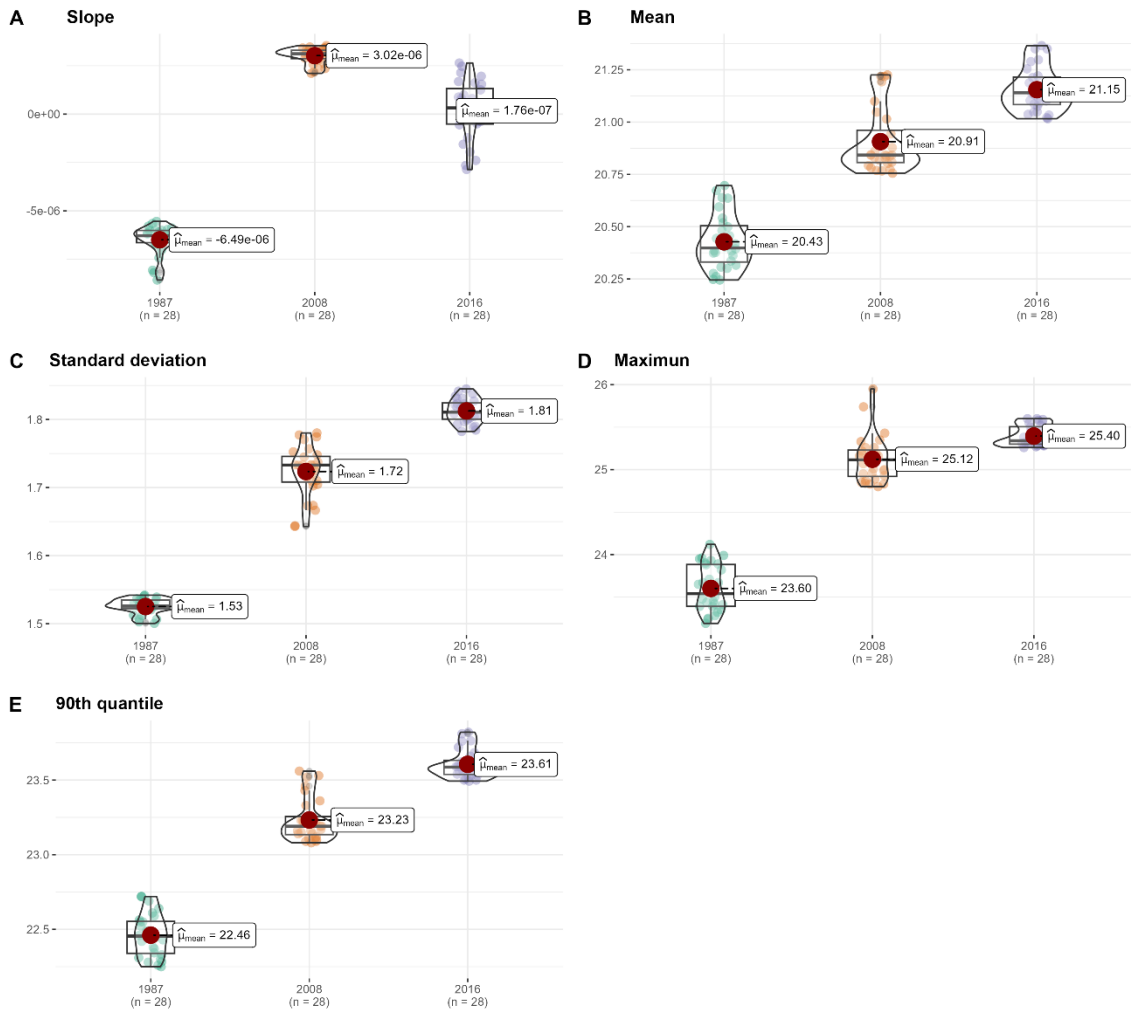


Figure S3. Metrics of patterns in monthly SST anomalies for each of the three time periods.

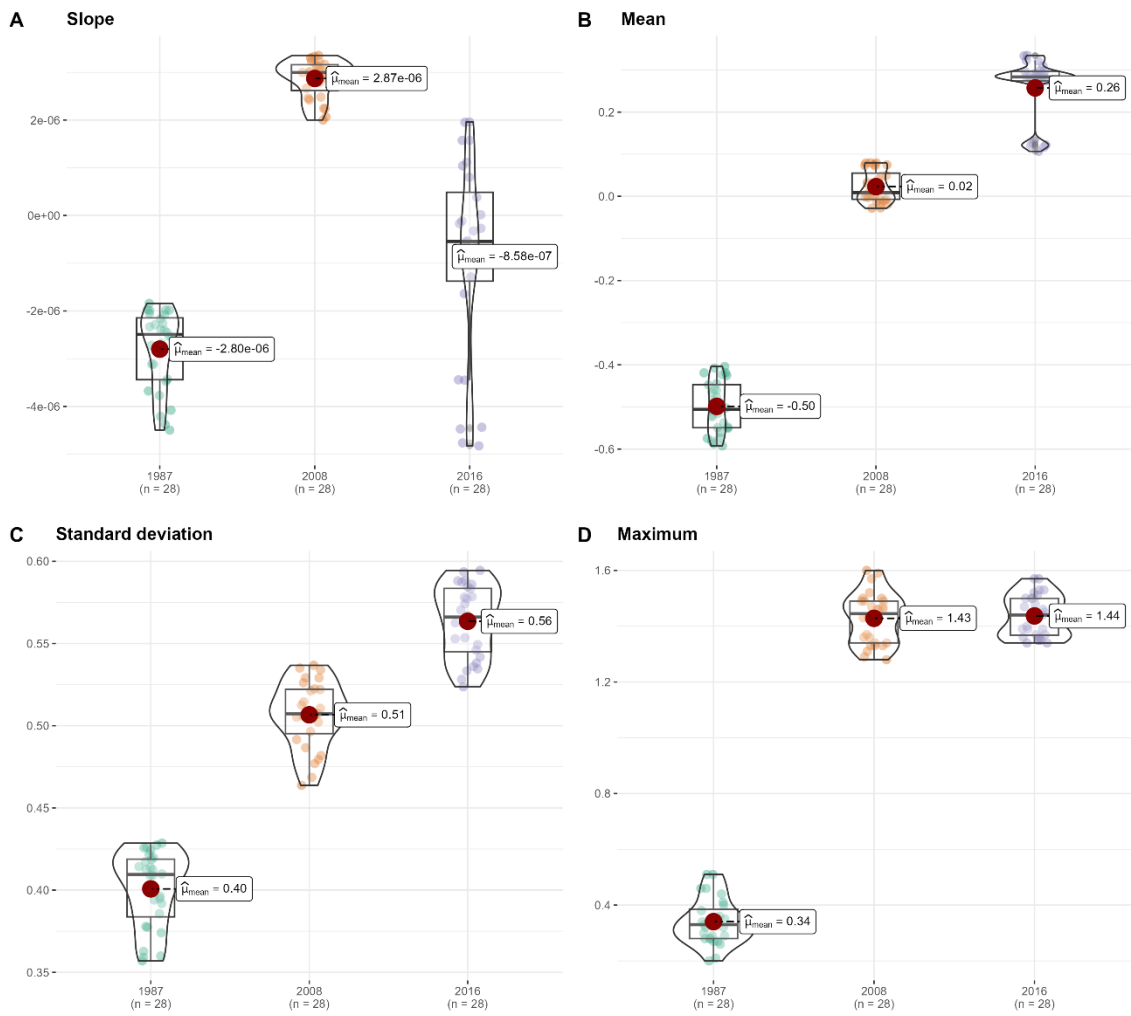


Figure S4. Metrics for patterns in UV radiation for each of the three time periods.

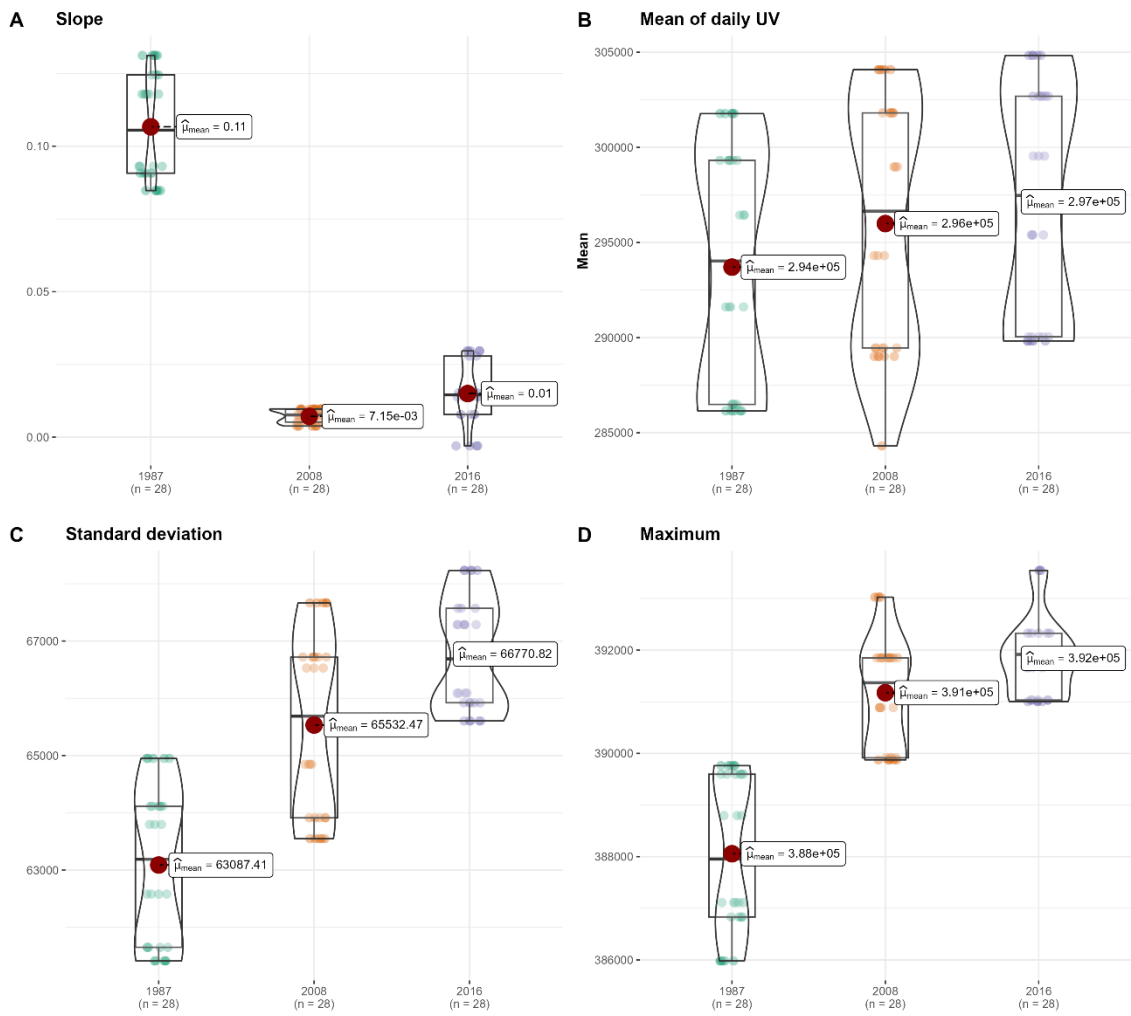


Figure S5. Metrics for patterns in SSRD for each of the three time periods.

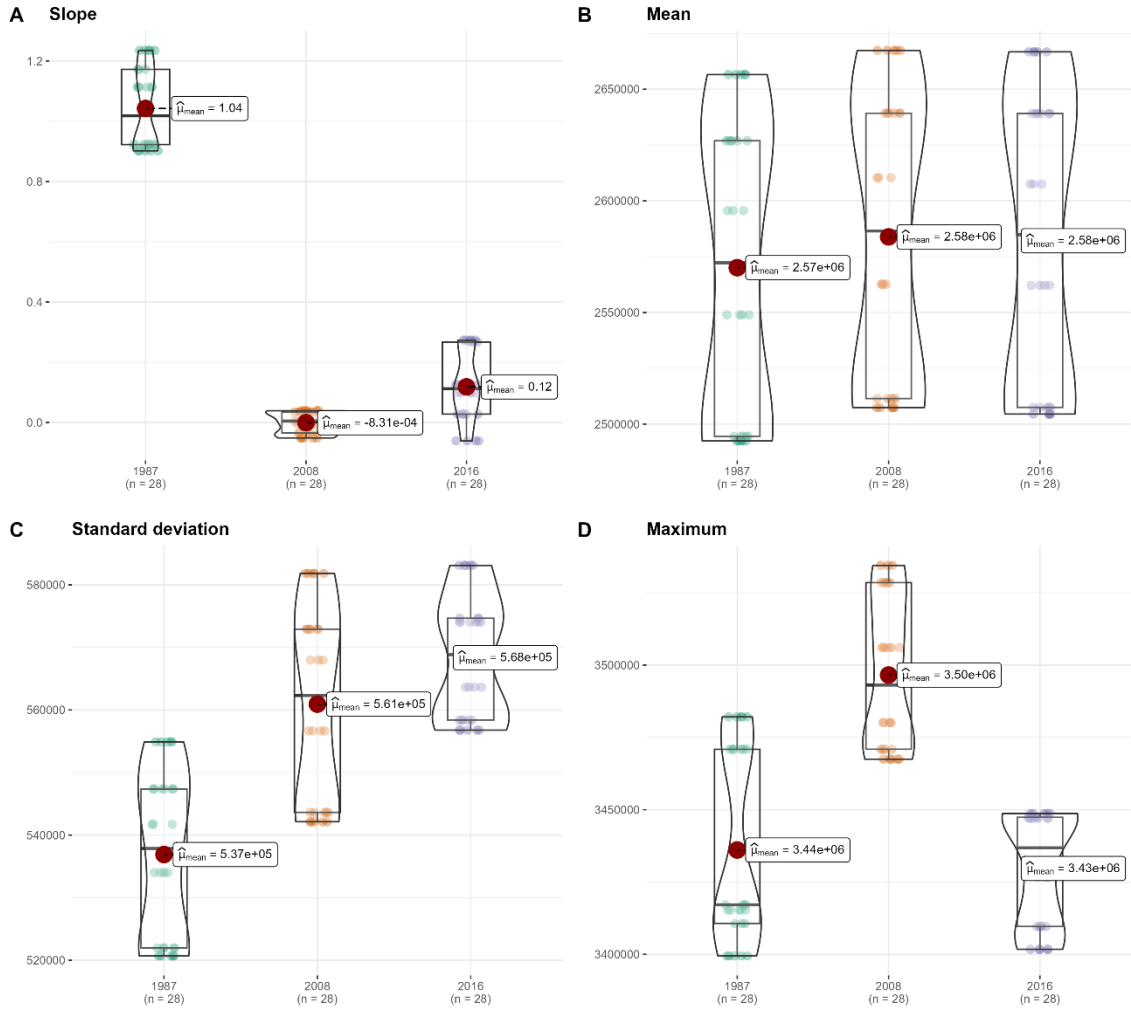


Figure S6. Metrics of patterns in MHWs for each of the three time periods.

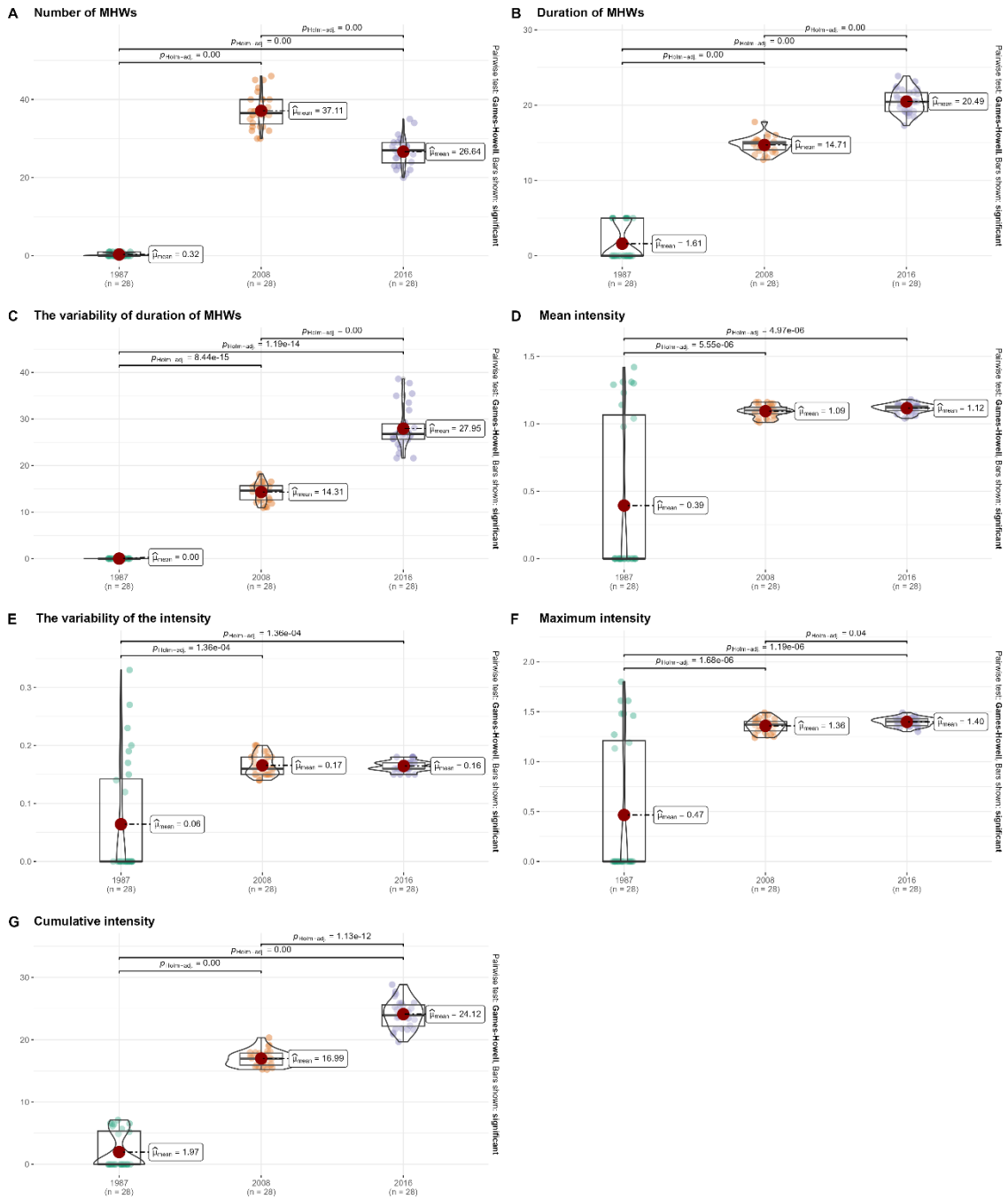


Figure S7. Correlation analysis of geomorphological predictor variables.

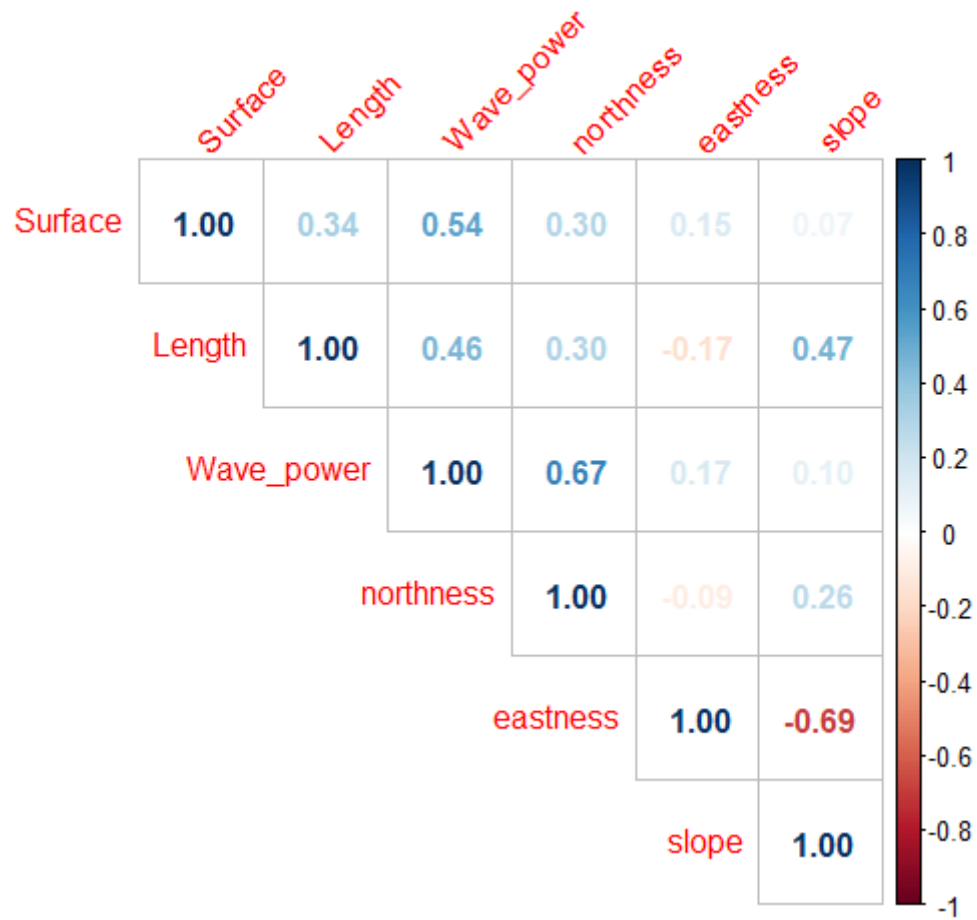


Figure S8. Correlation analysis of daily SST metrics.



Figure S9. Correlation analysis of monthly SST anomalies.

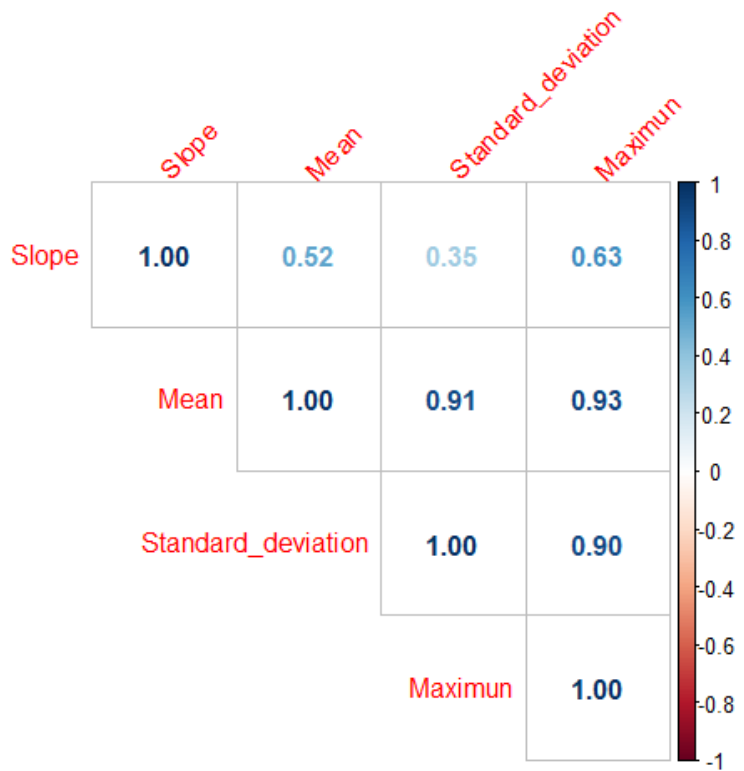


Figure S10. Correlation analysis of UV radiation metrics.

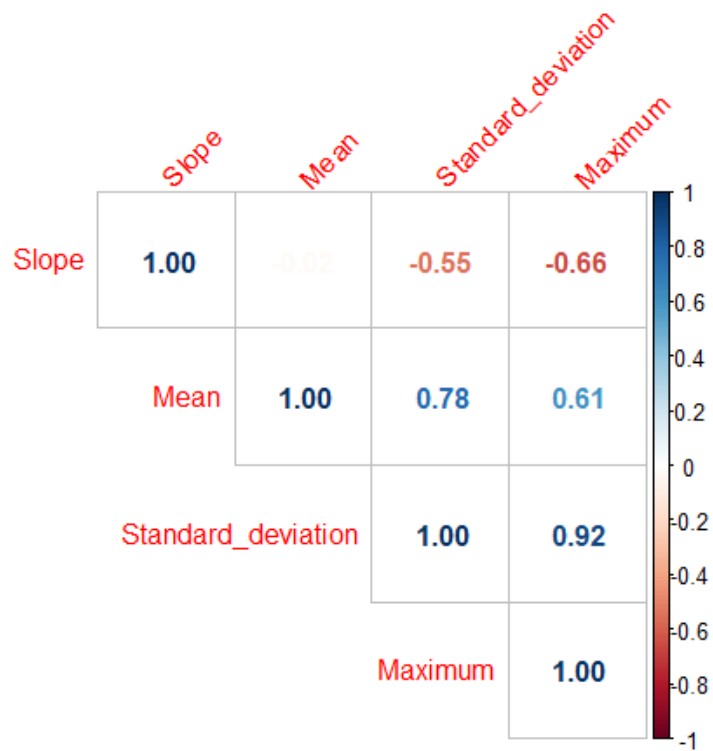


Figure S11. Correlation analysis of SSRD radiation metrics.

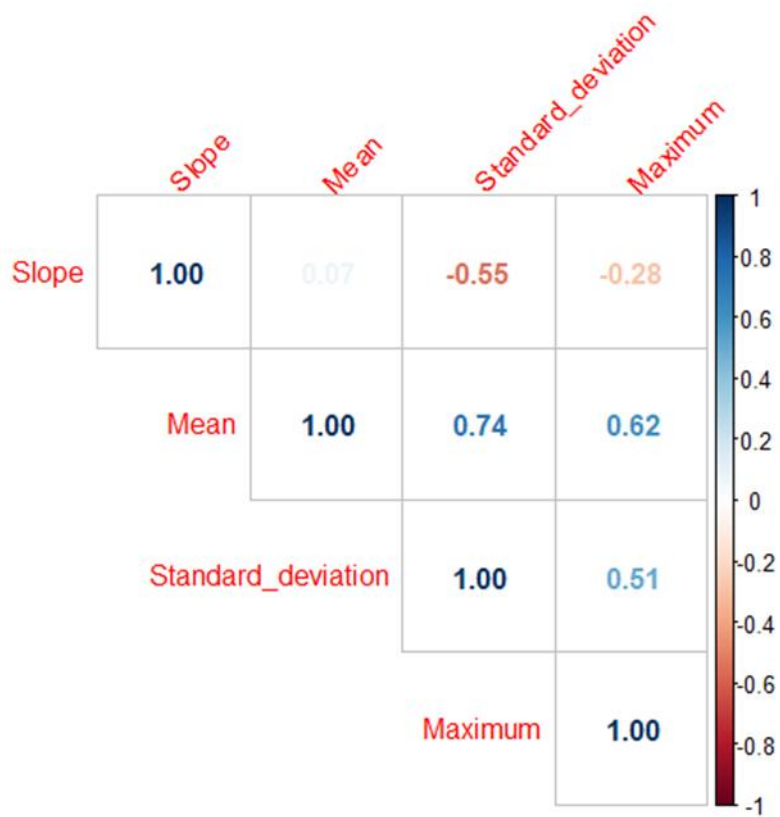


Figure S12. Correlation analysis of MHWs metrics.

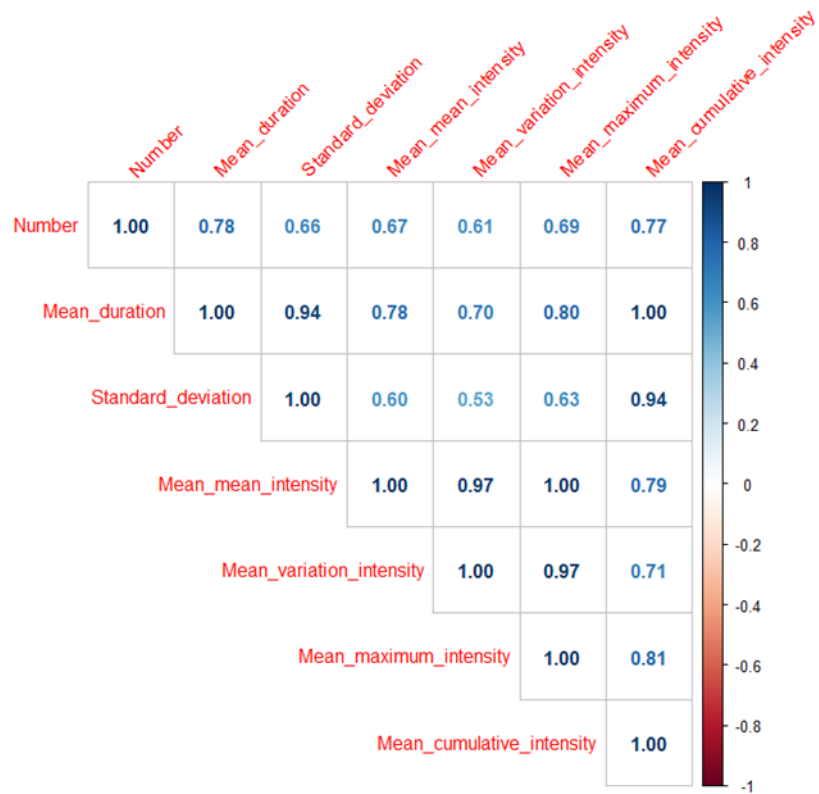


Figure S13. Correlation analysis of climatic metrics.

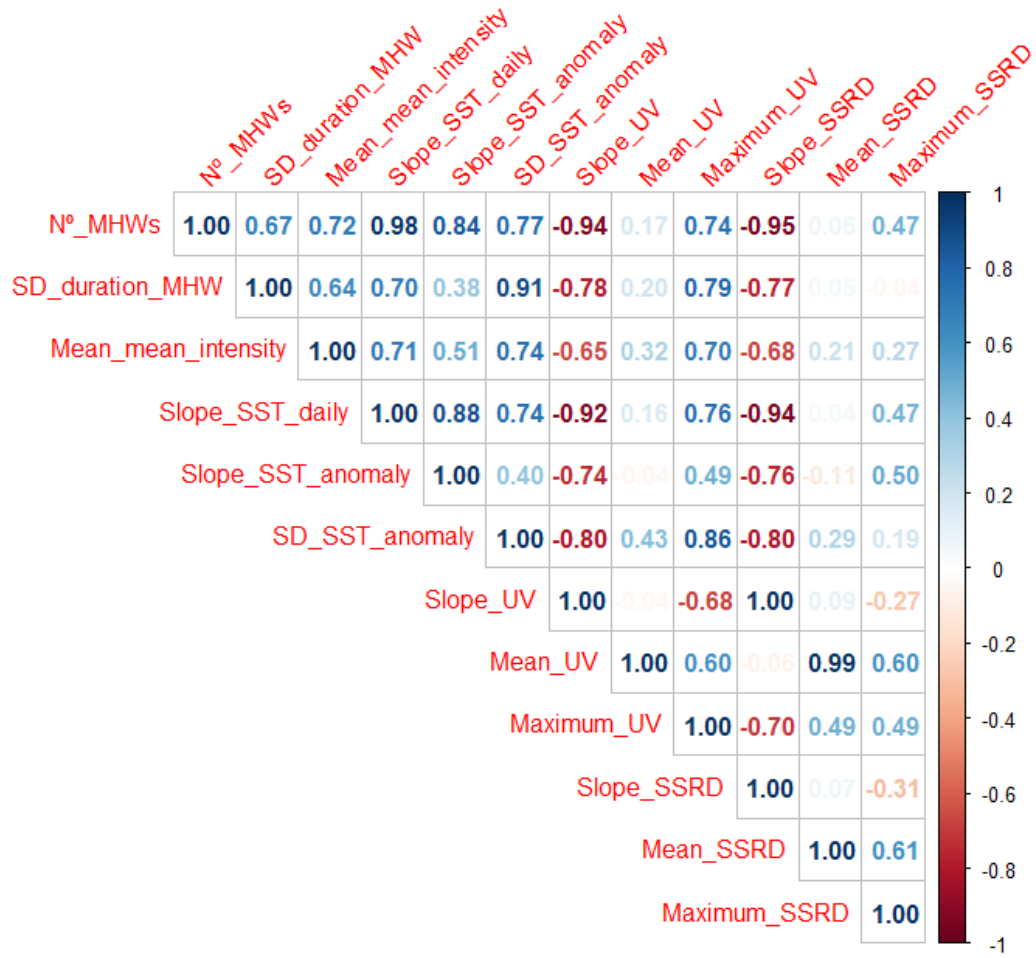


Figure S14. Correlation analysis of geomorphological and climatic variables.

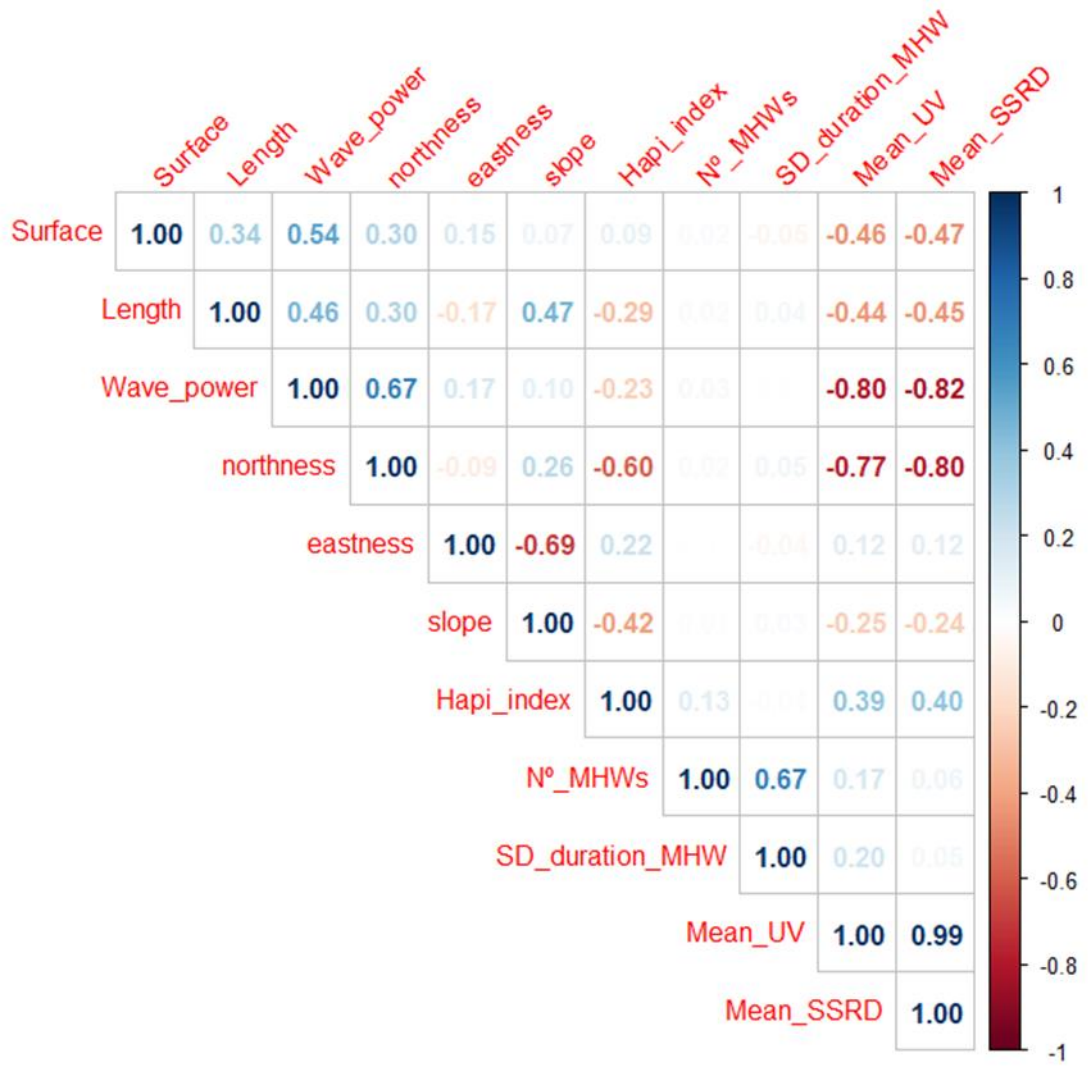


Figure S15. Annual mean climatology for the last 40 years in Gran Canaria Island. Thresholds to define MHWs are included with red and green dots showing the maximum and mean sea water temperatures (pooled by months), respectively.

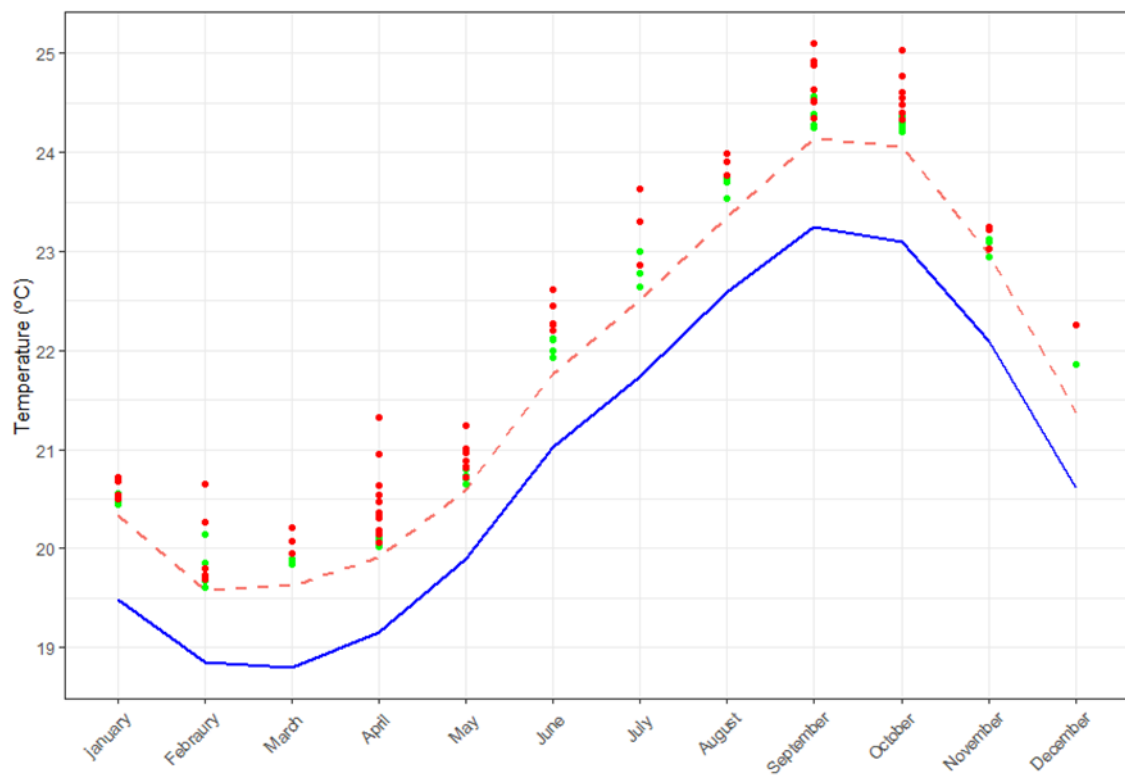


Figure S16. Algal embryos after (A) 1, (B) 5, (C) 14 and (D) 25 days.

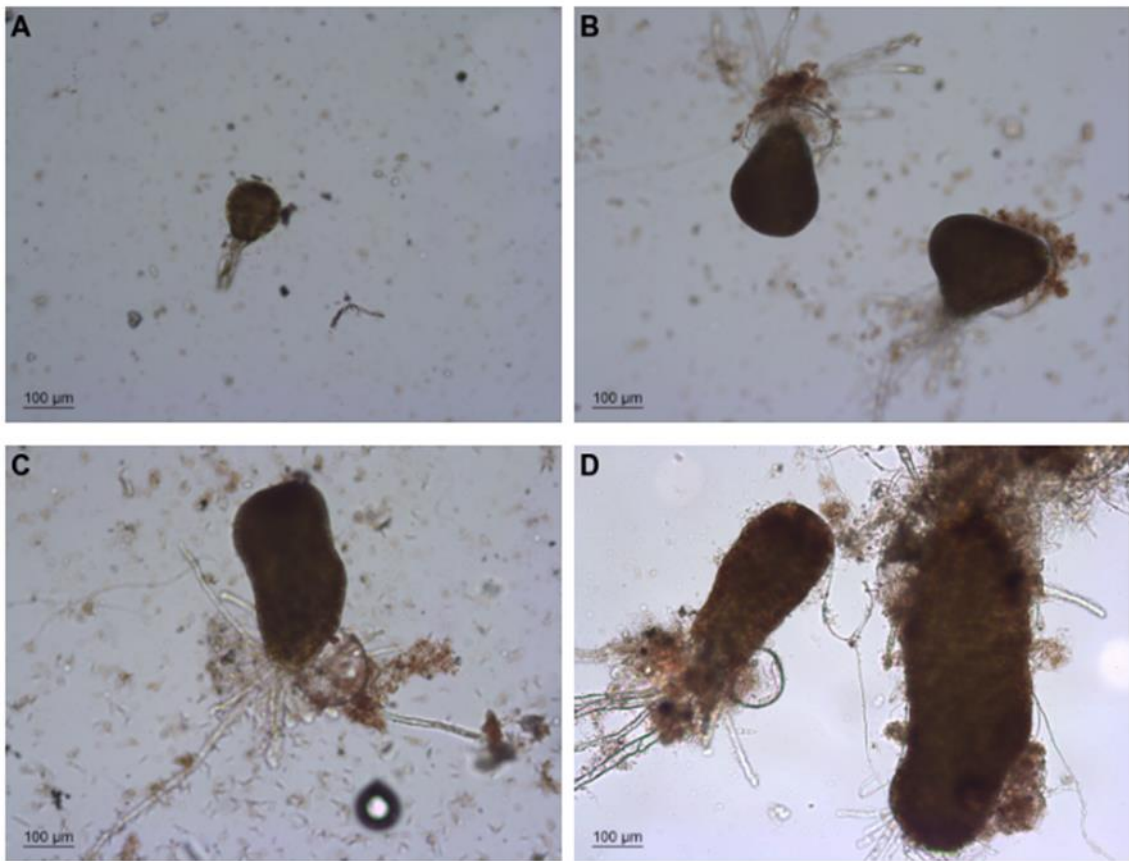


Table S3. Results of the model selection approach using the “dredge” function from the ‘MuMIn’ package. The 20 most parsimonious models are included, ranked according to the AICc, for a total combination of 256 models.

Models	Df	LogLik	AICc	Δ	Weight (Wi)
Surface + Length + Slope + Wave power + Hapi index + N ^o MHW + Maximum of SSRD	9	8.048	5.5	0.00	0.538
Surface + Length + Slope + Wave power + Hapi index + N ^o MHW + Maximum of SSRD + SD of duration of MHW	10	8.780	6.9	1.43	0.264
Surface + Length + Slope + Hapi index + N ^o MHW + Maximum of SSRD + SD of duration of MHW	9	5.981	9.6	4.14	0.068
Surface + Slope + Wave power + Hapi index + N ^o MHW + Maximum of SSRD +	8	4.254	10.3	4.81	0.049
Surface + Length + Slope + Hapi index + N ^o MHW + Maximum of SSRD	8	3.933	11.0	5.45	0.035
Surface + Slope + Wave power + Hapi index + N ^o MHW + Maximum of SSRD + SD of duration of MHW	9	4.949	11.7	6.20	0.024
Surface + Length + Slope + Hapi index + N ^o MHW + SD of duration of MHW	8	2.293	14.2	8.73	0.007
Surface + Slope + Hapi index + N ^o MHW + Maximum of SSRD + SD of duration of MHW	8	1.848	15.1	9.62	0.004
Surface + Slope + Hapi index + N ^o MHW + Maximum of SSRD	7	0.218	16.6	11.09	0.002
Surface + Slope + Hapi index + N ^o MHW + SD of duration of MHW	7	0.377	16.9	11.40	0.002

Table S4. Results of the multimodel averaging following model selection to address the relative importance of environmental variables to predict spatio-temporal variation in the area occupied by *G. abies-marina* along the coastal perimeter of Gran Canaria Island. Significant predictors ($P < 0.05$) are highlighted in bold.

	Estimate	Adjusted SE	Z value	P-value	Relative importance
Surface	0.0009	0.00017	5.353	1e⁻⁰⁷	1.00
Slope	-0.214	0.0545	3.924	9e⁻⁰⁵	1.00
N^o MHWs	-0.027	0.000314	8.503	2e⁻¹⁶	1.00
HAPI index	-0.052	0.0145	3.598	0.0003	1.00
Maximum of SSRD	0.000003	0.000001	3.212	0.001	0.99
Length	0.014	0.007	1.994	0.046	0.92
Wave power	0.02	0.0114	1.758	0.079	0.88
SD in the duration of MHWs	-0.00188	0.0035	0.0537	0.591	0.37

Table S5. Summary of GLMMs testing whether the proportion of *G. abies-marina* populations differed between micro-habitats (“open rock” and “refugia”) through the three time periods (1987, 2008 y 2016). Significant results ($P < 0.05$) are highlighted in bold.

Model	DF	χ^2	P-value
Time period	2	0.006	0.997
Micro-habitat	1	18.332	1.856e⁻⁰⁵
Time period x microhabitat	2	104.871	2.2e⁻¹⁶

Table S6. Lineal models testing whether the extent (area) of *G. abies-marina* in 2016 predicts the proportion of the macroalgae in each micro-habitat (“open rock” and “refugia”). Significant results ($P < 0.05$) are highlighted in bold.

“Open rock”	Estimate	SE	t-value	P-value
Intercept	0.078	6.26	0.013	0.99
Extent	36.35	8.50	4.28	0.0008
“Refugia”				
Intercept	99.92	6.26	15.96	2.23e⁻¹⁰
Extent	-36.35	8.50	-4.28	0.0008

Table S7. Summary of the GLMMs testing the effect of temperature on survival and growth of *G. abies-marina* embryos.

Response	DF	χ^2	P-value
Survival	4	1087.5	2.2e⁻¹⁶
Growth	4	530.29	2.2e⁻¹⁶

Table S8. Pairwise comparisons (Tukey test) for the survival of *G. abies-marina* embryos.

Contrast	Estimate	SE	Z ratio	P-value
18°-20°C	1.292	0.08095	14.440	<.0001
18°-22°C	1.708	0.0904	18.892	<.0001
18°-24°C	2.098	0.0896	23.418	<.0001
18°-25°C	2.951	0.0962	30.686	<.0001
20°-22°C	0.416	0.0684	6.089	<.0001
20°-24°C	0.806	0.0665	12.114	<.0001
20°-25°C	1.659	0.0751	22.085	<.0001
22°-24°C	0.389	0.0684	5.691	<.0001
22°-25°C	1.243	0.0767	16.205	<.0001
24°-25°C	0.854	0.0742	11.508	<0.001

Table S9. Pairwise comparisons (Tukey test) for the size of *G. abies-marina* embryos.

Contrast	Estimate	SE	Z ratio	P-value
18°-20°C	0.01544	0.0123	1.251	0.7215
18°-22°C	0.01191	0.0127	0.937	0.8826
18°-24°C	0.18335	0.0142	12.896	<.0001
18°-25°C	0.28531	0.0154	18.896	<.0001
20°-22°C	-0.00353	0.0126	-0.279	0.9987
20°-24°C	0.16792	0.0141	11.903	<.0001
20°-25°C	0.26988	0.0153	17.642	<.0001
22°-24°C	0.17145	0.0144	11.875	<.0001
22°-25°C	0.27340	0.0156	17.533	<.0001
24°-25°C	0.10196	0.0167	6.105	<0.001

Table S10. Summary of the GAM testing the effect of temporal changes in frond size of *G. abies-marina* embryos.

Parametric coefficients	Estimate	Std Error	Z-value	P-value
Intercept	2.23	0.027	81.29	<2e ⁻¹⁶
Approximate significance of smooth terms	Edf	Ref.df	Chi.sq	P-value
S(year)	2.95	2.99	28.79	1.92e ⁻¹⁶

CHAPTER 5. Conclusions

1. Changes in the distribution and extent of *Gongolaria abies-marina* on the island of Gran Canaria over the last few decades are evident and dramatic. In the late 1980s, *G. abies-marina* occupied 928 ha (12.84% of the rocky bottoms) and now it only covers 7.4 ha (0.1%). This decline of *G. abies-marina* forests was mainly related to a combination of human-driven environmental stressors operating at both global and local scales.
2. We found a temporal shift in the frond size structure of *Gongolaria abies-marina* on the island of Gran Canaria, mainly related to the prevalence of the fertile stage, which showed the largest variability in relation to environmental predictors.
3. The population structure of *G. abies-marina* was spatially and temporally variable, associated with wave power, demonstrating the importance of exposure to waves in determining algal canopy density, biomass and morphology.
4. The annual production of *G. abies-marina* in Gran Canaria (5,380.9 g dwt m⁻² year⁻¹) was higher than that previously estimated in the Canary Islands (1,293.2 g dwt m⁻² year⁻¹) and other Mediterranean *Cystoseira*-dominated assemblages. The primary annual production of *G. abies-marina* was as large as that observed for kelps and other fucoids around the world. The dramatic decline of *G. abies-marina* forests in recent decades, 928 ha in Gran Canaria, means the loss of high primary production (16,831.6 Mg C year⁻¹).
5. Results from the early stages thermo-tolerance assay, together with the increased severity in MHWs, provide solid evidence to explain declines of *G. abies-marina*.
6. The fragmented populations of *G. abies-marina* on Gran Canaria Island mostly persist in topographic microhabitats in the lower eulittoral (i.e., as scattered patches with underdeveloped branches), where they find small-scale refugia, as has been reported for other large brown macroalgae.

RESUMEN EN ESPAÑOL

Los bosques marinos de grandes macroalgas pardas, en su mayoría pertenecientes a los órdenes Fucales y Laminariales, son hábitats únicos que sostienen una gran variedad de organismos en zonas costeras de todo el mundo, y son comparables a los bosques terrestres por los servicios ecosistémicos que proporcionan (Steneck et al. 2002). Estas macroalgas que forman dosel son productores primarios muy importantes (Mann 1973). Aumentan la complejidad estructural donde viven, proporcionando refugio y alimento para las especies asociadas (Schiel y Foster 2006; Cheminée et al. 2013) y aumentando la biodiversidad (Chapman 1995; Steneck et al. 2002; Piazzì et al. 2018). Sin embargo, en el último medio siglo, las amenazas para las macroalgas pardas que forman dosel han aumentado en número y gravedad, lo que ha llevado a una disminución de su abundancia en muchos lugares de latitudes templadas (Mineur et al. 2015; Krumhansl et al. 2016). La pérdida de los bosques de macroalgas también implica un daño o empobrecimiento en la prestación de servicios ecosistémicos (Smale et al. 2019). Por lo tanto, la conservación de estas especies que forman hábitats es un objetivo crucial para ecólogos y gestores ambientales. Para lograrlo, es fundamental comprender mejor la estructura y dinámica del dosel de los bosques de algas en relación con los factores ambientales y las interacciones intraespecíficas (Schiel y Foster 2006; Bennett y Wernberg 2014; Smale et al. 2016). Además, entender las causas de la disminución de los bosques de macroalgas es esencial para implementar programas adecuados de conservación y restauración (Coleman y Wernberg 2017).

Los bosques de algas submareales e intermareales experimentan grandes variaciones en su distribución, abundancia y comportamiento en una variedad de escalas espaciales y temporales (Martínez et al. 2012; Ferreira et al. 2014; Yesson et al. 2015). Su estructura y extensión se ven influenciadas por diversas variables ambientales, incluyendo la temperatura (Tuya et al. 2012), la disponibilidad de luz (Creed et al. 1998), los nutrientes (Piazzì y Ceccherelli 2017) y la exposición al oleaje (Engelen et al. 2005). Procesos ecológicos, como la competencia y la facilitación intraespecífica e interespecífica, también pueden afectar su estructura y funcionamiento (Bennett y Wernberg 2014). Aunque las macroalgas son importantes formadoras de hábitat en los ecosistemas rocosos de zonas templadas y subtropicales, todavía hay pocos estudios sobre la estructura del dosel, especialmente en términos de su dinámica temporal (Åberg 1992; Schiel y Foster 2006).

Los cambios estacionales en el fotoperiodo son importantes para iniciar el crecimiento de las macroalgas después del período de letargo invernal. De manera similar, un aumento en la temperatura del agua está relacionado con el inicio del crecimiento y la reproducción (Graiff et

al. 2015; de Bettignies et al. 2018). Normalmente, en mares templados, no existe un acoplamiento entre el período de crecimiento máximo de las macroalgas y la concentración de nutrientes en el agua (Ballesteros 1988; Delgado et al. 1994). Por este motivo, las algas pardas del orden de las Laminariales acumulan reservas de nitrógeno en invierno que se utilizan para iniciar el crecimiento a principios de la primavera, cuando aumentan los niveles de luz (Chapman y Craigie 1977; Nielsen et al. 2014). Muchas especies de *Cystoseira* pueden almacenar reservas en sus tófulos, estructuras de almacenamiento situadas en la base de las ramas (García-Fernández y Bárbara 2016), aunque algunas especies como *Gongolaria abies-marina* carecen de tófulos u otras estructuras alternativas para almacenar reservas (González y Afonso-Carrillo 1990). Por otro lado, la exposición al oleaje es uno de los principales factores que afectan a la estructura y dinámica del dosel (Engelen et al. 2005; Kregting et al. 2016), incluida la adaptación local a las fuerzas hidrodinámicas (de Bettignies et al. 2015).

Una combinación de factores de estrés naturales y antropogénicos a menudo explica el deterioro de los bosques de macroalgas en todo el mundo (Strain et al. 2014; Mineur et al. 2015; Krumhansl et al. 2016). Entre estos factores de estrés, el cambio climático se ha convertido en uno de los impulsores más importantes de este cambio ecológico global (Wernberg et al. 2016). Actualmente, existen evidencias de que el cambio climático ha modificado la distribución de las especies, lo que ha alterado la estructura y el funcionamiento de los ecosistemas (Pech et al. 2017). Muchas especies han cambiado su distribución geográfica, colonizando hábitats más favorables (Vergés et al. 2014; Bevilacqua et al. 2019; Álvarez-Losada et al. 2020), mientras que se han extinguido en áreas previamente ocupadas (Gouvêa et al. 2017; de Bettignies et al. 2018; Gurgel et al. 2020). Eventos extremos de anomalías térmicas, en particular las olas de calor marina (MHWs, por sus siglas en inglés), han ocurrido con una intensidad, frecuencia y duración crecientes en todo el mundo (Hobday et al. 2016; Oliver et al. 2018; Thorat et al. 2022), alterando abruptamente la estructura y función de los ecosistemas marinos, incluyendo los bosques de macroalgas pardas (Wernberg et al. 2016; Straub et al. 2019; Gupta et al. 2020; Smale 2020; Pesarrodonna et al. 2021). Simultáneamente, las perturbaciones humanas locales, como la destrucción del hábitat, la contaminación y la eutrofización, actúan de manera acumulativa e incluso sinérgica, amplificando los efectos del cambio climático en los hábitats costeros (Gouvêa et al. 2017; Orfanidis et al. 2021). Desde el punto de vista de la conservación, es crucial determinar no solo la naturaleza de los diferentes factores involucrados en el declive de los bosques de macroalgas, sino también sus contribuciones relativas y cómo estos factores alteran los procesos en diferentes niveles de organización, desde efectos fisiológicos hasta interacciones ecológicas (Côté et al. 2016; Duarte et al. 2018).

Las macroalgas pardas de los géneros *Cystoseira*, *Ericaria* y *Gongolaria* (Fucales, Phaeophyceae), *Cystoseira* sensu lato (s.l.), son componentes clave de los bosques marinos del Mediterráneo-Atlántico, esenciales para la biodiversidad y el funcionamiento del ecosistema (Tuya y Haroun 2006), los cuales han experimentado declives severos en las últimas décadas (Thibaut et al. 2005; Blanfuné et al. 2016; Valdazo et al. 2017; Bernal-Ibáñez et al. 2021b). Debido a su alta sensibilidad a los impactos antropogénicos, varias especies de *Cystoseira* son indicadoras de aguas de alta calidad y facilitan la implementación de la Directiva Marco Europea del Agua (2000/60/CE) (Ballesteros et al. 2007, Blanfuné et al. 2016b, 2017). Todas las especies del Mediterráneo del género *Cystoseira* s.l., excepto *C. compressa*, han sido protegidas bajo el Anexo II de la Convención de Barcelona (2010). Cinco especies, *Ericaria amentacea*, *Ericaria mediterranea*, *Ericaria sedoides*, *Gongolaria montagnei* y *Ericaria zosteroides*, están protegidas bajo la Convención de Berna (Anexo I, 1979). Además, todas las especies mediterráneas de *Cystoseira* están bajo supervisión de organizaciones internacionales, como la UICN, RAP/ASP y MedPan (Thibaut et al. 2014). Por último, las especies de *Cystoseira* s.l. son consideradas "formadoras de hábitat" y, por lo tanto, se consideran hábitats de interés de la UE (Micheli et al. 2013).

El género *Cystoseira* C. Agardh fue descrito en 1820 y es muy diverso; incluye 37 especies, y su taxonomía y nomenclatura ha experimentado muchos cambios desde entonces (García-Fernández y Bárbara 2016). Las razones de estos cambios radican en el hecho de que la variabilidad en este género ocurre no solo entre especies, sino también entre individuos de una misma especie, incluso estacionalmente dentro del mismo individuo. En los últimos años, con el objetivo de completar el conocimiento del género *Cystoseira*, su taxonomía, origen y evolución, se han realizado varios estudios (Draisma et al. 2010; Orellana et al. 2019; Neiva et al. 2022). Específicamente, Orellana et al. (2019) estudiaron la diversidad y filogenia del género *Cystoseira* s.l. en el Mediterráneo y el Atlántico Este, y como resultado de sus estudios, realizaron cambios en los nombres de algunas especies, incluyendo nuestra especie de estudio, *Cystoseira abies-marina* (S.G. Gemelin) C. Agardh, que fue renombrada como *Treptacantha abies-marina* (S.G. Gmelin) Kützing. Sin embargo, Molinary y Guiry (2020) demostraron que el género *Gongolaria* Boehmer tenía prioridad nomenclatural sobre este nombre, y actualmente, nuestra especie de estudio se denomina *Gongolaria abies-marina* (S.G. Gemelin) Kuntze.

El presente estudio se centra en *Gongolaria abies-marina* (S.G. Gemelin) Kuntze, esta especie ha sido considerada la especie fucal más abundante en las costas rocosas del Archipiélago Canario (Wildpret et al. 1987; Tuya y Haroun 2006), y sus poblaciones suelen formar extensas comunidades tanto en el eulitoral como en el sublitoral somero, principalmente en zonas rocosas

expuestas al oleaje (Wildpret et al. 1987; Medina y Haroun 1993). Esta es una de las macroalgas más productivas en las Islas Canarias (Johnston 1969), y a finales del verano, después del pico máximo de reproducción, es posible encontrar una gran cantidad de restos, llamados arribazones, en las playas provenientes de bosques cercanos (Portillo-Hahnefeld 2008). Las poblaciones de *G. abies-marina* muestran una estructura compleja, lo que permite la presencia de muchas especies asociadas, tanto vegetales como animales.

G. abies-marina es una macroalga cespitosa con numerosas ramas erectas, de hasta 50 cm de longitud. Al igual que otras especies del género *Cystoseira*, esta especie experimenta una pérdida anual de su talo a finales del verano, cuando una alta proporción de las frondas se desprenden después del período reproductivo. Las hapterios adheridos al sustrato y pequeñas frondes sobreviven al invierno y de ellos vuelve a surgir el dosel al año siguiente. De esta manera, la planta nunca pasa por una fase de descanso total, ya que, durante los meses desfavorables, las frondes de diferentes estaciones coexisten (González-Rodríguez y Afonso-Carrillo 1990). Por lo tanto, aunque los individuos son perennes, los talos son anuales (Buonomo et al. 2017). Esta especie se propaga tanto a través de la propagación vegetativa como de la reproducción sexual (Medina 1997). Al igual que otras especies del género, los talos tienen una flotabilidad negativa, y los propágulos normalmente se asientan a menos de 20-40 cm de la población fuente (Mangialajo et al. 2012), lo que le otorga a la especie una capacidad de dispersión limitada (Bulleri et al. 2002).

A lo largo de las costas de los archipiélagos oceánicos de Azores y Webbnesia (Atlántico oriental), diversas actividades humanas locales han alterado los hábitats costeros (Tuya et al. 2014; Ferrer-Valero et al. 2017; Bernal-Ibáñez et al. 2021b). Al mismo tiempo, se ha atribuido al calentamiento del océano efectos negativos en las algas pardas (Sansón et al. 2013; Geppi y Riera 2022), y la aparición de olas de calor marina se ha vuelto más frecuente e intensa en las últimas décadas en el Atlántico oriental (Bernal-Ibáñez et al. 2022). En la costa del noreste Atlántico, se ha informado sobre la disminución e incluso la desaparición de bosques de algas pardas (Friedlander et al. 2017; Bernal-Ibáñez et al. 2021b; Martín-García et al. 2022), y se han señalado varios procesos en este sentido, como la herbivoría de los erizos de mar, el desarrollo humano, eventos extremos de oleaje y las olas de calor marina (Bernal-Ibáñez et al. 2021a, b; Martín-García et al. 2022). En la década de 1990, se registraron retrocesos de los bosques de *Gongolaria abies-marina* en las Islas Canarias (Medina y Haroun 1994). En la década de 2000, Rodríguez et al. (2008) registraron una gran erosión de las poblaciones de *Gongolaria abies-marina* en todo el archipiélago canario. Además, en la década de 2010, Martín-García et al. (2022) registraron una disminución del 90% en las poblaciones de *G. abies-marina* en las islas occidentales (Tenerife, La Gomera, La Palma y

El Hierro). Por esta razón, esta alga está incluida en el catálogo regional de especies en peligro de extinción (Catálogo Canario de Especies Protegidas; Ley 4/2010, 4 de junio de 2010). Recientemente, esta especie también fue incluida en el Catálogo Español de Especies amenazadas (Orden TEC/596/2019, 8 de abril de 2019).

Objetivos

En las últimas décadas, los bosques de *Gongolaria abies-marina* han experimentado un declive significativo en muchas áreas costeras de los archipiélagos de Azores y Webbnesia. La existencia de registros históricos de esta especie en las Islas Canarias permite evaluar los cambios temporales en su distribución y relacionarlos con series temporales de variables antropogénicas locales y globales. Además, existen pocos estudios sobre la fenología y la estructura del dosel de esta especie en las Islas Canarias. Por estas razones, y tomando la isla de Gran Canaria como área de estudio, los principales objetivos de esta tesis son:

1. Proporcionar una evaluación actualizada de la distribución y extensión actual de *Gongolaria abies-marina* y facilitar una comparación con datos históricos, incluyendo poblaciones de ciertos lugares.
2. Vincular la variación estacional en las condiciones ambientales con la estructura del dosel y la reproducción de esta macroalga en la isla de Gran Canaria a lo largo de un ciclo anual.
3. Evaluar los efectos de una variedad de factores de estrés ambientales y antropogénicos en la distribución temporal de los bosques marinos creados por *Gongolaria abies-marina* a nivel de la isla.

Conclusiones

1. Los cambios en la distribución y extensión de *Gongolaria abies-marina* en la isla de Gran Canaria en las últimas décadas son evidentes y dramáticos. A finales de la década de 1980, *G. abies-marina* ocupaba 928 hectáreas (12.84% del fondo rocoso) y ahora solo cubre 7.4 hectáreas (0.1%). Este declive de los bosques de *G. abies-marina* estuvo principalmente relacionado con una combinación de factores de estrés ambientales impulsados por actividades humanas a nivel global y local.
2. Encontramos un cambio temporal en la estructura del tamaño de las frondas de *G. abies-marina* en la isla de Gran Canaria, principalmente relacionado con la prevalencia de la etapa fértil, que mostró la mayor variabilidad en relación con los factores ambientales.
3. La estructura de la población de *G. abies-marina* fue variable espacial y temporalmente, asociada a la potencia de las olas, lo que demuestra la importancia de la exposición a las olas en la densidad, biomasa y morfología del dosel algal.
4. La producción anual de *G. abies-marina* en Gran Canaria (5,380.9 g de peso seco m⁻² año⁻¹) fue mayor que la estimada previamente en las Islas Canarias (1,293.2 g de peso seco m⁻² año⁻¹) y en otros ensamblajes dominados por *Cystoseira* en el Mediterráneo. La producción anual primaria de *G. abies-marina* fue tan grande como la observada en algas pardas y otras fucas en todo el mundo. La dramática disminución de los bosques de *G. abies-marina* en las últimas décadas, 928 hectáreas en Gran Canaria, significa la pérdida de una alta producción primaria (16,831.6 Mg C año⁻¹).
5. Los resultados del ensayo de termotolerancia en las etapas tempranas, junto con el aumento en la severidad de las olas de calor marina, proporcionan evidencia sólida para explicar el declive de *G. abies-marina*.
6. Las poblaciones fragmentadas de *G. abies-marina* en la isla de Gran Canaria en su mayoría persisten en microhábitats topográficos en el eulitoral inferior (es decir, como parches dispersos con ramas poco desarrolladas), donde encuentran refugios a pequeña escala, como se ha informado para otras macroalgas pardas grandes.

FUNDING

This research was partly funded by the University of Las Palmas of Gran Canaria through a research technician contract to José Valdazo. In addition, analyses of the time series of environmental and anthropogenic data were carried out by littoral enterprise within the framework of a project supported by the Government of the Canary Islands: "Study of the delimitation, characterisation, and dissemination of the coralline community and the monitoring of the conservation status of protected algal species of the genera *Treptacantha*, *Carpodesmia*, and *Gelidium*", co-financed by the FEDER Canarias operational program (2014-2020).

REFERENCES

- Åberg P (1992) A demographic study of two populations of the seaweed *Ascophyllum nodosum*. *Ecology* 73:1473–1487.
<https://doi.org/10.2307/1940691>
- Arenas F, Fernández C, Rico JM, et al (1995) Growth and reproductive strategies of *Sargassum muticum* (Yendo) Fensholt and *Cystoseira nodicaulis* (Whit.) Roberts. *Sci Mar* 59:1–8.
- Álvarez-Losada Ó, Arrontes J, Martínez B, et al (2020) A regime shift in intertidal assemblages triggered by loss of algal canopies: A multidecadal survey. *Mar Environ Res* 160:104981.
<https://doi.org/10.1016/j.marenvres.2020.104981>
- Andrews S, Bennett S, Wernberg T (2014) Reproductive seasonality and early life temperature sensitivity reflect vulnerability of a seaweed undergoing range reduction. *Mar Ecol Prog Ser* 495:119–129.
<https://doi.org/10.3354/meps10567>
- Ballesteros E (1988) Estructura y dinámica de la comunidad de *Cystoseira mediterranea* Sauvageau en el Mediterráneo Noroccidental. *Investigación Pesquera* 52:313–334.
- Ballesteros E (1990a) Structure and dynamics of the *Cystoseira caespitosa* Sauvageau (Fucales, Phaeophyceae) community in the north-western Mediterranean. *Sci Mar* 54:155–168.
- Ballesteros E (1990b) Structure and dynamics of the community of *Cystoseira zosteroides* (Turner) C. Agardh (Fucales, Phaeophyceae) in the north-western Mediterranean. *Sci Mar* 54:217–229.
- Ballesteros E, Torras X, Pinedo S, et al (2007) A new methodology based on littoral community cartography for the implementation of the European Water Framework Directive. *Mar Poll Bull* 55:172-180.
<https://doi.org/10.1016/j.marpolbul.2006.08.038>
- Barton K (2023) MuMIn: multi-model inference.
- Benedetti-Cecchi L, Pannacciulli F, Bulleri F, et al (2001). Predicting the consequences of anthropogenic disturbance: large-scale effects of loss of canopy algae on rocky shores. *Mar Ecol Prog Ser* 214:137-150.
<https://doi.org/10.3354/meps214137>
- Bennett S, Wernberg T (2014). Canopy facilitates seaweed recruitment on subtidal temperate reefs. *J Ecol* 102:1462–1470.
<https://doi.org/10.1111/1365-2745.12302>
- Berec L, Angulo E, Courchamp F (2007) Multiple Allee effects and population management. *Trends Ecol Evol* 22:185–191.
<https://doi.org/10.1016/j.tree.2006.12.002>

Bernal-Ibáñez A, Cacabelos E, Melo R, Gestoso I (2021a) The role of sea-urchins in marine forests from Azores, Webbnesia, and Cabo Verde: human pressures, climate-change effects and restoration opportunities. *Front Mar Sci* 8:649873.

<https://doi.org/10.3389/fmars.2021.649873>

Bernal-Ibáñez A, Gestoso I, Wirtz P, et al (2021b) The collapse of marine forests: drastic reduction in populations of the family Sargassaceae in Madeira Island (NE Atlantic). *Reg Environ Change* 21:71.

<https://doi.org/10.1007/s10113-021-01801-2>

Bernal-Ibáñez A, Gestoso I, Ramalhosa P, et al (2022) Interaction of marine heatwaves and grazing on two canopy-forming algae. *J Exp Mar Biol Ecol* 556:151795.

<https://doi.org/10.1016/j.jembe.2022.151795>

Bevilacqua S, Savonitto G, Lipizer M, et al (2019) Climatic anomalies may create a long-lasting ecological phase shift by altering the reproduction of a foundation species. *Ecology* 100:1–4.

<https://doi.org/10.1002/ecy.2838>

Blanfuné A, Boudouresque CF, Verlaque M, et al (2016a) The fate of *Cystoseira crinita*, a forest-forming Fucale (Phaeophyceae, Stramenopiles), in France (North Western Mediterranean Sea). *Est Coast Shelf Sci* 181:196-208.

<https://doi.org/10.1016/j.ecss.2016.08.049>

Blanfuné A, Boudouresque CF, Verlaque M, et al (2016b) Response of rocky shore communities to anthropogenic pressures in Albania (Mediterranean Sea): ecological status assessment through the CARLIT method. *Mar Poll Bull* 109:409-418.

<https://doi.org/10.1016/j.marpolbul.2016.05.041>

Blanfuné A, Thibaut T, Boudouresque CF, et al (2017) The CARLIT method for the assessment of the ecological quality of European Mediterranean waters: Relevance, robustness and possible improvements. *Ecol Indic* 72:249–259.

<https://doi.org/10.1016/j.ecolind.2016.07.049>

Brooks M, Bolker B, Kristensen K, et al (2023) glmmTMB: Generalized Linear Mixed Models using Template Model Builder.

Bulleri F, Benedetti-Cecchi L, Acunto S, et al (2002) The influence of canopy algae on vertical patterns of distribution of low shore assemblages on rocky coasts in the northwest Mediterranean. *J Exp Mar Biol Ecol* 267:89-106.

[https://doi.org/10.1016/S0022-0981\(01\)00361-6](https://doi.org/10.1016/S0022-0981(01)00361-6)

Bulleri F (2009). Facilitation research in marine systems: state of the art, emerging patterns and insights for future developments. *J Ecol* 97:1121–1130.

<https://doi.org/10.1111/j.1365-2745.2009.01567.x>

Buonomo R, Assis J, Fernandes F, et al (2017). Habitat continuity and stepping-stone oceanographic distances explain population genetic connectivity of the brown alga *Cystoseira amentacea*. *Mol Ecol* 26:766-780.

<https://doi.org/10.1111/mec.13960>

Campos-Cáliz A, Fernández AN, Sánchez de Pedro R, Bañares-España E (2019) Physiological responses of adults and juveniles of *Cystoseira tamariscifolia* to projected warming scenarios along Alboran sea populations. II International Congress of Young Marine Researchers 426–430.

Capdevila P, Hereu B, Salguero-Gómez R, et al (2019) Warming impacts on early life stages increase the vulnerability and delay the population recovery of a long-lived habitat-forming macroalga. *J Ecol* 107:1129–1140.

<https://doi.org/10.1111/1365-2745.13090>

Chapman ARO (1995) Functional ecology of furoid algae: twenty-three years of progress. *Phycologia* 34:1–32.

<https://doi.org/10.2216/i0031-8884-34-1-1.1>

Chapman ARO, Craigie JS (1977) Seasonal growth in *Laminaria longicuris*: relations with dissolved inorganic nutrients and internal reserves of nitrogen. *Mar Biol* 40:197–205.

<https://doi.org/10.1007/BF00390875>

Cheminée A, Sala E, Pastor J, et al (2013). Nursery value of *Cystoseira* forests for Mediterranean rocky reef fishes. *J Exp Mar Biol Ecol* 442:70–79.

<https://doi.org/10.1016/j.jembe.2013.02.003>

Chung IK, Beardall J, Mehta S, et al (2011) Using marine macroalgae for carbon sequestration: a critical appraisal. *J Appl Phycol* 23:877–886.

<https://doi.org/10.1007/s10811-010-9604-9>

Coleman MA, Wernberg T (2017) Forgotten underwater forests: The key role of furoids on Australian temperate reefs. *Ecol Evol* 7:8406–8418.

<https://doi.org/10.1002/ece3.3279>

Collado-Vides L (2002) Clonal architecture in marine macroalgae: ecological and evolutionary perspectives. *Evol Ecol* 15:531–545.

<https://doi.org/10.1023/A:1016009620560>

Côté IM, Darling ES, Brown CJ (2016) Interactions among ecosystem stressors and their importance in conservation. *Proc Royal Soc B* 283:20152592.

<https://doi.org/10.1098/rspb.2015.2592>

Creed JC, Kain JM, Norton TA (1998) An experimental evaluation of density and plant size in two large brown seaweeds. *J Phycol* 34:39–52.

<https://doi.org/10.1046/j.1529-8817.1998.340039.x>

de Bettignies T, Wernberg T, Gurgel CFD (2018) Exploring the influence of temperature on aspects of the reproductive phenology of temperate seaweeds. *Front Mar Sci* 5: 218.

<https://doi.org/10.3389/fmars.2018.00218>

de Bettignies T, Wernberg T, Lavery PS, et al (2015) Phenological decoupling of mortality from wave forcing in kelp beds. *Ecology* 96:850–861.

<https://doi.org/10.1890/13-2365.1>

de Caralt S, Verdura J, Vergés A, et al (2020) Differential effects of pollution on adult and recruits of a canopy-forming alga: implications for population viability under low pollutant levels. *Sci Rep* 10:1–12.

<https://doi.org/10.1038/s41598-020-73990-5>

De La Fuente G, Asnaghi V, Chiantore M, et al (2019) The effect of *Cystoseira* canopy on the value of midlittoral habitats in NW Mediterranean, an emergy assessment. *Ecol Modell* 404:1–11.

<https://doi.org/10.1016/j.ecolmodel.2019.04.005>

Delgado O, Ballesteros E, Vidal M (1994) Seasonal variation in tissue nitrogen and phosphorus of *Cystoseira mediterranea* Sauvageau (Fucales, Phaeophyceae) in the Northwestern Mediterranean Sea. *Bot Mar* 37:1–9.

<https://doi.org/10.1515/botm.1994.37.1.1>

Doney SC, Ruckelshaus M, Emmett Duffy J, et al (2012) Climate Change Impacts on Marine Ecosystems. *Ann Rev Mar Sci* 4:11–37.

<https://doi.org/10.1146/annurev-marine-041911-111611>

Draisma SGA, Ballesteros E, Rousseau F, Thibaut T (2010) DNA sequence data demonstrate the polyphyly of the genus *Cystoseira* and other Sargassaceae genera (Phaeophyceae). *J Phycol* 46: 1329–1345.

<https://doi.org/10.1111/j.1529-8817.2010.00891.x>

Duarte B, Martins I, Rosa R, et al (2018) Climate change impacts on seagrass meadows and macroalgal forests: an integrative perspective on acclimation and adaptation potential. *Front Mar Sci* 5:190.

<https://doi.org/10.3389/FMARS.2018.00190>

Eger AM, Marzinelli EM, Beas-Luna R, et al (2023) The value of ecosystem services in global marine kelp forests. *Nat Commun* 14:1894.

<https://doi.org/10.1038/s41467-023-37385-0>

Engelen AH, Aberg P, Olsen JL, et al (2005) Effects of wave exposure and depth on biomass, density and fertility of the fucoid seaweed *Sargassum polyceratum* (Phaeophyta, Sargassaceae). *Eur J Phycol* 40:149–158.

<https://doi.org/10.1080/09670260500109210>

Espino F, Tuya F, del Rosario A, et al (2019) Geographical range extension of the Spotfin burrfish, *Chilomycterus reticulatus* (L. 1758), in the Canary Islands: A response to ocean warming? *Diversity (Basel)* 11:1–15.

<https://doi.org/10.3390/d11120230>

Falace A, Marletta G, Savonitto G, et al (2021) Is the south-mediterranean canopy-forming *Ericaria giacconeii* (= *Cystoseira hyblaea*) a loser from ocean warming? *Front Mar Sci* 8:760637.

<https://doi.org/10.3389/fmars.2021.760637>

Ferreira JG, Arenas F, Martínez B, et al (2014) Physiological response of fucoid algae to environmental stress: comparing range centre and southern populations. *New Phytol* 202:1157–1172.

<https://doi.org/10.1111/nph.12749>

Ferrer-Valero N, Hernández-Calvento L, Hernández-Cordero AI (2017). Human impacts quantification on the coastal landforms of Gran Canaria Island (Canary Islands). *Geomorphology* 286:58-67.

<https://doi.org/10.1016/j.geomorph.2017.02.028>

Filbee-Dexter K, Wernberg T (2018) Rise of Turfs: A New Battlefield for Globally Declining Kelp Forests. *Bioscience* 68:64–76.

<https://doi.org/10.1093/biosci/bix147>

Fox J, Weisberg S (2008) *An R Companion to Applied Regression*, Third Edition. SAGE Publications, Inc

Franco JN, Wernberg T, Bertocci I, et al (2015) Herbivory drives kelp recruits into ‘hiding’ in a warm ocean climate. *Mar Ecol Prog Ser* 536:1-9.

<https://doi.org/10.3354/meps11445>

Friedlander AM, Ballesteros E, Clemente S, et al (2017) Contrasts in the marine ecosystem of two Macaronesian islands: A comparison between the remote Selvagens Reserve and Madeira Island. *PLoS ONE* 12(11):e0187935.

<https://doi.org/10.1371/journal.pone.0187935>

García-Fernández A, Bárbara I (2016). Studies of *Cystoseira* assemblages in Northern Atlantic Iberia. *An Jard Bot Madrid* 73:e035.

<https://doi.org/10.3989/ajbm.2403>

García-Romero L, Carreira-Galbán T, Rodríguez-Báez JÁ, et al (2023) Mapping Environmental Impacts on Coastal Tourist Areas of Oceanic Islands (Gran Canaria, Canary Islands): A Current and Future Scenarios Assessment. *Remote Sens* 15:1586.

<https://doi.org/10.3390/rs15061586>

Garrabou J, Coma R, Bensoussan N, et al (2009) Mass mortality in Northwestern Mediterranean rocky benthic communities: Effects of the 2003 heat wave. *Glob Chang Biol* 15:1090–1103.

<https://doi.org/10.1111/j.1365-2486.2008.01823.x>

Geppi EF, Riera R (2022) Responses of intertidal seaweeds to warming: A 38- year time series shows differences of sizes. *Estuar Coast Shelf Sci* 270:107841.

<https://doi.org/10.1016/j.ecss.2022.107841>

Giaccone G, Alongi G, Pizzuto F, et al (1994). La Vegetazione marina bentonica fotofila del Mediterraneo: 2: Infralitorale e Circalitorale: proposte di aggiornamento. *Boll Accad Gioenia Sci Nat Catania* 27(346):111-157.

Gil-Rodríguez MC (1978) Revisión taxonómica y ecológica del género *Cystoseira* C. Agardh en el Archipiélago Canario. *Vieraea* 9:115–148.

Gil-Rodríguez MC, Afonso-Carrillo J, Sansón M, et al (1988) Embriogénesis en *Cystoseira abies-marina* (Gmelin) C. Agardh (Phaeophyta). Importancia biosistemática. *Actes del Simposi Internacional de Botanica Pius Font i Quer* 123–127.

Gómez Garreta A, Barceló Martí M, Gallardo García T, et al (2000) *Flora phycologica ibérica*. I. Fucales (Vol.1). Servicio de publicaciones, Universidad de Murcia.

González-Rodríguez RM, Afonso-Carrillo J (1990). Estudio fenológico de cuatro especies de *Cystoseira* C. Agardh (Phaeophyta, Fucales) en Punta del Hidalgo, Tenerife (Islas Canarias). *Vieraea* 18:205-234.

Graiff A, Liesner D, Karsten U, Bartsch I. (2015). Temperature tolerance of western Baltic Sea *Fucus vesiculosus* – growth, photosynthesis and survival. *J. Exp Mar Biol Ecol* 471:8–16.

<https://doi.org/10.1016/j.jembe.2015.05.009>

Gómez Garreta A, Barceló Martí M, Gallardo García T, et al (2000) Flora phycologica ibérica. I. Fucales (Vol.1). Servicio de publicaciones, Universidad de Murcia.

Gouvêa LP, Schubert N, Martins CDL, et al (2017) Interactive effects of marine heatwaves and eutrophication on the ecophysiology of a widespread and ecologically important macroalga. *Limnol Oceanogr* 62:2056–2075.

<https://doi.org/10.1002/lno.10551>

Grimaldi CM, Lowe RJ, Benthuisen JA, et al (2023) Hydrodynamic and atmospheric drivers create distinct thermal environments within a coral reef atoll. *Coral Reefs* 42:693-706.

<https://doi.org/10.1007/s00338-023-02371-x>

Guern M (1962). Embryologie de quelques espèces du genre *Cystoseira* Agardh 1821 (Fucales). *Vie et Milieu* 13:649–679.

Gupta A Sen, Thomsen M, Benthuisen JA, et al (2020) Drivers and impacts of the most extreme marine heatwaves events. *Sci Rep* 10:1–16.

<https://doi.org/10.1038/s41598-020-75445-3>

Gurgel CFD, Camacho O, Minne AJP, et al (2020) Marine Heatwave Drives Cryptic Loss of Genetic Diversity in Underwater Forests. *Curr Biol* 30(7):1199-1206.e2.

<https://doi.org/10.1016/j.cub.2020.01.051>

Halpern BS, Walbridge S, Selkoe KA, et al (2008). A global map of human impact on marine ecosystems. *Science* 319(5865):948-952.

<https://doi.org/10.1126/science.1149345>

Hernández JC, Sangil C, Lorenzo-Morales J (2020) Uncommon southwest swells trigger sea urchin disease outbreaks in Eastern Atlantic archipelagos. *Ecol Evol* 10:7963–7970.

<https://doi.org/10.1002/ece3.6260>

Hijmans RJ (2023) terra: Spatial Data Analysis.

Hobday AJ, Alexander L V, Perkins SE, et al (2016) A hierarchical approach to defining marine heatwaves. *Prog Oceanogr* 141:227–238.

<https://doi.org/10.1016/j.pocean.2015.12.014>

Hoffmann L, Renard R, Demoulin V (1992) Phenology, growth and biomass of *Cystoseira balearica* in Calvi (Corsica). *Mar Ecol Prog Ser* 80:249–254.

Hurd CL (2000) Water motion, marine macroalgal physiology, and production. *J Phycol* 36:453–472.

<https://doi.org/10.1046/j.1529-8817.2000.99139.x>

Irving AD, Balata D, Colosio F, et al (2009) Light, sediment, temperature, and the early life-history of the habitat-forming alga *Cystoseira barbata*. *Mar Biol* 156:1223–1231.

<https://doi.org/10.1007/s00227-009-1164-7>

ISTAC. 2015. Anuario Estadístico de Canarias 2014. Instituto Canario de Estadística, Gobierno de Canarias.

IUCN. 2017. The IUCN Red List of Threatened Species. Version 2017-1. Accessed on 10 July 2017. www.iucnredlist.org

- Iveša L, Djakovac T, Devescovi M (2016) Long-term fluctuations in *Cystoseira* populations along the west Istrian Coast (Croatia) related to eutrophication patterns in the northern Adriatic Sea. *Mar Poll Bull* 106:162-173.
<https://doi.org/10.1016/j.marpolbul.2016.03.010>
- Johnston CS (1969). Studies on the ecology and primary production of Canary Island marine algae. *Proc Int Seaweed Symp* 6:213-222.
- Jones CG, Lawton JH, Shachak M (1994). Organisms as ecosystem engineers. *Oikos* 69:373-386.
<https://doi.org/10.2307/3545850>
- Krause-Jensen D, Duarte CM (2016) Substantial role of macroalgae in marine carbon sequestration. *Nat Geosci* 9:737–742.
<https://doi.org/10.1038/ngeo2790>
- Kregting L, Blight AJ, Elsässer B, Savidge G (2016) The influence of water motion on the growth rate of the kelp *Laminaria digitata*. *J Exp Mar Biol Ecol* 478:86–95.
<https://doi.org/10.1016/j.jembe.2016.02.006>
- Krumhansl KA, Scheibling RE (2012) Production and fate of kelp detritus. *Mar Ecol Prog Ser* 67:281–302.
<https://10.3354/meps09940>
- Krumhansl KA, Okamoto DK, Rassweiler A, et al (2016) Global patterns of kelp forest change over the past half-century. *Proc Natl Acad Sci* 113:13785–13790.
<https://doi.org/10.1073/pnas.1606102113>
- Lamela-Silvarrey C, Fernández C, Anadón R, et al (2012) Furoid assemblages on the north coast of Spain: past and present (1977-2007). *Bot Mar* 55:199-207.
<https://doi.org/10.1515/bot-2011-0081>
- Legendre, P. & Legendre, L. (1998). *Numerical Ecology*. Elsevier, Amsterdam.
- Lenth RV, Bolker B, Buerkner P, et al (2023) emmeans: Estimated Marginal Means, aka Least-Squares Means.
- Lima FP, Wetthey DS (2012) Three decades of high-resolution coastal sea surface temperatures reveal more than warming. *Nat Commun* 3:704.
<https://doi.org/10.1038/ncomms1713>
- Ling SD, Scheibling RE, Rassweiler A, et al (2015). Global regime shift of catastrophic sea urchin overgrazing. *Phil Trans R Soc B* 370:20130269.
<https://doi.org/10.1098/rstb.2013.0269>
- Losada IJ, Méndez F, Vidal C, et al (2010) Spatial and temporal variability of nearshore wave energy resources along Spain: methodology and results. In: *Oceans 2010 MTS/IEEE SEATTLE*. Seattle, WA, USA, pp 1–8.
- Lüdecke D, Ben-Shachar M, Patil I, et al (2021) performance: An R Package for Assessment, Comparison and Testing of Statistical Models. *J Open Source Softw* 6:3139.
<https://doi.org/10.21105/joss.03139>

Mancuso FP, D'Agostaro R, Milazzo M, et al (2022) The invasive seaweed *Asparagopsis taxiformis* erodes the habitat structure and biodiversity of native algal forests in the Mediterranean Sea. *Mar Environ Res* 173:105515.

<https://doi.org/10.1016/j.marenvres.2021.105515>

Mangialajo L, Chiantore M, Cattaneo-Vietti R (2008). Loss of furoid algae along a gradient of urbanisation and relationships with the structure of benthic assemblages. *Mar Ecol Prog Ser* 358:63-74.

<https://doi.org/10.3354/meps07400>

Mangialajo L, Chiantore M, Susini ML, et al (2012). Zonation patterns and interspecific relationships of furoids in microtidal environments. *J Exp Mar Biol Ecol* 412:72-80.

<https://doi.org/10.1016/j.jembe.2011.10.031>

Mann KH (1973). Seaweeds: their productivity and strategy for growth: the role of large marine algae in coastal productivity is far more important than has been suspected. *Science* 182:975–981.

<https://doi.org/10.1126/science.182.4116.975>

Martín-García L, Rancel-Rodríguez NM, Sangil C, et al (2022) Environmental and human factors drive the subtropical marine forests of *Gongolaria abies-marina* to extinction. *Mar Environ Res* 181:105759.

<https://doi.org/10.1016/j.marenvres.2022.105759>

Martínez B, Viejo RM, Carreño F, Aranda SC (2012) Habitat distribution models for intertidal seaweeds: responses to climatic and non-climatic drivers. *J Biogeogr* 39:1877–1890.

<https://doi.org/10.1111/j.1365-2699.2012.02741.x>

Medina M (1997). Estudio ecofisiológico de las praderas de *Cystoseira abies-marina* (S.G. Gmel.) C. Agardh en el Archipiélago Canario. PhD thesis, Tech. Univ. La Laguna, 155 pp.

Medina M, Haroun R (1993) Preliminary study on the dynamics of *Cystoseira abies-marina* population in Tenerife (Canary Island). *Cour Forschinst Senckenb* 159:109-112.

Medina M, Haroun R (1994) Dinámica regresiva de una pradera submareal de *Cystoseira abies-marina* (*Cystoseiraceae*, Phaeophyta) en la isla de Tenerife. *Vieraea* 23:65–71.

Micheli F, Levin N, Giakoumi S, et al (2013). Setting priorities for regional conservation planning in the Mediterranean Sea. *PLoS ONE* 8:e59038.

<https://doi.org/10.1371/journal.pone.0059038>

Mineur F, Arenas F, Assis J, et al (2015) European seaweeds under pressure: Consequences for communities and ecosystem functioning. *J Sea Res* 98:91–108.

<https://doi.org/10.1016/j.seares.2014.11.004>

M.M.A. (2001) Estudio Ecocartográfico de la zona sur del litoral de la Isla de Gran Canaria. Plan de Ecocartografías del Litoral Español.

M.M.A. (2005) Estudio Ecocartográfico de la zona norte del litoral de la isla de Gran Canaria. Plan de Ecocartografías del Litoral Español.

Molinari E, Guiry MD (2020) Reinstatement of the genera *Gongolaria* Boehmer and *Ericaria* Stackhouse (Sargassaceae, Phaeophyceae). *Notulae Algarum* 172:1-10

Montserrat M, Verdura J, Corneau S, et al (2023) The role of grazers in early-life stages of *Cystoseira sensu lato* can be crucial in the restoration of marine forests. *Front Mar Sci* 10: 1176780.

<https://doi.org/10.3389/fmars.2023.1176780>

Neiva J, Bermejo R, Medrano A, et al (2022) DNA barcoding reveals cryptic diversity, taxonomic conflicts and novel biogeographical insights in *Cystoseira* s.l. (Phaeophyceae). *Eur J Phycol* 58(3):351-375.

<https://doi.org/10.1080/09670262.2022.2126894>

Nielsen MM, Krause-Jensen D, Olesen B, et al (2014) Growth dynamics of *Saccharina latissima* (Laminariales, Phaeophyceae) in Aarhus Bay, Denmark, and along the species' distribution range. *Mar Biol* 161:2011–2022.

<https://doi.org/10.1007/s00227-014-2482-y>

Oliver ECJ, Donat MG, Burrows MT, et al (2018) Longer and more frequent marine heatwaves over the past century. *Nat Commun* 9:1–12.

<https://doi.org/10.1038/s41467-018-03732-9>

Oliveras M, Gómez A (1989). Corología del género *Cystoseira* C. Agardh (Phaeophyceae, Fucales). *An. Jard. Bot. Madrid* 46: 89-97.

Orellana S, Hernández M, Sansón M (2019) Diversity of *Cystoseira sensu lato* (Fucales, Phaeophyceae) in the eastern Atlantic and Mediterranean based on morphological and DNA evidence, including *Carpodesmia* gen. emend. and *Treptacantha* gen. emend. *Eur J Phycol* 54: 447–465.

<https://doi.org/10.1080/09670262.2019.1590862>

Orfanidis S, Rindi F, Cebrian E, et al (2021) Effects of Natural and Anthropogenic Stressors on Fucalean Brown Seaweeds Across Different Spatial Scales in the Mediterranean Sea. *Front Mar Sci* 8:658417.

<https://doi.org/10.3389/fmars.2021.658417>

Pebesma E (2023) sf: Simple Features for R.

Pecl GT, Araújo MB, Bell JD, et al (2017) Biodiversity redistribution under climate change: Impacts on ecosystems and human well-being. *Science* 355:eaai9214.

<https://doi.org/10.1126/science.aai9214>

Pessarrodona A, Filbee-Dexter K, Alcoverro T, et al (2021) Homogenization and miniaturization of habitat structure in temperate marine forests. *Glob Chang Biol* 27(20):5262–5275.

<https://doi.org/10.1111/gcb.15759>

Peterson BG, Carl P (2014). *PerformanceAnalytics: Econometric Tools for Performance and Risk Analysis*. R package version 1 (3541), 107.

Piazzini L, Bonaviri C, Castelli A, et al (2018) Biodiversity in canopy-forming algae: structure and spatial variability of the Mediterranean *Cystoseira* assemblages. *Estuar Coast Shelf Sci* 207:132–141.

<https://doi.org/10.1016/j.ecss.2018.04.001>

- Piazzì L, Ceccherelli G (2017) Concomitance of oligotrophy and low grazing pressure is essential for the resilience of Mediterranean subtidal forests. *Mar Pollut Bull* 123:197–204. <https://doi.org/10.1016/j.marpolbul.2017.08.061>
- Portillo-Hahnefeld E (2008) Arribazones de algas y plantas marinas en Gran Canaria. Características, gestión y posibles usos. Instituto Tecnológico de Canarias, 86 pp.
- Ramírez R, Tuya F, Haroun RJ (2008). El Intermareal Canario. Poblaciones de lapas, burgados y cañadillas. BIOGES, Universidad de Las Palmas de Gran Canaria, 52 pp.
- Ribera MA, Gomez-Garreta A, Gallardo T, et al (1992). Check-list of Mediterranean Seaweeds. I. Fucophyceae (Warming, 1884). *Bot Mar* 35:109–130.
- Rico JM, Fernández C (1997) Ecology of *Sargassum muticum* on the North Coast of Spain II. Physiological differences between *Sargassum muticum* and *Cystoseira nodicaulis*. *Bot Mar* 40: 405–410. <https://doi.org/10.1515/botm.1997.40.1-6.405>
- Riera R, Sangil C, Sansón M (2015) Long-term herbarium data reveal the decline of a temperate-water algae at its southern range. *Est Coast Shelf Sci* 165:159-165. <https://doi.org/10.1016/j.ecss.2015.05.008>
- Rivera M, Scrosati R (2008) Self-thinning and size inequality dynamics in a clonal seaweed (*Sargassum lapazeanum*, Phaeophyceae). *J Phycol* 44:45–49. <https://doi.org/10.1111/j.1529-8817.2007.00427.x>
- Rodríguez M, Pérez Ó, Ramos E, et al. (2008) Estudio de la distribución y tamaño de población de la especie *Cystoseira abies-marina* (S.G. Gmelin) C. Agardh, 1820 en Canarias. C.I.M.A. Informe Técnico 29, 188 pp.
- Román M, Román S, Vázquez E, et al (2020) Heatwaves during low tide are critical for the physiological performance of intertidal macroalgae under global warming scenarios. *Sci Rep* 10:1–15. <https://doi.org/10.1038/s41598-020-78526-5>
- Roskov Y, Abucay L, Orrell T, et al (2016). Species 2000 & ITIS Catalogue of Life, 2016 Annual Checklist. Naturalis, Leiden, the Netherlands. <http://www.catalogueoflife.org/annual-checklist/2016>
- Sales M, Cebrian E, Tomas F, et al (2011) Pollution impacts and recovery potential in three species of the genus *Cystoseira* (Fucales, Heterokontophyta). *Est Coast Shelf Sci* 92:347-357. <https://doi.org/10.1016/j.ecss.2011.01.008>
- Sales M, Ballesteros E (2012) Seasonal dynamics and annual production of *Cystoseira crinita* (Fucales: Ochrophyta)-dominated assemblages from the northwestern Mediterranean. *Sci Mar* 76:391–401. <https://doi.org/10.3989/scimar.03465.16D>
- Sangil C, Sansón M, Afonso-Carrillo J (2011) Spatial variation patterns of subtidal seaweed assemblages along a subtropical oceanic archipelago: Thermal gradient vs herbivore pressure. *Estuar Coast Shelf Sci* 94:322–333. <https://doi.org/10.1016/j.ecss.2011.07.004>

Sangil C, Sansón M, Clemente S, et al (2014) Contrasting the species abundance, species density and diversity of seaweed assemblages in alternative states: Urchin density as a driver of biotic homogenization. *J Sea Res* 85:92-103.

<https://doi.org/10.1016/j.seares.2013.10.009>

Sansón M, Reyes J, Afonso-Carrillo J (2001). Flora marina. In: Fernández Palacios J.M., Martín-Esquivel J.L. (eds). *Naturaleza de las Islas Canarias: ecología y conservación*. Ed. Turquesa. Santa Cruz de Tenerife. pp. 193-198.

Sansón M, Sangil C, Orellana S, et al. (2013). Do the size shifts of marine macroalgae match the warming trends in the Canary Islands? In: XIX Simposio de Botánica Criptogámica. Las Palmas de Gran Canaria, 24-28 June.

Santelices B (2004) A comparison of ecological responses among asexual (unitary), clonal and coalescing macroalgae. *J Exp Mar Biol Ecol* 300:31–64.

<https://doi.org/10.1016/j.jembe.2003.12.017>

Schiel DR, Foster MS (2006) The population biology of large brown seaweeds: ecological consequences of multiphase life histories in dynamic coastal environments. *Ann Rev Ecol Evol Syst* 37:343-372.

<https://doi.org/10.1146/annurev.ecolsys.37.091305.110251>

Schlegel RW, Smit AJ (2018) heatwaveR: A central algorithm for the detection of heatwaves and cold-spells. *J Open Source Softw* 3:821.

<https://doi.org/10.21105/joss.00821>

Scrosati R (2005) Review of studies on biomass–density relationships (including self-thinning lines) in seaweeds: main contributions and persisting misconceptions. *Phycological Res* 53:224–233.

<https://doi.org/10.1111/j.1440-183.2005.00390.x>

Shay JE, Pennington LK, Mandussi Montiel-Molina JA, et al (2021) Rules of Plant Species Ranges: Applications for Conservation Strategies. *Front Ecol Evol* 9:700962.

<https://doi.org/10.3389/fevo.2021.700962>

Smale DA, Burrows MT, Evans AJ, et al (2016) Linking environmental variables with regional-scale variability in ecological structure and standing stock of carbon within UK kelp forests. *Mar Ecol Progr Ser* 542:79–95.

<https://doi.org/10.3354/meps11544>

Smale DA, Wernberg T, Oliver ECJ, et al (2019) Marine heatwaves threaten global biodiversity and the provision of ecosystem services. *Nat Clim Chang* 9:306–312.

<https://doi.org/10.1038/s41558-019-0412-1>

Smale DA (2020) Impacts of ocean warming on kelp forest ecosystems. *New Phytologist* 225:1447–1454.

<https://doi.org/10.1111/nph.16107>

Smith KE, Burrows MT, Hobday AJ, et al (2023) Biological Impacts of Marine Heatwaves. *Ann Rev Mar Sci* 15:119-145.

<https://doi.org/10.1146/annurev-marine-032122-121437>

Steneck RS, Graham MH, Bourque BJ, et al (2002) Kelp forest ecosystems: biodiversity, stability, resilience and future. *Environ Conserv* 29: 436–459.

<https://doi.org/10.1017/S0376892902000322>

Stipcich P, Apostolaki ET, Chartosia N, et al (2022) Assessment of *Posidonia oceanica* traits along a temperature gradient in the Mediterranean Sea shows impacts of marine warming and heat waves. *Front Mar Sci* 9: 895354.

<https://doi.org/10.3389/fmars.2022.895354>

Strain EMA, Thomson RJ, Micheli F, et al (2014) Identifying the interacting roles of stressors in driving the global loss of canopy-forming to mat-forming algae in marine ecosystems. *Glob Chang Biol* 20:3300–3312.

<https://doi.org/10.1111/gcb.12619>

Straub SC, Wernberg T, Thomsen MS, et al (2019) Resistance, Extinction, and Everything in Between – The Diverse Responses of Seaweeds to Marine Heatwaves. *Front Mar Sci* 6:763.

<https://doi.org/10.3389/fmars.2019.00763>

Sunday JM, Pecl GT, Frusher S, et al (2015) Species traits and climate velocity explain geographic range shifts in an ocean-warming hotspot. *Ecol Lett* 18(9):944-953.

<https://doi.org/10.1111/ele.12474>

Susini ML, Thibaut T, Meinesz A, et al (2007) A preliminary study of genetic diversity in *Cystoseira amentacea* (C. Agardh) Bory var. *stricta* Montagne (Fucales, Phaeophyceae) using random amplified polymorphic DNA. *Phycologia* 46:605-611.

<https://doi.org/10.2216/06-100.1>

Thibaut T, Pinedo S, Torras X, et al (2005) Long-term decline of the populations of Fucales (*Cystoseira* spp. and *Sargassum* spp.) in the Albères coast (France, northwestern Mediterranean). *Mar Poll Bull* 50:1472-1489.

<https://doi.org/10.1016/j.marpolbul.2005.06.014>

Thibaut T, Blanfuné A, Markovic L, et al (2014) Unexpected abundance and long-term relative stability of the brown alga *Cystoseira amentacea*, hitherto regarded as a threatened species, in the north-western Mediterranean Sea. *Mar Poll Bull* 89:305-323.

<https://doi.org/10.1016/j.marpolbul.2014.09.043>

Thibaut T, Blanfuné A, Boudouresque CF, et al (2015) Decline and local extinction of Fucales in the French Riviera: the harbinger of future extinctions? *Medit Mar Sci* 16:206-224.

<https://doi.org/10.12681/mms.1032>

Thibaut T, Blanfuné A, Verlaque M, et al (2016^a) The *Sargassum conundrum*: highly rare, threatened or locally extinct in the NW Mediterranean and still lacking protection. *Hydrobiologia* 781:3-23.

<https://doi.org/10.1007/s10750-015-2580-y>

Thibaut T, Blanfuné A, Boudouresque CF, et al (2016) Unexpected temporal stability of *Cystoseira* and *Sargassum* forests in Port-Cros, one of the oldest Mediterranean marine National Parks. *Cryptogamie Algol* 37:61-90.

<https://doi.org/10.7872/crya/v37.iss1.2016.61>

Thomsen MS, Wernberg T (2005) Miniview: what affects the forces required to break or dislodge macroalgae?. *Eur J Phycol* 40:139–148.

<https://doi.org/10.1080/09670260500123591>

Thoral F, Montie S, Thomsen MS, et al (2022) Unravelling seasonal trends in coastal marine heatwave metrics across global biogeographical realms. *Sci Rep* 12:7740.

<https://doi.org/10.1038/s41598-022-11908-z>

Tuya F, Martín JA, Reuss GM, et al (2001) Food preference of the sea urchin *Diadema antillarum* in Gran Canaria (Canary Island, central-east Atlantic Ocean). *J Mar Biol Assoc UK* 81:1-5.

<https://doi.org/10.1017/S0025315401004672>

Tuya F, Boyra A, Sanchez-Jerez P, et al (2004a) Relationships between rocky-reef fish assemblages, the sea urchin *Diadema antillarum* and macroalgae throughout the Canarian Archipelago. *Mar Ecol Prog Ser* 278:157–169.

<https://doi:10.3354/meps278157>

Tuya F, Boyra A, Sanchez-Jerez P, et al (2004b) Can one species determine the structure of the benthic community on a temperate rocky reef? The case of the long-spined sea-urchin *Diadema antillarum* (Echinodermata: Echinoidea) in the eastern Atlantic. *Hydrobiologia* 519:211-214.

<https://doi.org/10.1023/B:HYDR.0000026599.57603.bf>

Tuya F, Haroun R (2006). Spatial patterns and response to wave exposure of photophilic algal assemblages across the Canarian Archipelago: a multi-scaled approach. *Mar Ecol Prog Ser* 311: 15-28.

<https://doi.org/10.3354/meps311015>

Tuya F, Martín JA, Luque A (2006) Seasonal cycle of a *Cymodocea nodosa* seagrass meadow and of the associated ichthyofauna at Playa Dorada (Lanzarote, Canary Islands, eastern Atlantic). *Ciencias Marinas* 32:695–704.

<https://doi.org/10.7773/cm.v32i4.1158>

Tuya F, Ramírez R, Sánchez-Jerez P, et al (2006). Coastal resources exploitation can mask bottom-up mesoscale regulation of intertidal populations. *Hydrobiologia* 553:337-344.

<https://doi.org/10.1007/s10750-005-1246-6>

Tuya F, Cacabelos E, Duarte P, et al (2012) Patterns of landscape and assemblage structure along a latitudinal gradient in ocean climate. *Mar Ecol Progr Ser* 466:9–19.

<https://doi.org/10.3354/meps09941>

Tuya F, Ribeiro-Leite L, Arto-Cuesta N, et al (2014) Decadal changes in the structure of *Cymodocea nodosa* seagrass meadows: Natural vs. human influences. *Est Coast Shelf Sci* 137:41-49.

<https://doi.org/10.1016/j.ecss.2013.11.026>

Valdazo J, Viera-Rodríguez MA, Haroun R, et al (2017) Massive decline of *Cystoseira abies-marina* forests in Gran Canaria Island (Canary Island, eastern Atlantic). *Sci Mar* 81:499–507.

<https://doi.org/10.3989/scimar.04655.23A>

Valdazo J, Viera-Rodríguez MA, Tuya F (2020) Seasonality in the canopy structure of the endangered brown macroalga *Cystoseira abies-marina* at Gran Canaria Island (Canary Islands, eastern Atlantic). *Eur J Phycol* 55(3):253-265.

<https://doi.org/10.1080/09670262.2019.1696989>

Verdura J, Santamaría J, Ballesteros E, et al (2021) Local-scale climatic refugia offer sanctuary for a habitat-forming species during a marine heatwave. *J Ecol* 109:1758–1773.

<https://doi.org/10.1111/1365-2745.13599>

Verges A, Alcoverro T, Ballesteros E (2009) Role of fish herbivory in structuring the vertical distribution of canopy algae *Cystoseira* spp. in the Mediterranean Sea. *Mar Ecol Prog Ser* 375: 1-11.

<https://doi.org/10.3354/meps07778>

Vergés A, Steinberg PD, Hay ME, et al (2014) The tropicalization of temperate marine ecosystems: Climate-mediated changes in herbivory and community phase shifts. *Proc R Soc B* 281:20140846.

<https://doi.org/10.1098/rspb.2014.0846>

Wahl M, Molis M, Hobday AJ, et al (2015) The responses of brown macroalgae to environmental change from local to global scales: direct versus ecologically mediated effects. *Perspect Phycol* 2:11-30.

<https://doi.org/10.1127/pip/2015/0019>

Wernberg T, Bennett S, Babcock RC, et al (2016) Climate driven regime shift of a temperate marine ecosystem. *Science* 353(169):169-172.

<https://doi.org/10.1126/science.aad8745>

Wernberg T, Filbee-Dexter K (2019) Missing the marine forest for the trees. *Mar Ecol Prog Ser* 612:209–215.

<https://doi.org/10.3354/meps12867>

Wernberg T, Thomsen MS, Tuya F, et al (2010) Decreasing resilience of kelp beds along a latitudinal temperature gradient: Potential implications for a warmer future. *Ecol Lett* 13:685–694.

<https://doi.org/10.1111/j.1461-0248.2010.01466.x>

Wildpret W, Gil-Rodríguez MC, Afonso-Carrillo J (1987). Cartografía de los campos de algas y praderas de fanerógamas marinas del piso infralitoral del Archipiélago Canario. Consejería de Agricultura y Pesca. Gobierno de Canarias, unpubl., Santa Cruz de Tenerife.

Wood SN (2006) *Generalized Additive Models: An Introduction with R*. Chapman & Hall/CRC, Boca Raton.

<https://doi.org/10.1201/9781315370279>

Wood SN (2008) Fast stable direct fitting and smoothness selection for generalized additive models. *J R Stat Soc. Series B Stat Methodol* 70:495–518.

<https://doi.org/10.1111/j.1467-9868.2007.00646.x>

Wood SN (2010) Fast stable restricted maximum likelihood and marginal likelihood estimation of semiparametric generalized linear models. *J R Stat Soc. Series B Stat Methodol* 73(1): 3-36.

<https://doi.org/10.1111/j.1467-9868.2010.00749.x>

Yesson C, Bush LE, Davies AJ, et al (2015) The distribution and environmental requirements of large brown seaweeds in the British Isles. *J Mar Biolog Assoc U K*, 95:669–680.

<https://doi.org/10.1017/S0025315414001453>

Zarco-Perello S, Bosch PNE, Vanderklift MA, et al (2021) Persistence of tropical herbivores in temperate reefs constrains kelp resilience to cryptic habitats. *J Ecol* 109(5):2081-2094.

<https://doi.org/10.1111/1365-2745.13621>

Zhang QS, Li W, Liu S, et al (2009) Size-dependence of reproductive allocation of *Sargassum thunbergii* (Sargassaceae, Phaeophyta) in Bohai Bay, China. *Aquat. Bot.* 91: 194-198.
<https://doi.org/10.1016/j.aquabot.2009.06.003>

Zuur AF, Ieno EN, Walker NJ, et al (2009) *Mixed Effects Models and Extension in Ecology with R*. Highland Statistics Ltd, UK.
https://doi.org/10.1111/j.1467-985X.2010.00663_9.x